REPORT NUMBER: WI/SPR-04-00

LAYER COEFFICIENTS FOR NEW AND REPROCESSED ASPHALTIC MIXES

FINAL REPORT

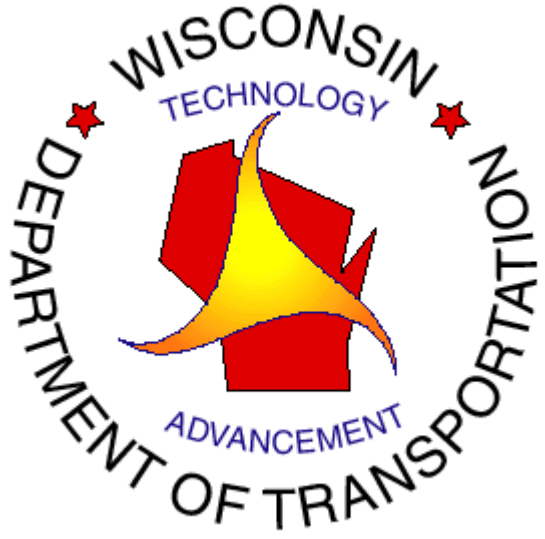

JANUARY 2000

Technical Report Documentation Page

1. Report No. WI/SPR-04-00	**2. Government Accession No.**	**3. Recipients Catalog No.**
4. Title and Subtitle Layer Coefficients for New and Reprocessed Asphaltic Mixes		**5. Report Date** January 2000 **6. Performing Organization Code**
7. Author(s) H. U. Bahia, Assistant Professor; P. J. Bosscher, Professor; J. Christensen, Research Assistant; and Yu Hu, Research Assistant		**8. Performing Organization Report No.**
9. Performing Organization Name and Address University of Wisconsin - Madison Dept. of Civil and Environmental Engineering 1415 Engineering Drive Madison, WI 53706-1490		**10. Work Unit No. (TRAIS)** **11. Contract or Grant No.** WisDOT SPR # 0092-45-86
12. Sponsoring Agency Name and Address Wisconsin Department of Transportation Division of Transportation Infrastructure Development Bureau of Highway Construction Pavements Section, Technology Advancement Unit 3502 Kinsman Blvd., Madison, WI 53704-2507		**13. Type of Report and Period Covered** Final Report **14. Sponsoring Agency Code** WisDOT Study # 97-02
15. Supplementary Notes		

16. Abstract

The objective of this study is to determine layer coefficients for selected types of asphalt mixtures used in Wisconsin including LV. MV, HV, SMA, SHRP, pulverize-Relay mixtures, Mill-Relay mixtures, asphalt base mixtures and recycled PCC-AC mixes combined at different percentages. The traditional method of resilient modulus was used as well as relating rutting damage functions to the layer coefficients. Tests were conducted in the field to measure deflections of actual pavement layers, as well as in the laboratory to measure the responses of samples under conditions that mimic field conditions. The results of the study show that laboratory and field measurements are consistent with the materials tested. The resilient modulus values measured show that different layer coefficients should be given to the recycled and reprocessed materials depending on the nature of the components. A list of layer coefficients is proposed for pavement design. The results of the asphalt materials did not show that there are significant differences in resilient modulus of asphalt mixtures tested; thus, layer coefficients for the asphalt mixtures, derived based on the resilient modulus, are similar for all asphalt mixtures. The results of laboratory rutting tests, however, were found to give different ranking of the materials, compared to the ranking using the resilient modulus results. It is observed that asphalt mixtures vary significantly in their rutting behavior in the laboratory and thus can have different contribution to pavement performance. It is recommended that proposed layer coefficients be used with caution due to lack of direct relation to materials damage behavior. A conceptual procedure for deriving layer coefficients based on resilient modulus, rutting behavior, and fatigue behavior is proposed in the study. The study recommends continued work to verify the proposed procedure and modify the layer coefficients to account for the damage behavior of pavement materials including fatigue and thermal cracking.

17. Key Words LAYER COEFFICIENTS, RESILIENT MODULUS, PAVEMENT DESIGN, RUTTING, FATIGUE, CRACKING		**18. Distribution Statement**	
19. Security Classif. (of this report)	**20. Security Classif. (of this page)**	**21. No. of Pages: 129**	**22. Price**

LAYER COEFFICIENTS FOR NEW AND REPROCESSED ASPHALTIC MIXES

FINAL REPORT WI/SPR-04-00
WisDOT Highway Research Study # 97-02

By

H.U. Bahia, Assistant Professor
P.J. Bosscher, Professor
J. Christensen, Research Assistant
Yu Hu, Research Assistant
University of Wisconsin - Madison
Department of Civil & Environmental Engineering
1415 Engineering Drive, Madison, WI 53706-1490

For

WISCONSIN DEPARTMENT OF TRANSPORTATION
DIVISION OF TRANSPORTATION INFRASTRUCTURE DEVELOPMENT
BUREAU OF HIGHWAY CONSTRUCTION
TECHNOLOGY ADVANCEMENT UNIT
3502 KINSMAN BLVD., MADISON, WI 53704-2507

January 2000

TABLE OF CONTENTS

LIST OF FIGURES

LIST OF TABLES

CHAPTER ONE

INTRODUCTION

1.1 Background

In the late 1950's and early 1960's, the American Association of State Highway Officials (AASHO) conducted a limited road test, the purpose of which was to determine a methodology for designing pavement structures. This organization, which later became the American Association of State Highway and Transportation Officials (AASHTO) used the AASHO Road Test results to introduce the 1972 AASHTO Asphalt Pavement Design Guide.

The AASHTO Guide methodology is based on using an abstract number that solved design equations called structural numbers (SNs). A SN expresses the structural capacity of the pavement structure required for given combinations of a total equivalent to 18-kip single axle loads (EASLs), soil support values, terminal serviceability indexes, and regional factors. This method is based on the pavement performance-serviceability concept developed during the AASHO Road Test. The method, which was updated in 1986 and 1993, utilizes layer coefficients (a_i values) to integrate a pavement structure using materials of varied supporting capacities. The SN combines the impacts of the layer coefficients, layer thicknesses, and drainage coefficients on the pavement structure.

The original layer coefficients were regression coefficients developed by relating layer thickness to a road performance determined on basis of the parameters of the AASHO Road Test. The development of the layer coefficients has been evolving; the most recent AASHTO Design Guide, published in 1993, stipulates that layer coefficients can vary depending on a number of factors. These factors include material type, material properties, type of layer, traffic level, and failure criterion. The principle variables are material types and material properties. Material types vary everywhere across the country and the material properties are dependent on construction practices and local environments. These conditions as well as traffic levels exhibit a wide range across the country. Therefore, the layer coefficients given in the AASHTO Design Guide are expected to be used universally, whereas different layer coefficients are expected to be developed for local conditions.

The 1993 AASHTO Design Guide recommends using the resilient modulus as the standard material quality measure to account for material types and material properties. Also, layer coefficients are still identified according to their treatment in the structural number design approach. In other words, a material with a certain resilient modulus will receive a lower layer coefficient if it is used as a base rather than a sub-base.

1.2 Problem Statement

Asphalt has advanced since the time of the original AASHO Road Test and the publication of the 1972 AASHTO Design Guide. In the 1980's, many states, including Wisconsin, started to change the specifications for Asphalt Concrete (AC) mix designs. More durable pavements were needed to support the ever-increasing traffic loads. Recently -in the 1990's- the use of reprocessed asphalt pavements as base courses has become more widely used.

Even though mix design and material types have evolved and changed, the layer coefficients for asphalt pavements have not been studied or revised to accommodate these changes in technology. Wisconsin, like many other states, does not differentiate between different types of AC surface mixes and base courses.

1.3 Research Objectives

The main objective of this research is to evaluate some of the new mixtures and materials using laboratory and field measures to determine if the layer coefficients need to be updated and differentiated for new and reprocessed materials.

To achieve this objective, the research is supposed to include actual pavement damage indicators in the calculation of the layer coefficients. During the last few years some research has suggested that using the resilient modulus alone for the calculation of a layer coefficient is not sufficient. Actual pavement damage, such as permanent deformation (rutting) and fatigue cracking, must be taken into account in order to formulate a layer coefficient that will reflect actual pavement behavior.

These goals will not only lead to updated layer coefficients, but also to the development of a more reliable method that will include pavement-rutting characteristics and other types of failure in the formulation of those layer coefficients. This approach can be used to evaluate new pavement and base course materials that are developed in the future.

1.4 Research Methodology

The methodology for this research starts with a literature review with a view to clarifying how the layer coefficients were derived, how they were calculated using resilient modulus, and how resilient modulus was determined. The literature review also sheds light on other material properties used to determine layer coefficients. The use of the Falling Weight Deflectometer (FWD) to determine resilient moduli and the concepts behind the method were also reviewed. In order to prepare for the testing in this project, the literature review was extended to include the development of tri-axial cells used to test granular materials and asphalt mixtures.

Material types were chosen to cover traditional mixture designs and two mix designs that represented more recent technologies (SHRP & SMA). Two types of recycled base courses were also included. The materials were collected from construction projects from different parts of Wisconsin.

Field measurements using the FWD were conducted at certain locations investigate how they would compare to compare with laboratory results. The laboratory results were generated using a tri-axial apparatus. Both resilient modulus and rutting tests were performed on all materials. Due to time and equipment limitations, fatigue cracking was not considered in this research plan.

Field data was processed using backcalculation techniques to determine resilient moduli. The laboratory resilient modulus data was analyzed using parameters developed for the testing of granular materials. The rutting data was analyzed by comparing cumulative strains to number of load repetitions. The field data was compared to laboratory data to validate the laboratory results. Finally, recommendations for future analysis, possible test method improvements, and suggestions for future research are presented.

1.5 Research Scope

To investigate the possibility of an improved method for estimating layer coefficients and possible relations between rutting and layer coefficients, several materials were tested using both field and laboratory methods. Field measurements were conducted with the use of the FWD. For certain sections each layer of the pavements was tested as they were being constructed. Materials from all the sites where field-testing took place were collected for laboratory testing.

Table 1.1 shows the material types and the projects from which they were gathered. The granular materials varied in terms of which type of machine recycled the existing asphalt pavement and how much outside aggregate was added into the recycled asphalt pavement material. The asphalt materials varied in terms of whether they were a base course or a surface course. They also varied with respect to their gradations, amount of asphalt used, and the asphalt binder type.

Table 1.1 Layer Coefficient Material and Project Table

Layer Coefficient Study				
Material Type	Project ID	Project Dates	Sample Pickup	FWD Testing
Asphalt Layers				
SMA	1028-05-77	Mid May - Mid June	6/12/97	None Scheduled
HV-2	1059-16-73	May - Mid July	7/2/97	Base 6/30/97
MV-2	1059-16-73	May - Mid July	7/11/97	Base 7/10/97 MV 9/24/97
SHRP	1059-16-73	Mid July - Oct	10/3/97	Base 9/10/97 SHRP 10/17/97
Base Layers				
Asphalt Base Coarse	1059-16-73	Mid July - Sept	10/9/97	Subgrade 9/10/97 Subbase 10/3/97 Base 10/10/97 HV 10/17/97
Pulverize	1581-12-70	Aug	8/14/97	Pre 8/13/97 Pul 8/15/97 MV 10/20/97
Mill and Relay	1644-01-71	End July - End Sept	9/8/97	None Scheduled

All laboratory results were obtained with the use of the tri-axial testing apparatus. The recycled granular materials were tested in wet and dry conditions for resilient modulus and under varying load

conditions for rutting. The asphalt materials were tested at 52°C and 64°C for resilient modulus and under varying load conditions for rutting.

The scope of the analysis in this report is limited to the analysis of the data collected from the above-mentioned field and laboratory tests. The first part covers the resilient modulus testing and the comparison between field and laboratory data. The second part covers the rutting results and how these can be formulated into damage functions.

1.6 Summary

This report is divided into seven chapters. The first chapter provides an introduction, objectives, methodology, scope, and summary of the research. In chapter 2, a literature review investigating the background of layer coefficients, resilient modulus, FWD methods, permanent deformation damage functions, and tri-axial test apparatus is presented. Chapter 3 describes both the field and laboratory data collection methods, including how the laboratory specimens were manufactured. Field data results and analyses are presented in Chapter 4. The laboratory results and analyses are discussed in the following chapter. Finally, the research findings and future recommendations are summarized in Chapter 6.

CHAPTER TWO

LITERATURE REVIEW

2.1 Introduction

The AASHO Road Test was developed in the late 1950's to provide information that could be used to develop pavement design criteria and procedures. When completed, the road test directly lead to the 1961 AASHO Interim Guide for the Design of Rigid and Flexible Pavements. This guide was modified in the following decade and published in 1972 as the AASHTO Interim Guide for Design of Pavement Structures – 1972. After that, major revisions to the guide were completed in 1986 and 1993.

The guide uses the concept of layer coefficients for asphalt pavements; these coefficients are based on research conducted on a number of pavement and material properties. The coefficients are indicators of the relative ability of a material to function as a structural component within the asphalt pavement.

According to the AASHTO 1986 Guide the resilient modulus of a material is the primary means of determining the layer coefficient of that material. However, there have been investigations that involved other material properties to determine layer coefficients. Over the past few years, some people have come to the conclusion that resilient modulus and strength are not enough to effectively gauge a material's behavior in a pavement structure. The literature review considers efforts put forth by researchers to model permanent deformation in asphalt pavements.

Finally, types of tri-axial cells developed by different researchers are reviewed in an effort to learn from their experiences. The tri-axial cell was the critical part of the entire laboratory testing. Therefore, an understanding of how this type of apparatus is set up was crucial.

2.2 Literature Review

2.2.1 Layer Coefficients

2.2.1.1 Background of AASHTO Layer Coefficients

The solution to the design equations in the different versions of the AASHTO pavement design

guide is in terms of a structural number (SN). The structural number is an abstract number expressing the structural strength of pavement required for a given combination of soil support value, total equivalent 18-kip (80 kN), single axle loads (ESALs), terminal serviceability index, and regional factor. The magnitude of the *SN* reflects the degree to which the sub-grade must be protected from the effects of traffic. The AASHTO Guide for the Design of Pavement Structures, based on the pavement performance-serviceability concept developed from the AASHO Road Test, utilized the concept of "layer coefficients" (a_i values) to synthesize a pavement structure employing materials of varied supporting capacities.

A value for this coefficient is assigned to each layer material in the pavement structure in order to convert actual layer thickness into structural numbers (SN). This layer coefficient expresses the empirical relationship between SN and thickness; it is a measure of the relative ability of the material to function as a structural component of the asphalt pavement.

The following general equation for the structural number reflects the relative impact of the layer coefficients (a_i), thickness (D_i), and the drainage coefficients (m_i) on the structural number:

$$SN = a_1 D_1 + a_2 D_2 m_2 + a_3 D_3 m_3 + ... + a_i D_i m_i \quad (1)$$

The AASHTO guide proposed numerical values for the structural layer coefficient of materials, a-values, which were originally regression coefficients that resulted from relating layer thickness to road performance under the conditions of the road test.

According to the most recent AASHTO guide (1993), the *a*-value can vary considerably depending upon a number of factors. These involve:

1. layer thickness
2. material type
3. material properties
4. layer location (base, sub-base)
5. traffic level
6. failure criterion

Material type and properties are the principle variables that affect the layer coefficient. In addition, material properties are dependent on environment and construction practices. Because of the wide variations in environments, traffic, and construction practices, the proposed *a*-values in the AASHTO

guide are not expected to apply to all cases. As a result, different *a*-values should be determined based on local conditions.

To account for material type and properties in the 1993 AASHTO guide, the elastic (resilient) modulus (M_r) is used as the standard material quality measure. It is still necessary to identify the corresponding layer coefficients because of their treatment in the SN design approach. For example, a granular material with a certain modulus will get a lower layer coefficient if used as a base course material than if used as a sub-base.

The relationship between the layer coefficients and the resilient modulus has been investigated in several research efforts. The layer coefficient does not only reflect the stress distribution in the layer, but is also an index of the strength of the material. The position of the material in the structure and the mode of distress may, therefore, influence the relation between the layer coefficient and the resilient modulus.

Other investigators have used another parameter, the layer thickness equivalency, mainly for the purpose of evaluating the support capacity of a given material compared to standard or commonly used materials. The layer thickness equivalency is determined as the thickness of the material in question required to replace 25 mm (1 inch) of the standard material (Mustaque et al. 1997).

Most of the methods used to evaluate either the layer coefficient or the layer thickness equivalency are based on the evaluation of limiting criteria at specific points in the pavement structure. To establish layer coefficients for the 1986 version of the AASHTO guide under various conditions and materials, three criteria based on the mechanistic response to loads were evaluated:

1. surface deflection,
2. tensile strain in the asphalt layer, and
3. vertical compressive strain on the roadbed soil.

To establish the relationship between the layer coefficient and the resilient modulus, a range of surface thicknesses (D_1) and base thicknesses (D_2) were used to calculate deflection, tensile strain, and vertical compressive strain. The results were used to evaluate the required increase in base thickness for a decrease in surface thickness while holding the deflection or strain level constant.

Layer coefficient values for different layers made of different materials can be determined using empirical equations derived from field experiments. The following equations are some of the commonly used relationships (Mustaque et al. 1997):

Asphalt concrete:

$$a_1 = 0.4 \times \log\left(\frac{E}{3000\ MPa}\right) + 0.44 \qquad 0.20 < a_1 < 0.44 \qquad (2)$$

Bituminous-treated Base:

$$a_2 = 0.3 * \log\left(\frac{E}{3000 MPa}\right) + 0.15 \qquad 0.1 < a_2 < 0.3 \qquad (3)$$

Granular Subbase:

$$a_3 = 0.23 * \log\left(\frac{E}{160 MPa}\right) + 0.15 \qquad 0.06 < a_3 < 0.2 \qquad (4)$$

In the AASHTO design procedure a number of relationships have been derived using layered elastic theory to evaluate a combination of pavement cross-sections and material properties. In addition to the following relationships, charts for estimation were developed for other materials:

Granular Base:

$a_2 = 0.249 \log E2 - 0.977$ (4a)

Granular Subbase:

$a_3 = 0.227 \log E3 - 0.839$ (4b)

Where a_i values are the layer coefficients and the E_i values are the resilient modulus values.

The relationship between layer coefficients and resilient moduli is generally based on layered elastic theory. Layer coefficients are affected by more factors than just material stiffness and strength, which is

why these empirical relationships are derived. Appendix G in the 1993 AASHTO guide provides values for a_1 as a function of the properties of the selected materials.

2.2.1.2 Structural Layer Coefficients as Determined by Different Departments of Transportation in the U.S.

2.2.1.2.1 NCHRP Report No. 128

As part of the National Cooperative Highway Research Program (NCHRP) project (McCullough 1972) a survey of state highway agencies was conducted to collect information regarding the layer coefficients to be used in the AASHTO design method. Table 2.1 summarizes the results of that survey. For a given layer, it appears that in most cases values for the layer coefficient have been associated only with a material description.

The Asphalt Institute also conducted a study to develop layer coefficients for asphalt layers.On the basis of that research, it was concluded that the structural components (surfacing, base, and sub-base) could be treated as linear combinations of equivalent thicknesses of each layer. That is:

$$D = a_1D_1 + a_2D_2 + a_3D_3. \quad (5)$$

The Asphalt Institute method for determining equivalency factors was based on the AASHTO Road Test survey of prior performance, together with theoretical considerations. The AASHTO Road Test Report 61-E included a development of structural coefficients based on Performance Serviceability Index, cracking, and deflection. Three separate multiple linear regression analyses were performed on the AASHTO road test data. On the basis of the analysis presented in the report, it was concluded that asphalt concrete can be 2 to 6 times more effective than good crushed stone.

Table 2.1 The Results of the 1972 AASHTO Survey of Layer Coefficients

SUMMARY OF STRUCTURAL COEFFICIENTS USED FOR DIFFERENT PAVEMENT COMPONENTS								
COMPONENT	ALABAMA	ARIZONA	DELAWARE	MASSA-CHUSETTS	MINNESOTA	MONTANA	NEVADA	NEW HAMPSHIRE
SURFACE COURSES								
Plant mix (high stab)	0.44	0.35-0.44	0.35-0.40	0.44	0.315	0.30-0.40	.030-.035	0.38
Road mix (low stab)	0.20	0.25-0.38				0.20	0.17-0.25	0.20
Sand Asphalt	0.40	0.25			Plant mix (low stab) 0.28			0.20
BASE COURSES								
Untreated	limestone 0.14	well graded sand&gravel 0.14	Waterbound Macadam 0.20	crushed stone 0.14	crushed rock (Cl. 5 & 6) 0.14	selected surfacing 0.10	crushed gravel 0.10-0.12	crushed gravel 0.10
	sandstone 0.13	sandy gravel, mostly sand 0.11-0.13	crusher run 0.14		sandy gravel 0.07	crushed gravel 0.12-0.14	crushed rock 0.13-0.16	bank run gravel 0.07
	granite 0.12	cinders 0.12-0.14	quarry waste 0.11					crushed stone 0.14
	slag 0.14		select borrow 0.08					
Cement Treated	> 650 psi 0.23	> 500 psi 0.25-0.30	soil-cement 0.20			> 400 psi 0.20		gravel 0.17
	400-650 psi 0.20	300-500 psi 0.18-0.25						
	< 400 psi 0.15	< 300 psi 0.15				< 400 psi 0.15		
Lime Treated						0.15-0.20		
Bituminous Treated	Coarse graded 0.30	sand-gravel 0.25-0.34	asph. stab. 0.10	black base 0.34	All 0.175-0.21	plant mix 0.30	plant mix 0.25-0.34	bit. conc. 0.34
	sand 0.25	sand 0.20		penetrated crushed stone .029		bit. stab. 0.20		gravel 0.24
SUBBASE COURSES								
	sand & sandy clay 0.11	well graded sand&gravel 0.14		select material 0.08	sandy gravel (Cl. 3 & 4) 0.105	special borrow borrow 0.07	select material 0.05-0.09	sand-gravel 0.05
	sand & silty clay 0.05	sand & silty clay 0.05-0.10			selected granular* 0.07	sand 0.05	gravel type 1 0.09-0.11	
	float gravel 0.09	cr. stone or cinders 0.12		gravel 0.11				
	chert low PI 0.10							
	top soil 0.09							

* 12% minus 0.075mm

Table 2.1 The results of the 1972 AASHTO Survey of Layer Coefficients-Continued

SUMMARY OF STRUCTURAL COEFFICIENTS USED FOR DIFFERENT PAVEMENT COMPONENTS								
COMPONENT	NEW MEXICO	OHIO	PENNSYL-VANIA	SOUTH CAROLINA	SOUTH DAKOTA	UTAH	WISCONSIN	WYOMING
SURFACE COURSES								
Plant mix (high stab)	0.30-0.45	0.40	0.44	0.40	0.36-0.42	0.40	0.44	0.30-0.40
Road mix (low stab)	0.20	AC Interim	0.20			0.20	0.20	
Sand Asphalt			0.35	AC Binder 0.35			0.40	
Plant Mix Seal	0.25					0.40		
BASE COURSES								
Untreated	quarry rock 0.10-0.15	aggregate 0.14	crushed stone 0.14	crushed rock 0.14		all untreated 0.12	crushed gravel 0.10	all untreated 0.05-0.12
	crushed rock 0.06-0.12	waterbound macadam 0.14	dense graded 0.18				waterbound macadam 0.15-0.20	
							sand-gravel 0.07	
Cement Treated								
650 psi or more	0.23		cement aggr. plant mix 0.30				0.23	all types 0.15-0.25
400 to 650 psi	0.17		soil cement 0.20			0.20	0.20	
400 psi or less	0.12						0.15	
Lime Treated	0.05-0.10		soil-lime 0.20		0.15		0.15-0.30	0.07-0.12
Bituminous Treated	plant mix 0.30		soil bit. 0.20	black base 0.30	hot mix 0.30	coarse graded 0.30	coarse graded 0.34	plant mix 0.20-0.30
	road mix 0.15		plant mix 0.30	sand 0.25	coarse sand 0.24		sand 0.30	emulsion 0.12-0.20
					fine sand 0.18		coarse H.M. 0.23	
					cold mix: coarse 0.14 fine 0.10			
SUBBASE	aggregate 0.06-0.12	0.11	sand-gravel 0.11		sand-silty clay 0.07	sand & gravel 0.10	sand gravel 0.11	special borrow & subbase 0.05-0.12
	borrow 0.05-0.10				3% lime 0.06 over 3% lime 0.05	sand or sandy clay 0.06-0.10		

Notes:

1. Indiana, Iowa, Montana, New Jersey, Tennessee, and Puerto Rico -- conform to AASHTO Guides
2. North Carolina -- conforms to AASHTO Guides, except 0.30 for Bituminous Treated Base
3. North Dakota -- conforms to AASHTO Guides, except 0.30 for Bituminous Aggregate Base
4. Maine -- conforms to AASHTO Guides with some modification. No further information
5. Maryland -- substitution values for materials to replace design thickness of asphalt hot-mix are the AASHTO structural coefficients expressed in equivalent values, in inches

It was found that 25.4 mm (1 in) of high-quality asphalt concrete surfacing would be equivalent to 50.8 mm (2 in) to 76.2 mm (3 in) of good dense-graded, crushed-stone base, and that 25.4 mm (1 in) of asphalt concrete base would be approximately equivalent to 50.8 mm (2 in) of such crushed stone. The Asphalt Institute decided on an equivalency factor of at least 2 to 1 for asphalt concrete surface or base to aggregate base and 2.67 to 1 for asphalt concrete surface or base to aggregate sub-base.

2.2.1.2.2 1997 Survey of Midwestern States

As part of the literature review for this project, a survey of State Departments of Transportation (DOT's) in the Midwest area was conducted. The survey focused on design methods and layer coefficients used in the design procedure. The states included were: Illinois, Indiana, Iowa, Kansas, Kentucky, Michigan, Minnesota, Missouri, Nebraska, North Dakota, Ohio, and South Dakota. Responses were received from all states that were contacted.

The results from the states varied depending on the research and layer coefficients involved. However, all of the states contacted used one form or another of the AASHTO design method. Illinois and Kentucky have switched to mechanistic design methods. These are methods that do not depend on any observed performance characteristics; they rely solely on design theory. Appendix A shows a summary of the contacts from the states and the design method that they use. It also shows the layer coefficients used by each state. There is a wide variation in how many layer coefficients they assign and how they identify materials. Most of the states, however, use a layer coefficient for AC of 0.4 or 0.44.

2.2.1.3 Using Probabilistic Fatigue Model to Determine Layer Coefficients

A new method for determining the layer coefficient of flexible pavement materials, using a pavement model, was developed by George (1984). According to this method, the material properties associated with the layer coefficient are:

1. Elastic constants (resilient modulus and Poisson's ratio), and
2. Fatigue susceptibility expressed in the ε-N diagram.

Layer coefficients of several pavement materials used widely in the State of Mississippi (asphalt concrete, soil-cement, and soil-lime) were developed in this research. The task of developing layer

coefficients was accomplished in two steps. The first step was to relate fatigue performance of asphalt mixes to the structural numbers based on a large database. The relationship (model) also included load, temperature, and sub-grade support values as independent variables. In the second step, this model was used to establish an "equivalence" between pavement materials and layer coefficients.

The primary purpose of the model is to predict the load applications that the pavement/sub-grade system can withstand and still provide minimum acceptable serviceability. Although the authors recognized that the three specific distress modes commonly considered in evaluating pavement performance are fatigue cracking, permanent deformation (rutting), and low-temperature cracking, they cite previous research which concluded that the most prevalent type of pavement distress in the United States is fatigue cracking.

The layer coefficient calculation using this model is based on the premise that it is possible to establish what is known as "thickness equivalency" between layers. The layer coefficient of soil-cement base, for example, is computed by comparing its fatigue life with that of the asphalt base.

2.2.1.4 Using Material Properties to Determine Layer Coefficients

Highway and materials engineers have investigated the relationships between layer coefficients and a wide variety of material characteristics. This section provides a summary of the main types of material properties that have been associated to layer coefficients.

2.2.1.4.1 Resilient Modulus

Many researchers have studied the nonlinear stress-strain characteristics of sub-grade soils. Pavement engineers have taken the stress-strain models developed by this research and applied them to asphalt layers. Regarding pavement analysis and research, these models `proved to be a powerful and more realistic representation of material performance than conventional tests, such as the California Bearing Ratio (CBR). However, these stress or deformation analyses are useless without a corrective equation that relates the asphalt behavior to the behavior of the soil used to develop the models.

Every time a load passes over a pavement structure, the pavement deflects and then recovers a portion of the original deflection. After many cycles of repeated loading and unloading, the layers begin to accumulate small amounts of permanent deformation, but most of the deflections are recovered. The

recovered deflections are termed resilient deformations. The resilient modulus (M_R), which was developed to explain this behavior, can be defined as:

$$M_R = \frac{\sigma_d}{\varepsilon_R} \quad (6)$$

where

M_R = resilient modulus

σ_d = repeated deviator stress (σ_1 - σ_3)

ε_R = recoverable axial strain in the direction of the principal stress σ_1

Many research studies have been conducted to investigate the sensitivity of various factors affecting resilient modulus. These factors include material type, sample preparation method, stress state, the strain sensitivity of the material, and the condition of the samples (George & Uddin, 1994). Chen and his co-researchers (1995) discussed the factors affecting the measurement of M_R.

The procedure for determining M_R has not yet been standardized. However, guidelines are given in several AASHTO test methods (T274-82, T292-91I, and T294-92I). Different testing procedures may result in different M_R values ; hence, differences in the design of the pavement. Therefore, it is very important to investigate the effects of pertinent factors on M_R and the variability of M_R values due to different testing procedures. Although both the 1986 and 1993 AASHTO pavement design guides emphasize the use of M_R as a basis for material characterization, the procedures recommend the use of a correlation between the modulus and the structure layer coefficients.

The results of several tests performed by the authors indicate that the greatest range of differences between backcalculated and laboratory-determined moduli are for the asphalt concrete layers, followed by the base and subgrade materials. They explained that these large differences between backcalculated and laboratory AC moduli are a result of the existing cracks in the pavement system.

The K-θ model, which is most commonly used in pavement design, reflects the stress dependency behavior of granular materials. It is recommended for describing the nonlinear characteristics of noncohesive or granular materials. The model is as follows:

$$M_R = K_1 \theta^{K_2} \quad (7)$$

where

K_1 and K_2 = material constants, and

θ = bulk stress

While this model is good for representing the measured shear strain for calculating the elastic stiffness, it may provide a very poor prediction of volumetric strain. Uzan (1985) suggested an improved M_R model that included the effect of shear stress. The new model is as follows:

$$M_R = K_3 \theta^{K_4} \sigma_d^{K_5} \quad (8)$$

where

K_3, K_4, and K_5 are material constants evaluated by a multiple regression analysis from a set of repeated load M_R tests and σ_d is the deviator stress.

Witczak and Uzan (1988) suggested replacing the deviator stress σ_d with the octahedral shear stress (τ_{oct}) as shown in the following equation. The bulk stress (θ) and the octahedral shear stress were normalized using atmospheric pressure (P_a).

$$M_R = K_6 P_a \left[\frac{\theta}{P_a} \right]^{K_7} \left[\frac{\tau_{oct}}{P_a} \right]^{K_8} \quad (9)$$

where K_6, K_7, and K_8 are the material constants. The variable τ_{oct} is given by:

$$\tau_{oct} = \frac{1}{9} \left[(\sigma_1 - \sigma_2)^2 + (\sigma_2 - \sigma_3)^2 + (\sigma_3 - \sigma_1)^2 \right] \quad (10)$$

For tests performed under isotropic confining pressure, Eq. 11 can be simplified by using the relationships $\sigma_2 = \sigma_3$ and $\sigma_1 - \sigma_3 = \sigma_d$.

$$\tau_{oct} = \frac{\sqrt{2}}{3} \sigma_d \quad (11)$$

Some design methods use the typical stiffness values for granular materials ignoring the stress-dependent aspect of behavior. The values are generally in the range of 100 to 300 MPa depending on

the aggregate type and its moisture condition (the moisture condition is dependent on the time of the year). Chen et al. (1995) suggested two relationships between K_1 and K_2 based on different test procedures. They are as follows:

$$\log K_1 = 4.7308 - 2.5179\, K_2 \text{, from T294-92I, and} \qquad (12)$$

$$\log K_1 = 4.19 - 1.7304\, K_2 \text{, from T292-91I.} \qquad (13)$$

Rada and Witczak (1981) investigated the feasibility of developing predictive M_R equations from physical properties of granular materials. They tried to develop a comprehensive evaluation of factors that affect the M_R response of granular materials. They analyzed six different aggregate types, for each of which three hand-blended gradations were used. On each aggregate-gradation combination, three compaction energies were used to develop moisture-density relations. The combined number of individual granular material results used in the report was 271. The results of the research show that there exist a relationship between the M_R and the physical properties of the granular materials do exist.

Rada and Witczak (1981) found that each class of aggregates has its relatively unique K_1-K_2 relation that distinguishes it from the other groups. In addition, the overall mean values for all granular materials is K_1=9240 and K_2=0.52. The largest variation of K_1 and K_2 is observed for the crushed stone group, which has a range of K_1 values from 1700 to 57,000 ; the mean is found to be K_1=7210 and K_2=0.45. The influence of the degree of saturation appears to be dependent on the aggregate type. The semilogarithmic relationship between K_1 and K_2 that they proposed is:

$$\log K_1 = 4.66 - 1.81\, K_2 \qquad (14)$$

This relationship is similar to the relationship proposed by Chen et al. (1995).

Studies performed prior to the Rada and Witczak's research indicate that the degree of saturation (for a given aggregate) plays a major role in the M_R response. It was found that the values of the modulus and the K_1 reduce with increased saturation. Although the influence of the saturation on K_2 for the different types of aggregates is not that large, there are recognizable trends in K_2 as opposed to saturation plots. However, there is no uniform trend among all the aggregates. In contrast, the influence of saturation on K_1 is significant.

Several research studies have indicated the effects of density on the M_R response of granular material. Rada and Witczak (1981) confirm the previous conclusions that an increase in density does cause an increase in the M_R, though this effect is relatively smaller compared with changes caused by stress level and moisture.

There is also reference to the influence of fines (percentage that passes no. 200 sieve) on the M_R response. In general, the degree of influence of this parameter appears to be related to the aggregate that has been investigated. There is no general or uniform trend applicable to all aggregate types. The relative sensitivity in the case of the sand-gravel material is more pronounced than in the case of the crushed, angular aggregate. Increasing the P_{200} beyond the 16-18 percent range would eventually have pronounced changes in the M_R response to these materials.

The major input variables are bulk stress (θ), degree of saturation (S_r), and percentage compaction relative to modified compaction effort (*PC*). Based on the results of their research, predictive equations were investigated to develop accurate M_R predictions from the significant variables.

2.2.1.4.2 Dynamic Shear Modulus

George and Uddin (1994) used strain sensitive models for the evaluation of dynamic shear modulus, G. The important findings in their paper include:

a. Shear modulus, *G*, is a function of shear strain amplitude.

b. At very low shear strain amplitude (below 10^{-3} percent), the dynamic shear modulus is strain independent and is typically referred to as G_{max} (maximum dynamic shear modulus). Moduli associated with higher strain amplitude are strain-sensitive.

c. Dynamic shear modulus attenuation curves show identical trends in non-dimensional plots of G/G_{max} (normalized shear modulus) versus shear strains.

d. For high strain amplitudes in the range of 10^{-3} to 10^{-1} percent, clay, sands and gravely soils exhibit strain softening.

e. If G_{max} is known, then the *G* associated with any higher shear strain amplitude can be determined using the appropriate normalized shear modulus versus shear strain curve. G_{max} can be obtained in the field with seismic tests.

2.2.1.4.3 California Bearing Ratio (CBR)

Rohde (1994) carried out a detailed study on 52 in-service pavement structures in order to cover a wide range of pavements. Four methods were used to calculate the structural number from the collected information:

1. Backcalculated Moduli: This method used two backcalculation programs that involve the mechanistic analysis of measured deflections. The layer moduli were translated to layer coefficients. Along with the recorded layer thicknesses, they were used to determine the structural number.
2. Dynamic Cone Penetration (DCP). This method involves the analysis of the DCP results. First, the *CBR* is calculated by using the DCP penetration rate through each granular pavement layer and by employing the following relationships:

$$\begin{aligned} CBR &= 410 \log DN^{-1.27} \qquad (DN > 2 \quad mm/blow) \\ CBR &= 66.66\, DN^2 - 330\, DN + 563 \qquad (DN \le 2 \quad mm/blow) \end{aligned} \tag{15}$$

where

CBR is the *in situ* California Bearing Ratio and *DN* is the penetration rate of DCP (mm/blow).

The *CBR* values were translated into layer coefficients using the following relationship:

$$a_i = 29.14\, CBR - 0.1977\, CBR^2 + 0.00645\, CBR^3 \tag{16}$$

where

a_i is the layer coefficient. For the surface layers, a coefficient was assumed based on visual conditions.

3. Surface Deflection: This method only involves the surface deflection. Outer sensors were used to determine the subgrade stiffness.
4. Surface Deflection and Total Layer Thickness: For each pavement section, the Structural Index of Pavement (SIP) parameter is determined. Then, by incorporating the layer thickness, H_p, the structural number is determined.

Rohde (1994) suggested obtaining seasonal variations in the structural number by measuring the deflections in various seasons and applying the above techniques.

In addition, another relationship between M_R, θ, and *CBR* was suggested by Chen et al. (1995):

$$M_R = (490 \cdot \log\theta - 243)CBR \qquad (17)$$

Because the M_R test result is stress-dependent, the coefficient that relates M_R to *CBR* must be stress dependent and not a unique or constant value.

Ping et al. (1996) conducted a study for the Florida Department of Transportation. This research tried to correlate limerock bearing ratio (*LBR,* a Florida modification of the *CBR*) test results to the AASHTO pavement design procedure. Twenty existing pavement sites were selected for the field plate bearing load test (the *LBR* test). Laboratory samples were also prepared to cover the entire range of desired moisture contents. In addition, selected laboratory compacted specimens were placed in a soaking tank for approximately 2 days.

The *LBR* test results were compared with the optimum moisture content and the maximum dry density values. The data were too scattered to infer suitable relationships between the optimum moisture content and *LBR* values. However, the general trend for the density and *LBR* relationship is that the *LBR* value augments as the density increases. This indicates that the *LBR* is more sensitive to density than to the moisture content. The moisture content at the maximum dry density is generally the same as the moisture content at the maximum *LBR*.

In general, the average moisture content obtained in the laboratory at the maximum *LBR* values for all soils was not significantly different from the measured field moisture content. The maximum dry densities compacted in the laboratory were also close to the average in situ-measured field densities. However, the data were very scattered. Comparisons between the laboratory *LBR* results and the field layer modulus were made and a general trend was observed. Although the data were scattered, there is a slight increase in field layer modulus as *LBR* increases.

The *LBR* value was used as a correlation for soil support value (*SSV*) for the design of pavements in Florida. Ping et al. (1996) identify two types of correlation :

$$SSV(1) = 4.596 \cdot \log(LBR) - 0.576 \qquad and$$
$$SSV(2) = 3.325 \cdot \log(LBR) + 0.672 \qquad (18)$$

In addition, a correlation between the field resilient modulus and *SSV* is identified:

$$SSV(3) = 6.24 \cdot \log(E_R) - 18.72 \quad (19)$$

Correlations between the SSV results were also made. It is apparent that *SSV(1)* is higher than *SSV(2)*. The values for *SSV(3),* calculated from the field plate modulus, are much greater than those for both *SSV(1)* and *SSV(2)*. This means that the *SSV* obtained by correlating the field layer modulus is greater than that obtained by correlating the laboratory *LBR* value. The difference between *SSV(3)* and *SSV(1)* or *SSV(2)* may be due to the fact that *LBR* is a laboratory value that occurs at the optimum moisture content and maximum density, whereas the field plate modulus (E_R) is a field strength value that is affected by many uncertain factors such as stress history of the pavement and the percentage of large aggregates. *SSV(1)* predicts a modulus that is closer to the field modulus, *SSV(3),* than the existing Florida design equation (*SSV(2)*); however, the field *SSV(3)* is generally higher than the laboratory *SSV(1)*. This is due to the major difference between the field and laboratory testing conditions.

2.2.1.4.4 Elastic Modulus of Base Layer

The use of the resilient modulus was extended by the 1986 AASHTO guide to be the predictor of the base layer coefficient (a_2). The following equation could be used to determine the layer coefficients for a granular material from its elastic modulus (E_{BS}):

$$a_2 = 0.249 \cdot \left(\log_{10} E_{BS}\right) - 0.977 \quad (20)$$

Richardson (1996) determined layer coefficients for cement-stabilized soil for use in the AASHTO pavement design method. Two types of soils were examined: fine sand and silty clay. These were blended with three different amounts of concrete sand. Three different cement contents were molded and tested for static compressive chord modulus and unconfined compressive strength.

The methodology consisted in determining the moduli of the various materials and then converting these moduli to layer coefficients. Layer coefficients were determined by using the modulus values from the AASHTO pavement design guide nomograph. Regression equations based on strength, dry unit weight, and cement content were developed to allow an for estimation of layer coefficients.

The best-fit equation for the data obtained is as follows:

$$E_c = 915.48 + 1314.9\, q_u \quad (21)$$

where

E_c = chord modulus (MPa), and

q_u = unconfined compressive strength.

A multiple regression model was fit to the obtained data. The best-fit model is as follows:

$$E_c = 17759 + 579.77(C) + 9.6113(\gamma_d) \quad (22)$$

where

E_c = chord modulus (MPa),

C = cement content (% by weight), and

γ_d = dry unit weight (kg/m^3).

Layer coefficients were determined by use of the AASHTO nomograph. The equation for the relationship between a_2 and the modulus was derived from the nomograph:

$$a_2 = -2.7170 + 0.49711 \log E_c \quad (23)$$

where E_c = elastic modulus (psi).

Substitution of the elastic moduli for the previous equation resulted in the layer coefficients. The layer coefficient values ranged from 0.09 to 0.27, depending on the clay content, dry unit weight, and cement content. Increasing the cement content and dry unit weight increased the layer coefficient, whereas increasing the clay content lowered the layer coefficient.

A sensitivity analysis was performed by examining the effects of certain mixture variables (cement and sand content) on the required thickness. It was found that all changes in cement content and sand content are significant.

2.2.1.5 Wisconsin Department of Transportation

During the late 1980's WisDOT began to rewrite the asphaltic specifications for mixture designs to meet the demand for more durable asphaltic pavements that would accommodate the increased traffic loading. During the 1990's the reprocessing of asphaltic pavements into base course materials became more prevalent.

Wisconsin's flexible pavement design process, contained in the WisDOT Facilities Development Manual (FDM), is based on the AASHTO design method. A structural number is used without the

drainage coefficients. The FDM refers to the layer coefficients as strength coefficients. These are listed in Table 2, page 33. The FDM specifies that the strength coefficients are not absolute in the sense that they represent a minimum strength value that can be expected throughout the state. Some of the materials, such as Milled and Relayed Asphaltic Concrete, have a range of layer coefficients caused by variable strength and stability. The FDM also provides a table titled "Relative Strength Coefficients for Granular Subbase", which supplies a strength coefficient based on % passing #40 sieve. The FDM states that when recycled materials are used, the strength coefficients can be expected to be similar to those of virgin materials.

The FDM limits to 10% the portion of strength a that granular sub-ase will contribute to the total pavement structure. This takes place regardless of the strength coefficient or thickness involved. This will ensure that the surface and base thicknesses used in the pavement structure are adequate and have a built-in factor of safety.

In 1990, WisDOT published a report on layer coefficients for flexible pavements. The purpose of the study, entitled "Layer Coefficients for Flexible Pavements," was to evaluate new materials that are used in flexible pavements. The goals were to establish AASHTO layer coefficients for use in the design, establish a procedure that would allow for the determination of these coefficients, and provide input for the new 1986 AASHTO design procedure. The study was to establish layer coefficients for new materials being used and to evaluate the ones used at that time. The study also intended to develop a method of determining layer coefficients for the new materials and provide inputs for the 1986 AASHTO Design Guide. That study included both field and laboratory testing of typical asphalt mixes and base course materials. It consisted in a comparison between the AASHTO empirical approach, as revised in the 1986 manual, and mechanistic analysis and design procedures.

Field-testing was conducted on several different pavements, including bases, subbases, recycled asphalt concrete mixtures, and crack and seated overlays. The test sites varied in age from 1 to 9 years. Field cores were taken as well as sample pits to determine laboratory determinations of layer coefficients. Seasonal variations were investigated as well. Weaker pavement structures were found in spring, with the subgrade as the culprit. The base materials were weaker in the fall, with this being exaggerated if a subbase was present.

The study provided recommendations to use one layer coefficient for virgin asphalt mixes and another for recycled mixes. The study did not address the specific type of mixes currently used by WisDOT. Another important finding of that study was the need to relate layer coefficients to pavement performance based on measuring load-induced material damage. The study also indicated that the principle of the "weakest season" must be examined for individual materials. The researchers of the study indicated that reliance on resilient modulus alone was tenuous at best. They suggested developing rutting tests for asphalt layers and shear strength tests for granular materials to represent a parameter that relates to performance. They found seasonal variations during the course of their testing and suggested that these weakest seasons be taken into account. Finally, they recommended that a mechanistic design approach be developed. They believed that this would provide a more in-depth evaluation of material properties and their effects on pavement life.

Asphalt concrete layer coefficients were not changed and it was recommended that recycled asphalt concrete be given the same layer coefficient as virgin material. Granular bases were given values of 0.10, 0.14, and 0.16 for low, medium and high quality respectively. Open graded bases received a layer coefficient of 0.12. A single value layer coefficient for crack and seated pavements were not developed due to the randomness or the amount of cracks imparted on the concrete. It was suggested in the study that the layer coefficient for cracked and seated pavement be reduced by 15 to 20% from the layer coefficients published at the time of the study.

2.2.2 Background to Field Measurements

The need for non-destructive methods to measure *in situ* material properties has resulted in developing several methods. These methods can generally measure the total response of pavement layers to loading or the transfer speed of loading waves in pavement layers. One of the most commonly used methods is the Falling Weight Deflectometer (FWD).

2.2.2.1 The Falling Weight Deflectometer (FWD)

Applying a load to the pavement surface and measuring the resulting deflection can assess the structural integrity of pavements. The FWD is one of the widely used deflection-based equipment in pavement evaluation due to its ability to best simulate the dynamic moving wheel load at a wide range of

load levels. The FWD theory, field-testing procedures, analysis methods, and application in pavement engineering are presented in this section.

The FWD equipment tests the pavement by dropping a weight from a specified height, which corresponds to the load being simulated onto the pavement surface. Upon impact, several sensors located at various radial distances from the loading center measure pavement deflections. The FWD test is relatively quick, inexpensive, and closely simulates the deflection caused by a moving wheel load; therefore, it has been widely used throughout the world in both academic research and industrial practice (Houston et al. 1990).

Surface deflections constitute a bowl-shaped depression known as a deflection basin. The size, depth, and shape of the deflection basin are a function of several variables, including the applied load, the thickness, stiffness, and Poisson's ratio, as well as other properties of the pavement structure (Huang, 1993). Numerous backcalculation techniques have been developed to analyze deflection data obtained from various types of pavement deflection equipment. Empirical correlations, such as deflection parameters, which combine some or all of the measured deflections into a single value, are often used to show the reciprocal relation between pavement properties. Horak (1987) provided a summary of deflection parameters. Unfortunately, except for the subgrade layer, using these indices to predict the properties of pavement structures is limited. Therefore, the use of deflections as a direct measure of the pavement structural capacity should be avoided and a mechanistic analysis of the deflections is recommended instead (FHWA, 1994).

Numerous studies have utilized FWD for the purpose of pavement evaluation and material characterization. Two volumes of special technical reports from the American Society for Testing and Materials (1989, 1994) are representative documents summarizing the development and application of the FWD test. In this report, examples are presented from a previous research project, also sponsored by WisDOT, that used FWD as one of the techniques to investigate the effect of freeze-thaw action on pavement performance (Bosscher et al. 1997).

2.2.2.2 The Use of the Falling weight Deflectometer

Two procedures for determining layer coefficients from FWD deflections are documented in the 1986 AASHTO design guide. The first technique involves the backcalculation of layer moduli and relating

them to layer coefficients. This approach, which requires an exact knowledge of layer thickness, is time-consuming and relies heavily on backcalculation expertise. The second approach uses outer deflection sensors to determine subgrade stiffness and then applies the peak deflection, D_0, to determine structural number of he pavement. The problem with the second approach is that the subgrade is assumed to be an infinitely thick linear-elastic material. Real pavements are not like that ; hence, only the first method will be detailed.

The peak deflection measured below a FWD is a combination of the deflection in the subgrade and the elastic compression of the pavement structure. Based on the fact that approximately 95 percent of the deflections measured on the surface of a pavement originated below a line deviating 34 degrees from the horizontal axis, it can be assumed that the surface deflection measured at an offset of 1.5 times the pavement thickness originates entirely in the subgrade. By comparing this deflection to the peak deflection, an index associated with the magnitude of deformation that occurs within the pavement structure has been defined by Rohde (1994):

$$SIP = D_0 - D_{1.5Hp} \tag{24}$$

where

SIP = structural index of pavement,

D_0 = peak deflection,

$D_{1.5Hp}$ = surface deflection, and

Hp = total pavement thickness.

Rohde (1994) hypothesized that the *SIP* is strongly correlated with the stiffness of the pavement structure and subsequently with its structural number. To investigate this hypothesis and to develop a relationship between FWD-measured surface deflections and the structural number of a pavement, a large number of pavements were analyzed using the layered-elastic theory. A total of 7776 pavement structures with a wide range of stiffness-thickness combinations were used. For each of the pavement structures, the structural number was calculated using AASHTO guidelines:

$$SN = \sum_{i=1}^{n} h_i \, a_g \left(\frac{E_i}{E_g} \right)^{1/3} \tag{25}$$

where

a_g = layer coefficients of standard material,

E_g = resilient modulus of standard material,

h_i = layer thickness (in), and

SN = structural number.

The best relationship was found after including the pavement thickness in the analysis. A relationship with the following format was selected:

$$SN = k_1 SIP^{k_2} Hp^{k_3} \quad (26)$$

where

SN = structural number,

SIP = structural index of pavement (μm),

Hp = total pavement thickness (mm), and

k_1, k_2, k_3 = coefficients.

The same rationale used to determine *SN* from surface deflections might be used to obtain the sub-grade stiffness. Rohde (1994) has defined the Structural Index for the sub-grade (SIS) as:

$$SIS = D_{1.5Hp} - D_s \quad (27)$$

where

SIS= structural index of the sub-grade

D_s = surface deflection measured at an offset of (*1.5Hp + 450 mm*).

The *SIS* and the total pavement thickness were subsequently related to the sub-grade stiffness using the following relationship:

$$E_{sg} = 10^{k_4} SIS^{k_5} Hp^{k_6} \quad (28)$$

where

E_{sg} equals the sub-grade stiffness in MPa, and k_4, k_5, and k_6 are coefficients.

Sebaaly et al. (1989) investigated the relationship between surface cracking and the structural capacity of both thin and thick pavement structures. The research examined the relationship between the

structural and functional performance parameters. Among the various performance parameters studied were the surface cracking and the load-deflection response of the pavement structure under FWD loading. By using cracking to indicate the structural condition, these systems assume the existence of a relationship between surface cracking and the loss of structural capacity.

The results indicated that if pavement section showed an average rutting of 12.7 mm (0.5 in), the failure mode was considered to be rutting; however, if the section showed a linear cracking value of 13670.6 mm/m^2 (50 in/ft^2), the failure mode was considered to be fatigue. The rate of crack propagation through the asphalt depends on a combination of various factors:

1. the thickness of the asphalt layer,
2. the maximum size of the aggregate in the asphalt mix,
3. environmental conditions, and
4. the magnitude and frequency of loading.

Therefore, no general rate of crack propagation can be identified for any pavement system. When a crack is initiated; the structural capacity of the pavement section is reduced. The crack decreases the section of the asphalt layer available to resist tension, resulting in higher pavement deflections. In layer theory analysis, it is assumed that the reduced structural capacity from fatigue cracking results from a decrease in the modulus of the asphalt concrete layer.

2.2.3 Permanent Deformation Damage Functions

The research discussed in sections 2.2.1.3 and 2.2.1.4 indicates that various material properties, measured through laboratory testing or field testing, have been correlated with layer coefficients. However, this research has largely neglected to consider the failure behavior of materials. Several studies, however, looked at the use of failure behavior using what are called damage functions.

Damage functions are defined as mathematical equations that can predict distresses or reductions in performance measures as a fraction of a reference level of distress or reduction in performance established as a failure condition. The failure condition can be represented as a structural failure or a level of distress or loss of performance that may be expected to produce the need for major repair or rehabilitation. The AASHO Road Test developed the following damage function for serviceability:

$$g = \left(\frac{W}{\rho} \right)^{\beta} \quad (29)$$

where

g = damage function, which ranges from 0 to 1 with increasing damage

W = number of 18-kip Equivalent Single Axle Loads (ESAL's) applied

ρ = ESAL producing a damage level defined as failure

β= rate of damage increase

The values of ρ and β, which represent different types of distress and environmental zones, are functions of a variety of independent variables. AASHO generally used a Present Serviceability Index (PSI) of 1.5 to represent total failure. This would be the terminal serviceability. A reduction of PSI to 1.5 caused by a number of axle loads of an established magnitude is represented by a g equal to unity. Also, if a damage function equals 0.5, this means that the PSI has been reduced by one-half the difference between the initial PSI and the terminal PSI.

Cowher et al. (1975) summarized many previous studies on damage functions. A few of these are described below. Cowher et al. (1975) also conducted an investigation into the cumulative damage of asphalt materials.

Deacon (1965) studied the effects of compound loading on bituminous mixtures under laboratory conditions. He developed a test that used a rectangular asphalt beam specimen. It had a two-point, pneumatically-driven loading apparatus that produced a constant bending moment at the center of the beam. With the simple and compound loading fatigue data used during the study, he developed the following relationship to calculate the stiffness modulus:

$$E = \frac{K * P}{I * \Delta} \quad (30)$$

where

E = deflection-based stiffness modulus

K = constant dependent on specimen geometry

P = total dynamic load applied upwards

I = moment of inertia of beam

Δ = dynamic center deflection

The stiffness decreased rapidly during the initial and the final phases of the test. During the intermediate phases the stiffness was observed to gradually increase.

Deacon analyzed his data relying on Miner's Hypothesis and its variations to derive the best predictive relationship for a mean compound loading fracture life. Deacon found the best predictive model by taking the experimental compound loading data and comparing it to the predicted results of nine techniques. He compared the numbers generated in the following way:

$$Deviation = \frac{Predicted\ (Y) - Measured\ (Y)}{Measured\,(Y)} \tag{31}$$

where

Y = fracture life

The technique that had the least average squared deviation was considered the best technique. It was concluded that a modification of Miner's Hypothesis was the best predictive model. Deacon also found that the order and magnitude of stress application was important. Finally, Deacon found that the standard deviation of fracture life tends to increase as the stress level is decreased for simple loading conditions.

For simple loading conditions, Deacon found the existence of a linear relationship between the logarithm of the mean fatigue life and the logarithm of stress. Deacon also found that a larger load duration would decrease the measured value of fracture life.

Cowher et al. (1975) also summarized a study done by McElvaney (1972) on the compound loading behavior of bituminous mixtures. McElvaney studied the fatigue response of asphalt base course specimens to compound loading in order to determine the predictive accuracy of Miner's hypothesis. Three types of constant loading tests were employed: sequence tests, repeated-block tests, and temperature sequence tests. The tests consisted of a rotating cantilevered beam that was submersed in a controlled temperature water bath. The specimen was rotated at 1000 RPM with a constant load applied perpendicular to the axis of rotation. This produced a maximum bending stress at the necked down portion of the specimen. Simple loading tests were also performed.

McElvaney found the existence of a linear relationship between the logarithm of applied stress and the logarithmic mean number of cycles to failure. He also found that the fatigue life of a bituminous material was sensitive to temperature changes; an increase in temperature caused a decrease in fatigue life. Material variability on the cumulative cycles ratio was found to be significant at all stress levels. Finally, McElvaney stated that a linear damage rule such as Miner's Hypothesis is adequate for predicting fatigue life under compound loading conditions.

Cowher et al. (1975) conducted their tests to determine the applicability of Miner's hypothesis to fatigue data obtained from dynamic indirect tensile tests. The indirect tensile test equipment used by Cowher and his co-researchers is similar to the apparatus that will be used for this research project. Two stress levels were used to evaluate the hypothesis.

Cowher et al. (1975) concluded that a log-log plot of stress as opposed to fatigue life for a given set of environmental conditions is essentially linear. They also concluded that the aggregate type had no effect on fatigue life for the entire range of stresses considered. For compound loading, they found that the order and magnitude of the applied stresses have a significant effect on the fatigue life. It was also concluded that Miner's hypothesis is valid for the asphalt mixtures tested. Finally, they concluded that the time deformation under compound loading conditions could be predicted from simple loading considerations using a technique of linear summation of damage increments.

Cowher et al. (1975) recommended that future studies take into account the pseudo-random loading spectra, which are more representative of actual field conditions. It was also recommended that field conditions be incorporated into the laboratory testing so that a direct comparison can be made between field and laboratory findings.

Rauhut et al. (1984) developed damage functions for both flexible and rigid pavements. The damage functions developed were used to develop load equivalence factors for each of the significant distresses investigated. They developed a computer program called DAMAGE that converted the damage functions into load equivalence factors.

Rauhut et al. (1984) developed damage functions for rutting and serviceability loss using the AASHO Road Test data. Their purpose was to investigate and validate the use of a combined mechanistic and empirical modeling approach to develop damage functions. When Rauhut and his co-

researchers attempted to develop a damage function for fatigue cracking, they ran into problems with the data. Most of the cracking failures occurred during the spring thaw, which resulted in clustered data. As a result, it was not possible to develop meaningful regression analyses from that data.

They also modified ρ and β from the AASHO Road Test damage function (Eq. 29) to predict rutting damage in the following way:

$$\log \rho = 7.5470 - 2.5221 * \log(L_1 + L_2) + 1.4786 * \log L_2 + 1.3852 * \log SN + 1.2291 * \log t_{ac} \quad (32)$$

$$\log \beta = 0.1432 - 0.7302 * \log(L_1 + L_2) + 0.8890 * \log L_2 + 0.0759 * \log SN + 0.7180 * \log t_{ac} \quad (33)$$

where

L_1 = axle load, kips

L_2 = axle code (1 for single axle, 2 for tandem)

SN = structural number

t_{ac} = asphalt concrete surface thickness, inches.

For serviceability loss the new ρ and β were:

$$\log \rho = 8.3647 + \log(L_1 + L_2)[-3.5658 + 0.222 t_{ac}] + \log L_2[2.819 - 0.3539 t_{ac}] + 3.512 * \log SN - 1.6412 * \log t_{ac} \quad (34)$$

$$\log \beta = -0.7179 + \log(L_1 + L_2)[0.3706 - 0.4017 t_{ac} + 0.0302 t_{ac}^{\ 2}] + \log L_2[0.0728 + 0.2854 t_{ac} - 0.0265 t_{ac}^{\ 2}] - 0.0204 * \log SN + 2.4155 * \log t_{ac} \quad (35)$$

where the variables are similar to those in the rutting equations above.

For both the rut damage and serviceability loss Rauhut et al. (1984) found the existence of a good correlation between their damage functions and the AASHO Road Test data.

2.2.4 Rutting and Resilient Characteristics as Determined by Tri-Axial Testing

Unbound granular materials have a major function in the structural capacity of a highway pavement. They provide a foundation that supports asphalt concrete layers and helps to support the traffic that will use the constructed asphalt pavement. The unbound layers must exhibit high resilient moduli and show low permanent deformation in order to reduce resilient deformation and rutting in the asphalt pavement. The paragraphs that follow describe some studies that have been done in Europe on the use of a tri-axial cell test to analyze the use of unbound granular materials as a structural layer in pavements.

It is known that the characteristics of unbound granular materials are non-linear for both resilient and permanent deformation. These characteristics include applied stress level (Hicks & Monismith, 1971), material type, density moisture content (Thom & Brown, 1987; 1988; 1989), and grading (Kamal & Dawson, 1993). This literature review will concentrate on how the permanent deformation characteristics or rutting features can be predicted by the use of the tri-axial test.

Dawson et al. (1993) conducted a study characterizing unbound granular materials as a function of condition. They tested three aggregates in a pneumaticall-controlled 160-mm diameter, variable confining pressure (VCP), tri-axial chamber. The purpose was to determine the effects of the moisture content of the aggregate on the permanent and resilient deformations.

The samples were compacted using vibrocompression. This involves imparting an external vibration onto a tube while subjecting the sample to a light static axial pressure. The sample diameter to height ratio was held at 2 to 1 and air was used for the cell's confining pressure.

Conditioning was achieved by cycling the confining pressure zero to 100 kPa and cycling the deviator stress from 0 to 600 kPa. 20,000 conditioning cycles were applied. This resulted in a 2.0 gradient between the p-q in an invariant stress space, where p is the mean normal stress and q is the deviator stress. The permanent deformation tests were run by subjecting the specimens to 80,000 load repetitions very similar to the ones used for conditioning.

To model plastic strain ($\varepsilon_1^{p^*}$) they used an equation developed by Hornych et al. (1993).

$$\varepsilon_1^{p^*}(N) = \varepsilon_1^{p}(N) - \varepsilon_1^{p}(100) \quad (36)$$

$$\varepsilon_1^{p^*} = A_1\left[1-\left(\frac{N}{100}\right)^{-B}\right] \quad (37)$$

where

A_1 = the difference of strain at 100 cycles and strain after infinite cycles

B = rate at which a consistant and fully resilient response is developed

This equation showed a very good fit for the data produced by their tests. The strains rose quickly during the first 1000 cycles and increased slightly after. It was also found that permanent shear deformations rose with the increase of moisture content. All of the materials tested showed that the highest maximum stress ratio, (q/p max), correlated with the greatest permanent deformation. Some of the materials, however, showed that maximum stress ration was somewhat sensitive to moisture.

The study concluded that increasing the moisture content from pessimism to optimum will increase the permanent deformation as Poisson's ratio is experienced under repetitive loading. The moisture content has little to no effect on the nonlinearity of the unbound granular material. It was also determined that moisture content might cause greater changes in permanent deformations than significant alterations in magnitude of applied loading. Finally, they recommended that a new classification system be developed which assesses the material on resilient and permanent characteristics. This would allow for material source differences, as well as density, moisture and grading differences to be taken into account.

Galjaard et al. (1993) conducted an investigation of the different types of tri-axial apparatus. At the time there was no standard concerning the set-up or characteristics of the proper apparatus. Four separate laboratories located in Europe set-up their own tri-axial testing equipment and ran similar experiments. The methods of compaction, physical, and mechanical set-up of each tri-axial cell was different.

The University of Nottingham (UNOT) used a variable confining cells that had specimen dimensions of 150mm by 300mm. The maximum grain size allowed in such cells was 30mm. A silicone

oil was used as the cell fluid. The load cell and the axial LVDTs were located inside the cell as well as radial deformation rings. There was also an additional pressure sensor located inside the cell to measure cell pressure.

The compaction was done in an alluminum split ring mold. Four layeres were compacted using an external vibration on the split ring while a small surcharge load was applied axially. When completed, the split ring was removed. Then, a vacuum was applied to the inside of the specimen ; a second membrain was placed on the specimen, and it was moved to the cell base.

The Laboratorio Nacional de Engenharial Civil (LNEC) used a 300mm by 600mm vacuum constant confining pressure rig. The system has no tri-axial cell ; confining pressure was simulated by applying a vacuum to the inside of the specimen. The compaction was completed by using a split ring mold. A ten-layer compaction was implemented with the use of a vibrating hammer.

Le Laboratoire Central des Ponts et Chaussees (LCRF) employed a pneumatically powered 160 mm by 320 mm variable confining pressure rig. The maximum grain size allowed in this set-up was 31.5 mm. They positioned their load cell inside the pressure cell and used axial LVDTs, also located inside the tri-axial cell. Three radial LVDTs, placed 120° apart, were used instead of a radial ring device that was employed by the previous two laboratories mentioned. The confining pressure was developed by air pressure.

A vibrocompression technique was used to complete the compaction of the specimens. This consisted of a PVC container that experienced a horizontal vibration and a system to apply a small vertical load during the vibrating. The compaction using this method was completed in one layer at optimum moisture content. To achieve the proper water content, the specimens would be dried at 40° C until the desired moisture content was met.

Delft University of Technology (DUT) had an apparatus that was a 400mm by 800mm vacuum constant confining pressure rig. Like the LNEC the confining pressure was induced by applying a vacuum to the inside of the specimen. Again, there was no tri-axial cell needed to complete the test. Like all the others, they used axial transducers placed at the 1/3 and 2/3 points of the specimen to avoid edge effects. To measure radial deformations, proximity transducers located on the rings that hold the axial transducers were used.

Manual compaction took place in eight layers using a heavy tamper. After every second layer, further compaction was completed by using a compaction plate at the end of an actuator, a static load of 10kN for 30 minutes, plus a cyclic half-sine load with a frequency of 7Hz and an amplitude of 40kN.

Each laboratory completed three identical tests using a q/p stress ratio of 3. The specimens experienced 20,000 cycles of conditioning. The conditions were 50kPa confining pressure (σ_3), a minimum deviator stress of 0kPa (q_{min}), and a cyclic deviator stress set at 130kPa (q_r). Before and after the coditioning, the specimens received five cycles of isotropic loading. For these loadings, the initial cell pressure was zero and cyclic cell pressure was 50kPa. The testing portion of the tests was done in a series of 12 cyclic loadings of 100 cycles each. The parameters are as follows:

σ_3 = 15kPa, q_{min} = 0, q_r = 15; 30; 45; 60kPa (38)

σ_3 = 30kPa, q_{min} = 0, q_r = 25; 50; 75; 100kPa (39)

σ_3 = 45kPa, q_{min} = 0, q_r = 30; 60; 90; 120kPa. (40)

Finally, an additional isotropic loading identical to the previous ones was applied.

The permanent strains used for the analysis were obtained during the conditioning of the specimens. The axial permanent strains (ε_1^p) turned out to be quite different from all the laboratories. It was concluded that the differences could be attributed to the differences in the compaction methods used.

The study developed recommendations for tri-axial testing unbound materials. The first thing mentioned was the necessity of using a reliable compaction method. The vibrocompression method used at the LRSB was recommended. The method was quick and provided specimens with a homogenous density profile. They also qualified the results coming from this method of compaction as being good.

A testing system that has a resolution of 10^{-5} in strains should be used due to the nature of the very small resilient strains. The larger the specimen, the more reliable the results. The 300mm by 600mm size was pointed out because of the larger size and the ability to still perform a variable confining pressure test (VCP). The VCP was found to yield more reliable results.

LRSB conducted a separate analysis on compaction profiles produced from both a vibrocompression method and a vibrating hammer method compacted in 3, 5, and 7 layers. The densities varied from 70kg/m^3 (vibrocompression and 7-layer vibration hammer) to 300kg/m^3 (3-layer vibration

hammer). The density profile for the vibrocompression method was found to be rather consistent. The profile for the layered compaction tended to be high at the top of each layer and then fall off towards the bottom of each layer. As the number of layers increased this behavior decreased and the profile became more consistent. The permanent strains also varied considerably according to the particular compaction used. The seven-layer compaction showed the lowest strain $46*10^{-4}$. The deformation increased through five and three-layer compaction until they came to the vibrocompression method, which displayed the highest permanent strain, $122*10^{-4}$. This represents an increase by a factor of 2.6.

The conclusions of this study were focused around the compaction method used to create the specimens. It was recommended that the vibrocompression method of compaction be used. The study sighted the uniform density profile that this method created as one of its reasons for choosing this method. They also noted the relative easiness and quickness of this method. No correlation between laboratory data and field measurements was attempted during this study.

Paute and his co-researchers used the previous study as a starting point and expanded it using their recommendations for equipment and compaction method discussed previously. Therefore they used the vibrocompression apparatus mentioned before to compact each specimen. The tri-axial set-up used was similar to the ones used at UNOT or LCPC, although the one that was actually used was not specified. However, the two set-ups are very similar.

To characterize the permanent behavior of the unbound granular material, they resorted several tests at different loadings. The following table shows the stress levels used for the permanent deformation tests.

Table 2.2 Stress Levels For Permanent Deformation Tests

Path Name	Confining stress, σ_3 (kPa)		Deviator stress, q (kPa)		q_r/p_r
	min	Max	min	max	
P1	0	20	0	300	2.5
P2	0	100	0	600	2
P3	0	200	0	600	1.5
P4	0	75	0	300	1.7

The test consisted in applying 80,000 cycles to each specimen. Stress and strain values were recorded at the cycles numbering 20, 50, 100, 200, 400, 1000, 2500, 5000, 7500, 10000, 12500, 15000, 20000, 40000, 60000, and 80000.

The modeling of the permanent behavior consisted of two aspects: the variations between the number of cycles and the permanent strains and any relations between the stresses and the permanent strains. The model used here was the one developed by Hornych et al. (1993), the same model that was used in the research by Dawson et al. (1993).

$$\varepsilon_1^{p*}(N) = \varepsilon_1^{p}(N) - \varepsilon_1^{p}(100) \tag{41}$$

$$\varepsilon_1^{p*} = A_1\left[1-\left(\frac{N}{100}\right)^{-B}\right] \tag{42}$$

where

A_1 = the difference of strain at 100 cycles and strain after infinite cycles

B = rate at which a consistant and fully resilient response is developed

The model deals with the axial permanent strain occurring at 100 cycles. To create the power law relation, the first equation was integrated after it had been noticed that unbound granular materials have a linear relation between the ln ($\delta\varepsilon_1^p/\delta N$) versus ln (N).

$$\ln(\delta\varepsilon_1^{p} / \delta N) = a + b*\ln(N) \tag{43}$$

The integration led to:

$$\varepsilon_1^{p} = \frac{e^a}{b+1} * N^{b+1} + c \tag{44}$$

where

c = a constant.

The expression then becomes the power law shown above with two parameters A_1 and B. A_1 represents the limit of the permanent strain for a given cyclic loading.

A relation between the A_1 parameter and the axial permanent strain was found. This represents the influence of the stress level on the specimen.

$$A_1 = \frac{\left(\frac{q}{p+p^*}\right)}{a-b\left(\frac{q}{p+p*}\right)} \tag{45}$$

where

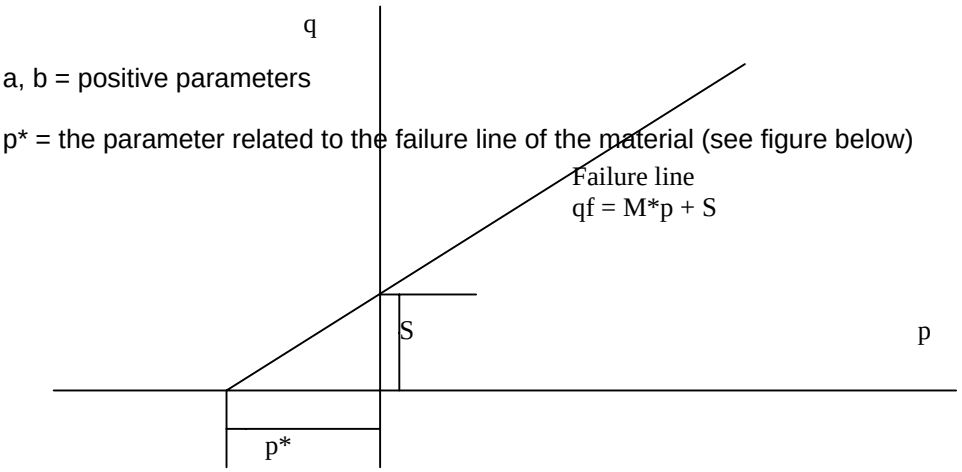

Figure 2.1 Determination of the stress p*

This hyperbolic relationship is similar to the one proposed by Lentz and Balady (1980). A_1 depends only on the ratio q/(p+p*). When A_1 increases, the stress ratio increases as well. The equation for A_1 also shows that there is a maximum limit for q/(p+p*) ; this represents the failure of the material: q/(p+p*) max = a/b = M, the slope of the failure lin. It was also observed that p* = S/M.

Puate and his co-researchers explained that these properties of the A_1 and failure line relationships present a simple method to accurately describe the plastic behavior of unbound granular materials. It was also noted that the parameters a, b, M, and S can be obtained by successive approximations to the value of p*. When the correlation ratio is at its highest the representative value can be obtained.

CHAPTER THREE

MATERIAL COLLECTION, SPECIMEN PREPARATION, DATA COLLECTION, AND CALCULATION

This chapter is divided into three sections: material and project descriptions, collection and analysis of the field data, and laboratory data collection and analysis. To collect a wide range of materials, the Wisconsin Department of Transportation (WISDOT) specified a list of projects to choose from and specified a group of materials to potentially analyze.

The particular projects to focus on were selected by the research group at the University of Wisconsin, Madison, based primarily on when the individual projects were being constructed. After collecting the materials and the field data, the members of the Technical Oversight Committee (TOC) for the project, organized by the WISDOT, narrowed down the list of materials to those they felt were the most important for immediate analysis and implementation of results.

3.1 Material and Project Descriptions

Two general types of materials were selected for this project: hot mix asphalt (HMA) and recycled granular base course. Four types of HMA and three types of base course materials were collected from various projects throughout the state. Table 3.1 on page 43 summarizes the materials used in this research.

3.1.1 Bound Materials

Four types of bound materials were selected: Superpave (SHRP), Stone Matrix Asphalt (SMA), High Volume (HV) mix, Medium Volume (MV) mix and Asphalt Base Course (ABC). These asphalt mixtures vary mainly in their gradations; however, the asphalt binder type and optimum content also vary.

Four of the five mixtures came from the same project located near Wausau, WI and the SMA came from a project near Eau Claire, WI.

Table 3.1 Materials Analyzed for the Layer Coefficient Project

Layer Coefficient Study				
Material Type	Project ID	Project Dates	Sample Pickup	FWD Testing
Asphalt Layers				
SMA	1028-05-77	Mid May - Mid June	6/12/97	None Scheduled
HV-2	1059-16-73	May - Mid July	7/2/97	Base 6/30/97
MV-2	1059-16-73	May - Mid July	7/11/97	Base 7/10/97 MV 9/24/97
SHRP	1059-16-73	Mid July - Oct	10/3/97	Base 9/10/97 SHRP 10/17/97
Base Layers				
Asphalt Base Coarse	1059-16-73	Mid July - Sept	10/9/97	Subgrade 9/10/97 Subbase 10/3/97 Base 10/10/97 HV 10/17/97
Pulverize	1581-12-70	Aug	8/14/97	Pre 8/13/97 Pul 8/15/97 MV 10/20/97
Mill and Relay	1644-01-71	End July - End Sept	9/8/97	None Scheduled

The SHRP mixture was one of three mixtures that came from Project No. 1059-16-73. This project was an expansion of Wisconsin State Highway 29 (STH 29) from two lanes to four lanes. The project was included in a study by the long Term Pavement Performance Program (LTPP) of the Federal Highway Administration (FHWA). Part of the FHWA project was to construct many different test section of asphalt pavement and monitor their performance for several years. The sections varied in structure, material type, and individual material properties.

The SHRP mixture was designed using the Superpave protocols. These protocols were recently developed from the Strategic Highway Research Program (SHRP). The SHRP mix consists of larger

sized aggregates with minimum amounts of natural sands. The binder used for this mix was a PG58-22. The material properties for the SHRP mix, as reported by the HMA producer, are shown in Table 3.2.

Table 3.2 SHRP Mixture Properties

Aggregate Sources

	Percent	Material	Source	SG
1	45%	Hy 29 1/2" Chip	Cisler Marathon	2.644
2	35%	Hy 29 3/8" Chip	Cisler Marathon	2.688
3	10%	Hy 29 1/4" Chip	Cisler Marathon	2.666
4	10%	Hy 29 Sand	River Pit Marathon	2.636
		Effective SG 2.699	Total SG	2.661

Aggregate Gradations

Sieve	1	2	3	4	Job Mix	CP*	RZ**
1"	100	100	100	100	100	100	
3/4"	100	100	100	100	100	90-100	
1/2"	93	100	100	100	96.8		
3/8"	43	100	100	99	74.3		
#4	4.5	59	80	95	40.2		
#8	3.1	33	56	89	27.5	23-49	34.6
#16	3	22	39	82	21.2		22.3-28.3
#30	3	14	27	58	14.8		16.7-20.7
#50	2.5	10	19	13	7.8		13.7
#100	2	7	13	1.5	4.8		
#200	1.5	5	10	1	3.5	2-8	
Thin&Elong					0.3	10	

Mix Properties

Asphalt Material PG 58-22 Binder SG 1.029

Material Property	Actual	Spec
AC Content (%)	5.2	--
Air Voids	4	4
VMA	15.2	13 min
Density @ N_i	88.3	89 max
Density @ N_m	97.4	98 max

* Control Points ** Restricted Zone

The SMA is a coarse mix with gap-graded aggregates. SMA has its origins in Europe and is used commonly because it exhibits high resistance to permanent deformation or rutting (Brown et al. 1997). The mix exceeds the boundaries of acceptable gradations; because of this, the asphalt binder must be modified in order to facilitate its construction. If the asphalt binder were not modified, it would run out of the mixture during construction. Therefore, fibers - and in some cases polymers - are added to the binder to prevent binder run-down.

The SMA project is located on Interstate 94 (I-94) near Osseo, WI. This project involved constructing an overlay on an existing asphalt pavement. The SMA has only recently been utilized in

Wisconsin. This project is one of the first in the state to use this type of mixture. The SMA material properties are shown in Table 3.3.

Table 3.3 SMA Mixture Properties

Aggregate Sources							
	Percent	Material		Source		SG	
1	44%	5/8" X 3/8" Chip		Burns Chippewa		2.700	
2	35%	3/8" X 3/16" Chip		Burns Chippewa		2.686	
3	15%	3/16" Man. Sand		Burns Chippewa		2.693	
4	6%	Fly Ash		NSP-Sherco MN		2.400	
		Effective SG	2.714	Total SG		2.674	
Aggregate Gradations							
Sieve	1	2	3	4	5	Job Mix	Spec
1"	100	100	100	100	--	100	100
3/4"	100	100	100	100	--	100	100
1/2"	77	100	100	100	--	89.9	90-97
3/8"	33	99	100	100	--	70.2	58-72
#4	4	18	89	100	--	27.4	25-35
#8	2.8	7.4	60	100	--	18.8	15-25
#16	2.6	5.8	41	100	--	15.3	
#30	2.4	5.1	34	99	--	13.4	8-18
#50	2.2	4.3	21	98	--	11.5	8-14
#100	1.9	3.3	14	96	--	9.9	
#200	1.4	2.4	9.5	93	--	8.5	8-12
Thin&Elong	3.6	1.9	18.4	--	--	3.3	10
Mix Properties							
Asphalt Material	PG 58-28*			Binder SG	1.029		
	Material Property	Target	Actual				
	AC Content % by	6	6.6				
	Rice SG	2.471	2.449				
	Air Voids (%)	4.6	3-4%				
	Bulk SG	2.357	2.364				
	VMA	17.1	+15.5%				

* 0.3% Cellulose Fibers Added

The HV mixture also came from the STH 29 project located near Wausau. This mix is more traditional than the two previous mixtures. This mix is made up of more fine materials making it a more dense mixture. This type of mixture has been widely used in Wisconsin for many years for high volume roads. It comes from a family of mixtures that were originally developed using the Marshall mixture design procedure. Table 3.4 shows the properties of the HV mixture

The three divisions of these types of mixes are HV, MV, and Low Volume (LV) (Roberts et al. 1996). The designations are based on traffic volumes. For each volume level, a subdivision is determined

by the mixtures gradation. A number represents the gradations: lower numbers represent courser mixtures and higher numbers signify finer gradations. The numbers range from one to five. The courser gradations are used for binder course layers and the finer gradations are used for surface course layers. The HV and MV collected for this project were both of gradation type 2.

The MV mixture was used for the construction of temporary traffic crossovers. The main difference between this mixture and the HV is that the MV has less manufactured sand. Therefore its percentage of screenings and natural sand is higher. Out of all the surface mixes it has the finest gradation and the greatest percentage of natural sands. The MV mixture properties are shown in Table 3.5.

The ABC material was also collected from the STH 29 project near Wausau. Since these mixes are designed as base courses, they tend to be gap-graded with a relatively large amount of natural sand. The conventional wisdom is that mixes with large amounts of natural sand are weak mixtures. Since the stresses at the base level will be lower than those at the surface level, the quality and strength of the mix need not equal those of a surface mixture. The addition of the asphalt is believed to strengthen the mixture to a level above that of an open-graded base course. The ABC mixture properties are shown in Table 3.6.

All of these mixes were designed and constructed by the Mathy Construction Co. The data for the material's property tables was taken directly from their reports on each asphalt mixture design.

Table 3.4 HV-2 Mixture Properties

Aggregate Sources							
	Percent	Material	Source			SG	
1	17%	#1 Concrete Stone	Cisler Marathon			2.682	
2	20%	3/8" Crushed Stone	Cisler Marathon			2.664	
3	18%	1/4" Screenings	Cisler Marathon			2.663	
4	20%	Blend Sand	River Pit Marathon			2.636	
5	25%	Manufactured Sand	Manakee Marathon			2.704	
		Effective SG	2.696	Total SG		2.671	

Aggregate Gradations							
Sieve	1	2	3	4	5	Job Mix	Spec
1"	100	100	100	100	100	100	100
3/4"	98	100	100	100	100	99.7	90-100
1/2"	58	100	100	100	100	92.9	60-95
3/8"	31	100	100	99	100	88.1	50-90
#4	2.3	67	85	93	89	69.9	30-70
#8	1.6	40	56	83	56	49	15-55
#16	1.5	25	37	76	36	36.1	--
#30	1.4	17	26	54	22	24.6	7-40
#50	1.3	12	19	15	10	11.5	5-25
#100	1.1	7.4	13	3.1	3.4	5.5	--
#200	0.9	6.3	10	1.4	107	3.9	3-8
Thin&Elong	0.3	1.9	19.3	1	10.1	3.3	10

Mix Properties				
Asphalt Material	PG58-28		Binder SG	1.029
	Material Property	Target	Actual	
	AC Content % by	6	6.3	
	Rice SG	2.457	2.446	
	Air Voids	5	4.1	
	Bulk SG	2.355	2.345	
	VMA	17.8	17.6	

Table 3.5 MV-2 Mixture Properties

Aggregate Sources							
	Percent	Material	Source			SG	
1	26%	1/2" Crushed Stone	Cisler Marathon			2.661	
2	15%	3/8" Crushed Stone	Cisler Marathon			2.670	
3	32%	3/8" Screenings	Cisler Marathon			2.664	
4	27%	Blend Sand	River Pit Marathon			2.629	
5	--	--	--			--	
		Effective SG	2.671	Total SG		2.655	

Aggregate Gradations							
Sieve	1	2	3	4	5	Job Mix	Spec
1"	100	100	100	100	--	100	100
3/4"	100	100	100	100	--	100	90-100
1/2"	82	100	100	100	--	95.3	60-95
3/8"	33	100	97	98	--	81.1	50-90
#4	106	60	68	94	--	56.6	30-70
#8	105	31	50	89	--	45.1	15-55
#16	1.4	18	35	81	--	36.1	
#30	103	13	26	58	--	26.3	7-40
#50	1.3	9.5	19	13	--	11.4	5-25
#100	1.2	6.3	13	0.9	--	5.7	
#200	1.1	4.9	8	0.3	--	3.7	3-8
Thin&Elong	0.5	3.1	14.1	1.3	--	4.1	10

Mix Properties				
Asphalt Material	120-150		Binder SG	1.029
	Material Property	Target	Actual	
	AC Content % by Weight	5.5	5.6	
	Rice SG	2.456	2.452	
	Air Voids	3.7	3.4	
	Bulk SG	2.365	2.369	
	VMA	15.8	15.8	

Table 3.6 ABC Mixture Properties

Aggregate Sources

	Percent	Material	Source	SG
1	55%	1" Crushed Rock	Zoromski Pit Mara.	--
2	13%	1/4" Screenings	Cisler Marathon	--
3	30%	Blend Sand	River Pit Marathon	--
4	2%	3M Fines	Plant Stockpile	--
		Effective SG --	Total SG	--

Aggregate Gradations

Sieve	1	2	3	4	5	Job Mix	Spec
1"	99.9	100	100	100	--	99.9	90-100
3/4"	82.9	100	100	100	--	90.6	70-95
1/2"	47.7	100	98.7	99.2	--	70.8	55-90
3/8"	38.2	100	97	98.6	--	65.1	40-80
#4	28.3	83.6	90	97.5	--	55.4	25-65
#8	23	57	82.1	96.8	--	46.6	15-50
#16	19	40.1	73.5	95.2	--	39.6	
#30	16.1	29.1	50.3	92.8	--	29.6	7-30
#50	10.2	20.8	10.6	62.4	--	12.7	5-20
#100	7.8	14.9	1.5	38.2	--	7.4	
#200	4.2	11.3	0.9	25.7	--	4.6	3-8
Thin&Elong	--	--	--	--	--	--	

Mix Properties

Asphalt Material	PG 58-28	Binder SG	1.027

Material Property	Target	Actual
AC Content % by	5	4.6
Rice SG	2.492	--
Air Voids	--	--
Bulk SG	2.387	--
VMA	--	--

3.1.2 Unbound Materials

Using recycled surface course materials for base layers is becoming popular given today's concerns with environmental protection. Recycling materials eliminates them from landfills by actually putting them to good use after their life as a surface course has come to an end.

There are two primary methods of recycling asphalt surface layers. One is called pulverizing and the other milling. They basically involve the same process: the pavement is ground using large metal teeth on a rotating drum until no pieces generally larger than one inch are left. The difference between the two methods is in the machinery. The pulverizing equipment grinds up the material and then drops it in the same location from where it was taken. On the other hand, the milling equipment lifts up the recycled pavement and puts it on a conveyor. The conveyor leads to the end of the machine where the recycled material can either be put into a truck or dropped to the ground. Project design and equipment availability determine which process will be used, but the two are essentially the same.

Many times virgin or shoulder aggregates are added to the recycled material. Some projects will recycle the entire surface layer, whereas at other times only a partial milling will be performed. Once these materials are broken down they are compacted and used as base layers for a new asphalt pavement that will be paved over the top. They are generally compacted to 95% of their maximum density. Other processes are then introduced to add asphalt at low contents or emulsion to help bind the recycled material.

The materials used for this project consisted of a pulverized asphalt pavement and a milled asphalt pavement. The pulverized material had a 13% shoulder aggregate added in during the pulverization process. The pulverizer ground up the entire surface layer and part of the granular shoulder. The milled material had no outside aggregates added during the recycling process. However, it was decided by the WDOT to add a 50% #2 of open-graded virgin aggregate for the laboratory testing.

The virgin aggregate for the milled asphalt was collected from the Payne and Dolan facility located in Verona, WI. The two materials were mixed by weight in the laboratory at equal proportions making a 50-50 blend.

The milled material was gathered from a project on US Highway 14 (USH 14) just south of La Crosse, WI. The project was a full-depth mill. The material was dropped onto the existing base

course, smoothed, compacted, and used as the new base course. The HV asphalt was paved on top of the milled asphalt completing the construction. The pulverized material came from Prentice, WI on USH 8. It was a full-depth pulverize with part of the existing shoulder added in as mentioned above. Like the milled material, the pulverized asphalt was evened out, compacted, but this time it was paved over with the MV asphalt.

The other three recycled materials consist of mixtures of recycled portland cement concrete and asphalt concrete (PCC-AC). The PCC was collected from a Payne and Dolan plant in Milwaukee and the recycled asphalt used for the mixtures came from eastern Rock County. These materials consist of recycled pavements only; no aggregates were added either in the field or in the lab. The mixtures were mixed by weight in the laboratory.

Modified proctor tests were conducted on all the unbound materials, according to the ASTM D 1557-91 Test Method in order to determine their compaction characteristics. Maximum specific gravity and sieve tests were also conducted on the materials. The test for Theoretical Maximum Specific Gravity and Density of Bituminous Paving Mixtures (ASTM D 2041-95) was used along with ASTM C 136-96a for the sieve analysis. The results of the sieve tests are shown in Table 3.7 and Figure 3.1. The modified proctor results are shown in Figures 3.2 through 3.6.

Table 3.7 Recycled Material Gradations

50% Virgin 50% Milled			13% Shoulder 87% Pulverized		
sieve (mm)	sieve U.S.	%pass	sieve (mm)	sieve U.S.	%pass
50	2"	100	50	2"	100
37.5	1.5"	100	37.5	1.5"	99.4
25	1"	99.7	25	1"	97.7
19	3/4"	93.7	19	3/4"	93.5
12.5	1/2"	76.2	12.5	1/2"	83.8
9.5	3/8"	64.3	9.5	3/8"	76.3
4.75	#4	39.5	4.75	#4	57.4
2.36	#8	24.9	2.36	#8	45.9
1.18	#16	16.1	1.18	#16	34.4
0.6	#30	11.2	0.6	#30	22.6
0.3	#50	7.9	0.3	#50	11.3
0.15	#100	5	0.15	#100	4.5
0.075	#200	2.5	0.075	#200	1.9

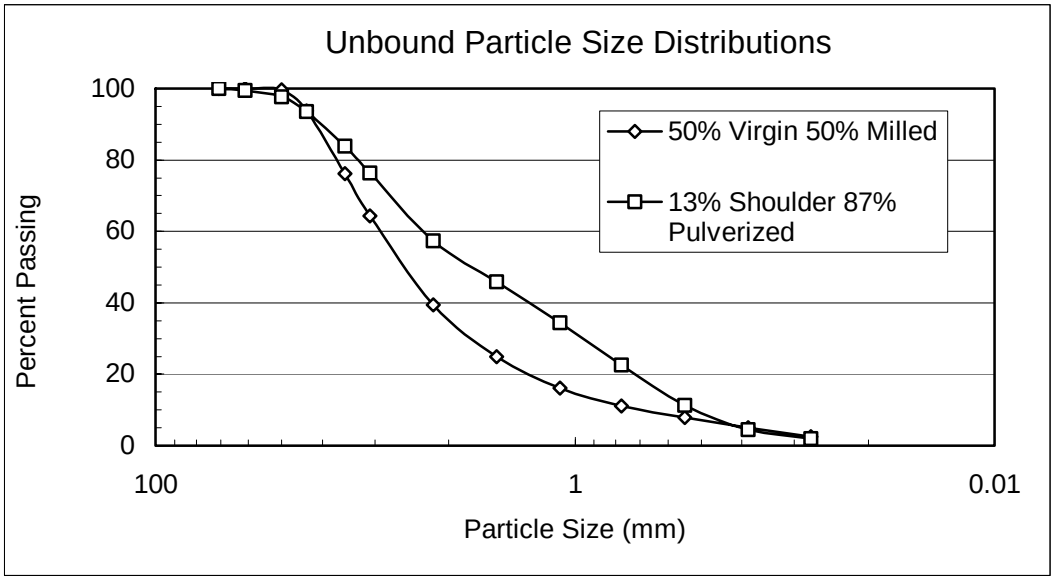

Figure 3.1 Recycled Material Gradation Curves

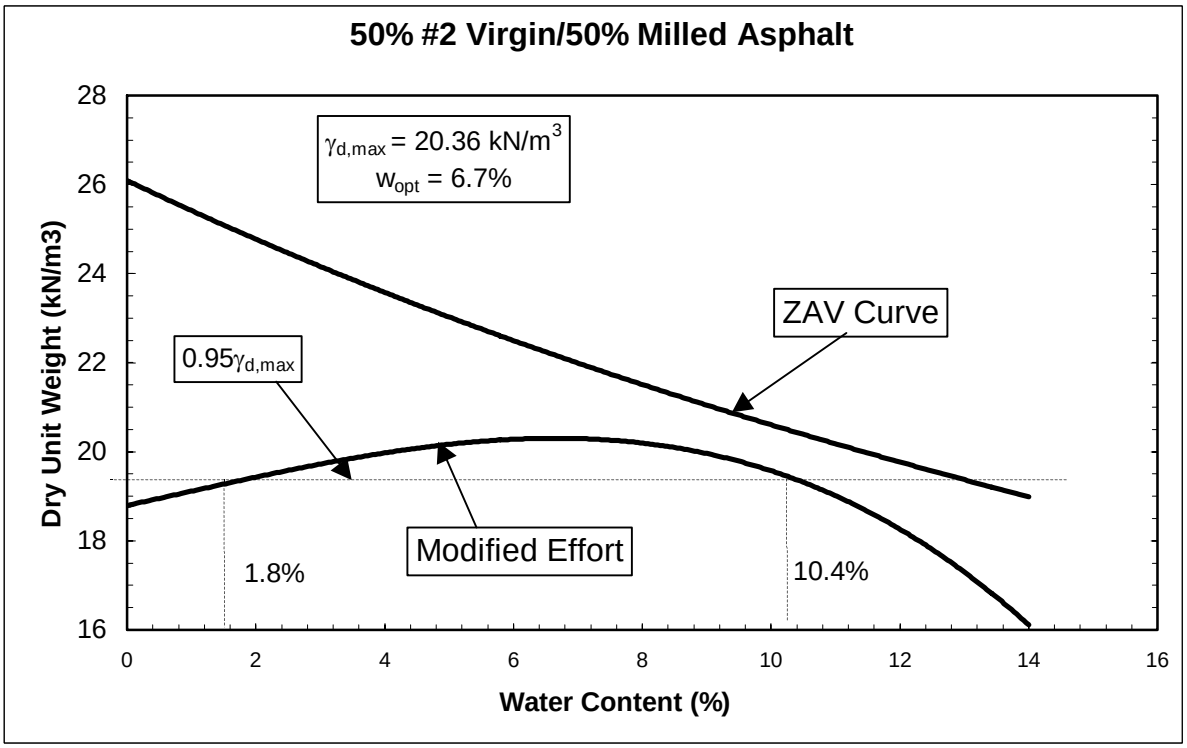

Figure 3.2 50-50 Modified Proctor Curve

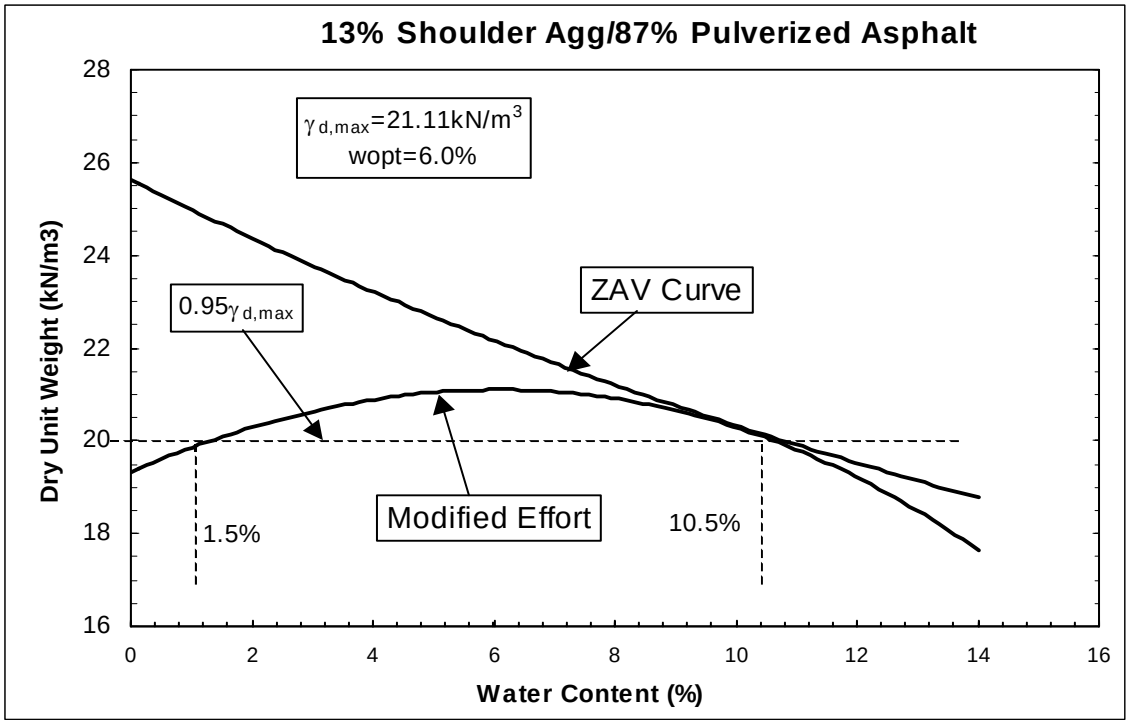

Figure 3.3 Pulverize Modified Proctor Curve

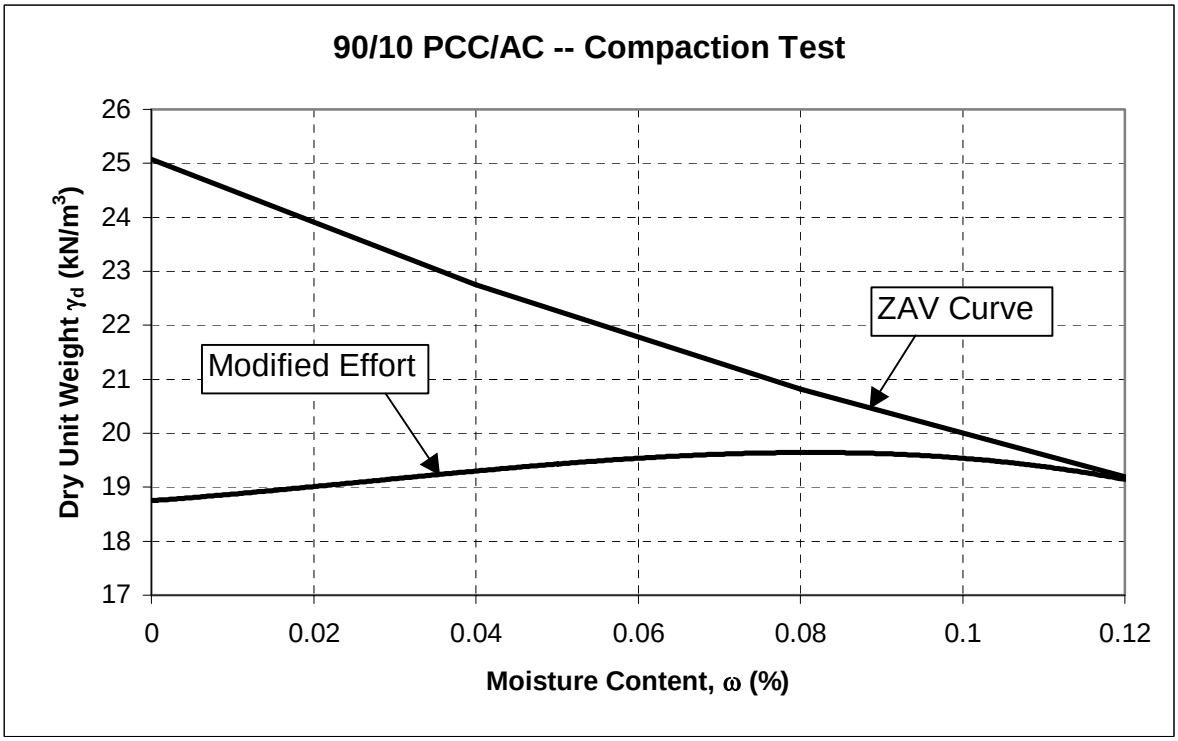

Figure 3.4 90P-10A Modified Proctor Curve

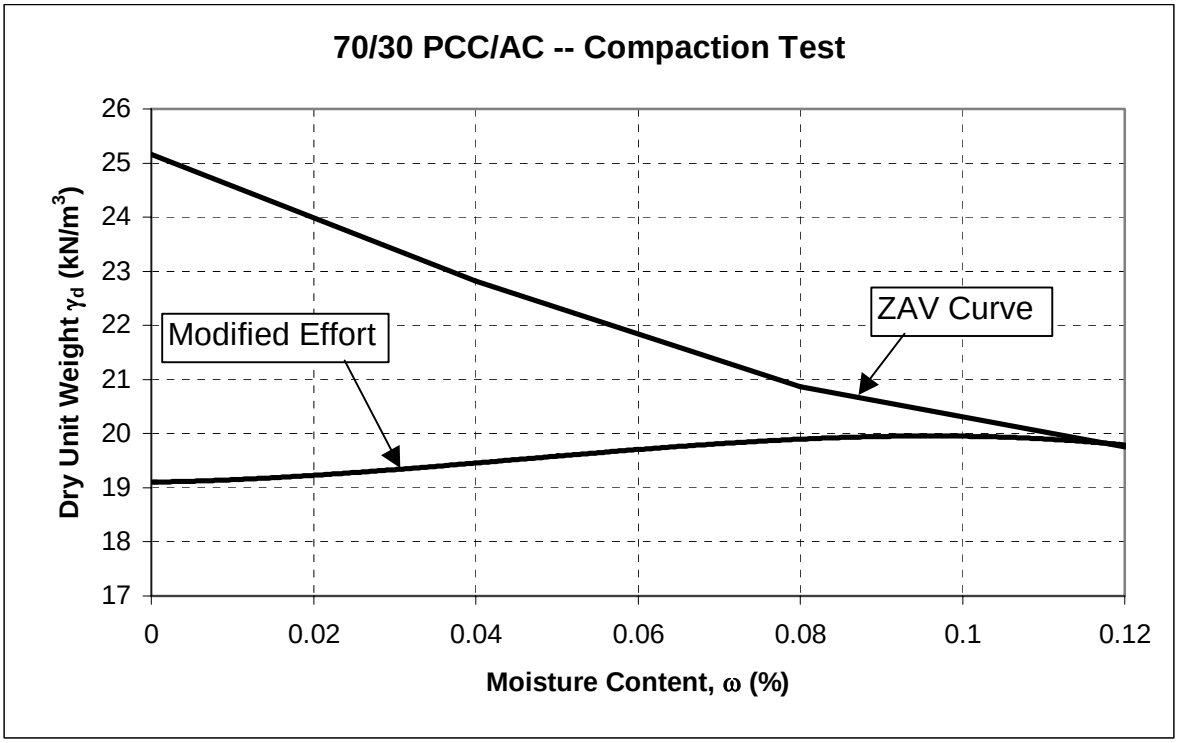

Figure 3.5 70P-30A Modified Proctor Curve

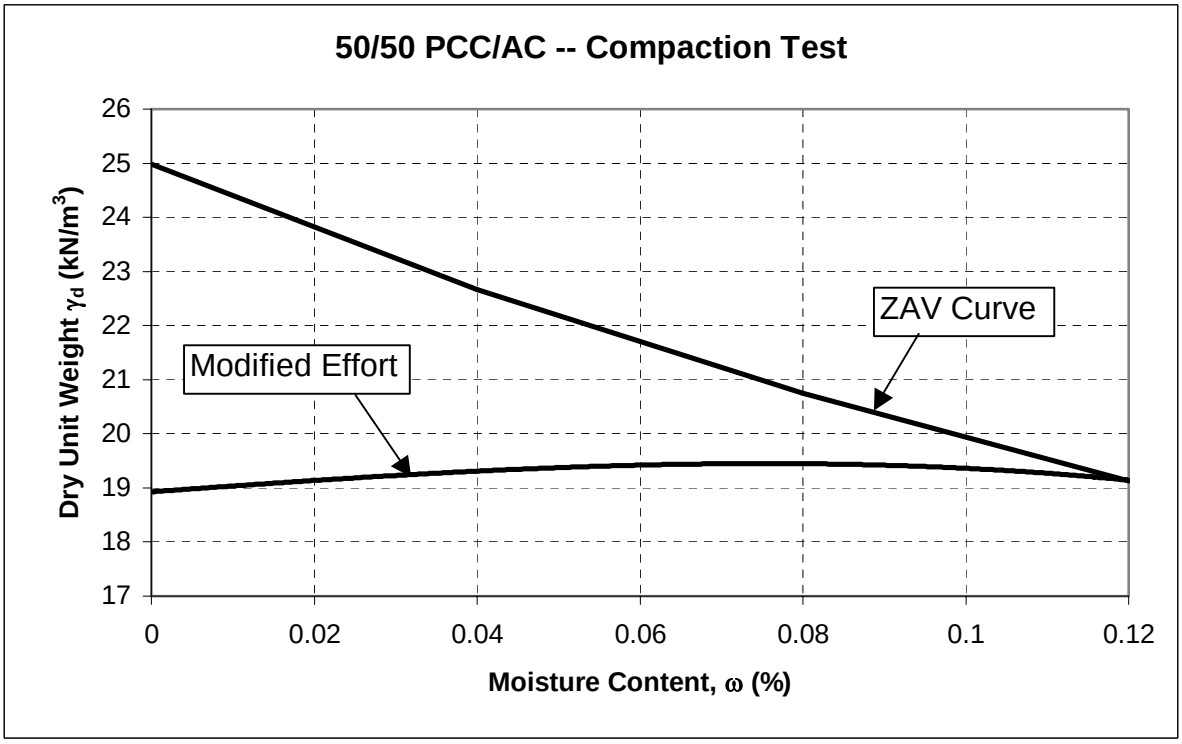

Figure 3.6 50P-50A Modified Proctor Curve

3.2 Field Data Collection and Analysis

3.2.1 Field Data Collection

The FWD was used to collect all of the field data for this research. The mechanism and the methods behind it were explained in Chapter 2. It was not feasible to test all of the asphalt sections considered as part of the original work plan. Also, some sections could not be tested due to the manner in which they were constructed. The reason for fieldwork in this research project was to be able to verify the laboratory numbers with actual field data.

Pavement sections that will be covered in this section include the MV, ABC, and the SHRP sections. Field and laboratory tests were conducted on all the materials just listed. The remaining materials did not undergo FWD testing.

The spacing of the FWD testing locations was determined from project to project depending on the geometry of the individual projects. An attempt was made to cover the entire length of the project. All of the projects varied in length; therefore, the spacing between test locations varied as well. Using the project particulars, the length of the test spacing was determined for each project so that at least 20 FWD testing locations were covered.

For the SHRP and MV projects, the base and surface layers were tested. The sub-grade could not be tested for either of these mixes because the- sub-grade material would not support the FWD trailer and the truck used to pull it. The ABC section was constructed on an existing roadbed; therefore, the sub-grade and every layer constructed on top of the sub-grade were tested.

3.2.2 Field Data Backcalculation Methods

The transformation of the data was performed using a backcalculation software program that goes through a computational process to determine the values of the resilient modulus (M_r). The program used to analyze the field data was MODULUS. The analysis of the data was not always simple. Whether or not to introduce the stiff layer in the M_r backcalculation process and how to pursue the process are critical to the accuracy of the M_r backcalculation in FWD tests. The stiff layer is the theoretical point at which deformations no longer occur. The location of this stiff layer is critical. At this time, there is no precise answer to the question of what is the best depth at which the stiff layer should be placed (Jong, 1997).

3.3 Laboratory Data Collection and Analysis

This section describes the entire process for the gathering of laboratory data. The first section describes how the granular and asphalt materials were prepared. Next, the determination of the testing parameters is discussed. Then the testing process is outlined and explained. Finally, the data analysis techniques are presented.

3.3.1 Specimen Preparation

The bound and unbound materials were prepared in different manners. However, achieving density was the important factor for each method. The granular material specimens have 12in heights and 6in diameters, which keeps them within the 2 to 1 ratio that is required for granular resilient modulus testing. The bound specimens were 8.8in in height and 6in in diameter. This geometry was dictated by the Superpave Gyratory mold limitations.

Once the granular material properties were known (presented in section 3.1.2), the amount of material to compact in each layer could easily be determined. Using a volumetric relationship, the amount of material needed in each layer to achieve the required density of 95% was calculated. A five-layer compaction was used for ease of compaction and to keep the density profile in the axial direction constant. The heights of the layers and the mass used per layer were dependent on the material type and the water content used.

The compaction was performed with a rotary impact hammer. Once the material was distributed into a split ring mold, a metal plate was placed on top of the material. The dimensions of the plate are just slightly smaller than the inside diameter of the split ring mold. The impact hammer was used to compact the material to the height determined by the volumetric relationships. Between layers the material surface was scarified to facilitate continuity between layers. The method produced good density results with little amounts of particle fracture.

Different methods of compaction for the bound materials were considered and some were attempted. A Compaction of a 12in specimen with the rotary impact hammer was attempted with little success. The compaction was attempted in 5 layers using volumetric relationships to determine mass per layer and layer heights. The rotary hammer could not produce a 12in specimen ; the final height was 13

in and the density profile over the entire height was not constant. The final air void content was calculated at 10%. The target air voids for this research is 7%. The use of the Superpave Gyratory Compactor (SGC) and the shorter specimens were the final choices.

The SGC does not facilitate 12in specimens. The insides of the molds are 10in in height. This allowed for a maximum height of approximately 8.8in. The gyratory was the method chosen for this research for different reasons. First, the gyratory compactor is the compaction method specified by Superpave. Second, the method is simple and yields repeatable results. Third, the ability to achieve a specimen that had uniform density through other means of compaction was not feasible with the equipment available. The protocols used to compact the specimens using the SGC are shown in Table 3.8. Figure 3.7 shows the density profiles of the asphalt mixtures several trials were made before the selection of the final protocols. Again volumetric relationships were used to determine the mass per layer and the heights similar to the unbound layers. The asphalt materials were compacted at 140°C and the material was loosened up between lifts to facilitate homogenous bonds between lifts.

Table 3.8 Asphalt Material Compaction Specifications

Material Properties	Layer	Asphalt Type				
		ABC	HV	SMA	SHRP	MV
G_{mm}		2.477	2.442	2.463	2.504	2.440
Target V_a		7	7	7	7	7
Actual V_a	4	6.827	7.305	7.243	6.340	6.362
	3	6.983	7.485	7.054	7.396	7.015
	2	7.130	6.977	6.696	6.936	7.314
	1	7.345	6.631	6.354	6.309	7.014
Mass/Layer (g)		2262	2228	2181	2261	2240
Specimen Height (mm)	4	226	226	226	226	226
	3	179	177	177	177	176
	2	125	125	124	125	125
	1	66	72	70	70	68

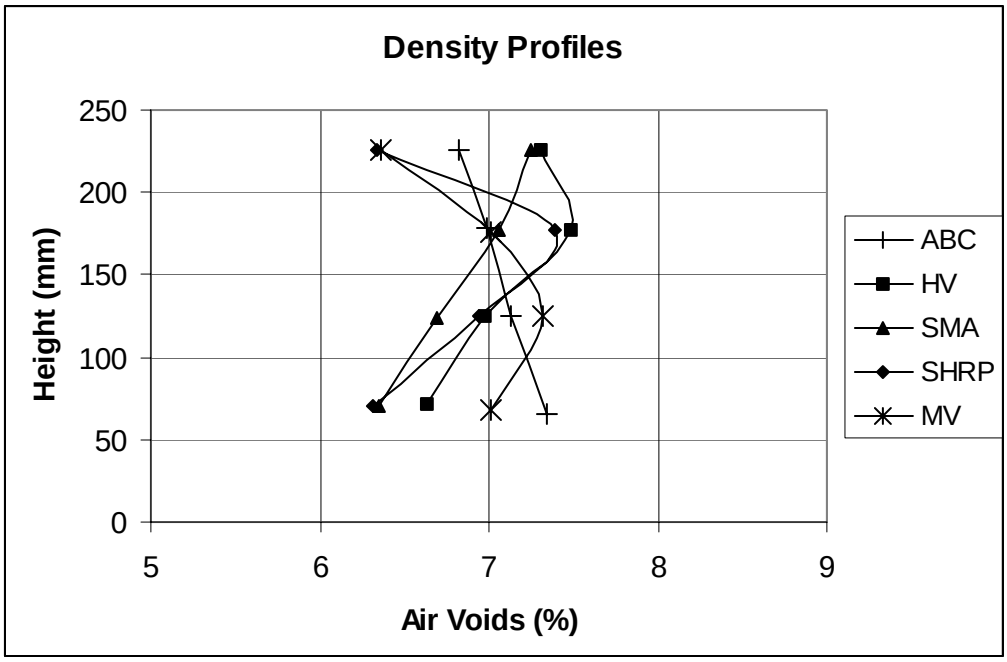

Figure 3.7 Density Profiles of Compacted Asphalt Mixes

Bulk specific gravity values were determined for the first several specimens. The total air voids were within ±0.5%. The number of gyrations to achieve the specified heights was recorded for all of the specimens. It was noticed that for each lift, the number of gyrations needed for compaction varied only by one or two each time for every specimen. This was determined to be a sufficient check of bulk specific gravity. As long as the mass per layer and the specified height are correct, the level of air voids was expected to meet the target if the number of gyrations needed was met. The number of gyrations required for lift compaction turned out to be a good check to determine if the mass, height, and air voids were correct. When problems in compaction occurred, it was observed that the number of gyrations was incorrect. Therefore, this was used to first determine if any problems occurred. If the number of gyrations for each lift was within ±2 of the average from the bulked tests, the specimen was not bulked. When the gyrations did not meet the determined averages, bulk specific gravity was measured every time the air voids were off.

3.3.2 Testing Parameters

The structural failure of asphalt layers under traffic is generally attributed to two modes of failure: fatigue and rutting. In order to assign proper layer coefficients to various materials used in asphalt pavement, each of the materials should be tested for these failure modes. Due to time and equipment

limitations, the work in this thesis covers only rutting behavior. The rutting testing was conducted in a tri-axial cell apparatus that is designed to create compressive stresses combined with some shearing action. The resilient modulus was also investigated since this is the traditional method employed to determine layer coefficients.

3.3.2.1 Unbound Material Parameters

The unbound granular material was tested at ambient temperature (22°C) on the assumption that there is no freezing and the material drains adequately. Ambient temperatures are used because granular materials are not generally dependent on temperature unless the water within them freezes.

The materials were tested at two moisture contents. Originally the moisture contents that corresponded with the 95% density line drawn against the modified proctor results were used. For the 50-50 material this corresponded with moisture contents of 1.8% and 10.4%. For the pulverized material the moisture contents were 1.5% and 10.5%. The 95% of maximum density mark was chosen because this is generally the density targeted in field construction. However, it was discovered early on in the testing that the 10% moisture contents were too high. Results could not be generated due to rapid specimen failures. The wet level moisture contents had to be dropped to 5%. This level generated completed tests and repeatable results. The PCC-AC materials were tested in their dry conditions only.

As for resilient modulus testing, the AASHTO T294-94 (SHRP P46) specification was used. The materials in this project fall into the type 1 soil category. All the specified confining pressures (σ_3) and deviator stresses (σ_d) specified in AASHTO T294 were used in the testing.

The determination of σ_3 and σ_d applied for the rutting tests was approached from two directions. First σ_3 values needed to be established. This was first done by performing a wedge analysis under a strip load to approximate the horizontal pressure at the edge of a loaded area. This assumes that rutting occurs as a series of bearing capacity failures. This analysis generated a σ_3 of 52.4kPa. Confining pressure was also checked under a circular flexible, uniformly loaded plate using elastic theory. This gave a σ_3 of approximately 75kPa; it also suggested that at σ_3 mid-depth of an assumed 18" base course was 35kPa. From these analyses a starting σ_3 value of 34kPa (5psi) was used in a series of rutting step tests. These tests used varying principle stress ratios (σ_1/σ_3) to determine the key stress parameters to use for the final rutting tests. Three different load repetition values were tried: 100, 1000, and 10,000. From the

results of the trials, σ_1/σ_3 ratios of 2 and 4 were selected; when the ratio increased much above 4, the specimens failed. The number of repetitions was set at 1000. It was noticed that the granular materials stabilized after approximately 100 repetitions and that the increase in permanent deformation became linear.

Once the σ_1/σ_3 ratios were established, a pavement analysis was performed using the KENLAYER program. Actual pavement geometries were used in the analysis along with material properties. The stresses calculated by KENLAYER ranged from 30kPa to 241kPa. The 85th percentile was picked from this range, using the following tri-axial relationship

$$\sigma_3 + \sigma_d = \sigma_1 \quad (46)$$

where

σ_3 = confining pressure

σ_d = deviator stress

σ_1 = total axial stress.

From this relationship along with a σ_1/σ_3 ratio of 2, a high end σ_3 of 103kPa was determined. Finally, using the σ_1/σ_3 ratios of 2 and 4, σ_d values were established.

3.3.2.2 Asphalt Surface Course Parameters

The parameters for temperature, stress, and density were picked based upon the levels expected in actual field conditions. A σ_3 equal to 103kPa with a σ_1/σ_3 ratio of 4 was used so that comparisons with the ABC materials could be made. However, the upper σ_1/σ_3 ratio was raised to 5.4 to represent the higher stress levels experienced by the surface layers. The higher total axial stress (σ_1) was selected to simulate a 553kPa (80psi) pressure.

The density issue was resolved by looking at field construction conditions. Since roads are generally opened to traffic at 7% air voids, it was decided to mimic that level to better simulate field conditions. The gyratory compactor was used to produce samples with a density of 93% G_{mm}.

Two temperatures were selected that would bracket the average high pavement surface temperature of 58°C, which is commonly experienced in Wisconsin. A range of 12°C was chosen to establish if there was any temperature effect and if so how severe the temperature effect is. Therefore, all

bound material rutting tests were conducted at 52°C and 64°C. The resilient modulus tests were conducted at 20°C. This is the temperature that is traditionally used to derive layer coefficients from resilient modulus data.

The rutting tests for the asphalt materials were run for 6000 cycles or 6% strain, which ever came first. The 6% strain was considered as representative of pavement failure conditions. The number of cycles was increased because of the visco-elastic nature of the material. The 6000 cycles were selected to limit the time of testing with a reasonable time period. All of the testing parameters are presented in Table 3.9.

As described previously ABC is a bound material. However, it is used as a base course rather than a surface course. Therefore, a special protocol was established to include some of the testing parameters used for granular materials and the parameters used for the bound materials.

This material is produced, transported, paved, and compacted like a surface asphalt mixture. Surface mixes experience relatively high temperatures when manufactured as well as during their life spans. To compare the ABC to the other mixes, the ABC was tested at the same temperatures as the surface mixtures. Those temperatures and how they were determined are discussed in the next section.

Testing the ABC was done at some of the same stress conditions that the granular material was tested at because the ABC will be in a lower layer of the asphalt pavement and, therefore, will naturally experience lower stresses. One confining pressure was used: σ_3= 103kPa, which is one of the stress conditions used for testing the surface materials.

Resilient modulus tests for this material were conducted according to the AASHTO T294-94 (SHRP P46) specification. This is not the traditional testing method for resilient testing of asphalt materials. Resilient modulus tests for asphalt materials are specified by ASTM D 4123-82 (1995), which is an indirect tensile type test. The tri-axial M_r was done because the rutting tests were performed in the tri-axial apparatus and this method of testing better simulates the actual pavement loading, experienced under traffic. Also, using the tri-axial method for both the rutting and resilient modulus tests would allow for an easy comparison between the results from both tests. The M_r test was conducted at both temperatures used for the rutting tests as well as at 20°C. There was no deviation from the stress levels specified by AASHTO T294-94.

3.3.3 Data Collection Methods

All of the testing took place in a steel and aluminum tri-axial cell. The cell was built to fit the AASHTO T294-94 (SHRP P46) specification for granular resilient modulus testing. The design, however, deviated from the specifications in two respects: first, the load cell was positioned outside of the cell rather than inside. Second, the porous stones were not included in the set-up. Both changes were assumed to have a negligible effect.

Table 3.9 Laboratory Testing Parameters

Unbound Recycled Granular Materials					
Pulverize w/13%			50-50 Milled Asphalt &		
ω (%)	σ_3 (kPa)	σ_d (kPa)	ω (%)	σ_3 (kPa)	σ_d (kPa)
1.5	34	34	1.8	34	34
1.5	34	103	1.8	34	103
1.5	103	103	1.8	103	103
1.5	103	310	1.8	103	310
5	34	34	5	34	34
5	34	103	5	34	103
5	103	103	5	103	103
5	103	310	5	103	310

	90P-10A		70P-30A		50P-50A	
ω (%)	σ_3 (kPa)	σ_d (kPa)	σ_3 (kPa)	σ_d (kPa)	σ_3 (kPa)	σ_d (kPa)
0	34	103	34	103	34	103
0	103	103	103	103	103	103

Load Repetitions (N)	1000
Density	$0.95\gamma_{d,max}$
Temperature (°C)	20

Asphalt Materials														
ABC			SMA			SHRP			HV			MV		
T °C	σ_3 (kPa)	σ_d (kPa)	T °C	σ_3 (kPa)	σ_d (kPa)	T °C	σ_3 (kPa)	σ_d (kPa)	T °C	σ_3 (kPa)	σ_d (kPa)	T °C	σ_3 (kPa)	σ_d (kPa)
52	103	103	52	103	310	52	103	310	52	103	310	52	103	310
52	103	310	52	103	450	52	103	450	52	103	450	52	103	450
64	103	103	64	103	310	64	103	310	64	103	310	64	103	310
64	103	310	64	103	450	64	103	450	64	103	450	64	103	450

Load repetitions (N)	6000
Density	0.93 G_{mm}

A top-mounted hydraulic actuator was used to apply the load. An environmental chamber located below the actuator supplied the desired temperature conditions. Two Linear Variable Differential Transducers (LVDTs) recorded the vertical deformations; they were placed on opposite sides of the

loading rod at an 180° angle. The LVDTs were attached directly to the cell, eliminating noise caused by the deformations in the load cell or testing frame. Figure 3.8 shows a diagram of the tri-axial cell.

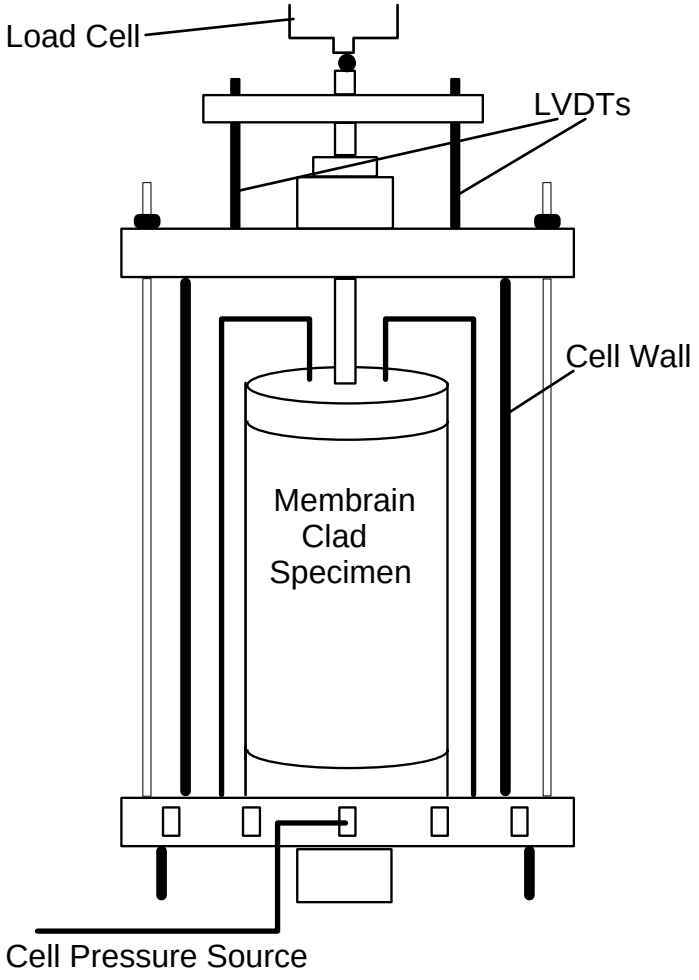

Figure 3.8 Schematic Diagram of a Tri-Axial Cell

3.3.4 Laboratory Data Transformation Techniques

This section describes how the data generated from the resilient modulus and rutting tests were analyzed. The data was collected in a text file format that listed the measurements recorded and it included step and sequence numbers. An example of the data file is shown in Figure 3.9.

3.3.4.1 Laboratory Resilient Modulus Calculations

The resilient modulus calculation was performed by importing the text files into an Excel

spreadsheet and then copying and pasting it into a calculation template. The template first sorts the data and removes any negative displacement readings. Next, the maximum load deviator stress (σ_d) was calculated by taking the absolute value of the high deviator stress reading. A dynamic deviator stress ($\sigma_{d\ dynamic}$) was determined by subtracting the low deviator stress from the high deviator stress. The bulk stress (Θ), the final stress needed, was calculated using the following equation;

$$\Theta = \sigma_d + 3\sigma_3 \tag{47}$$

1999	2	12	10:47:54							
Test Seq.# Test Step 0 Test Step 1	High Dev Stress (kPa)	High Disp #1 (mm)	High Disp #2 (mm)	High Cox (mm)	Low Dev Stress (kPa)	Low Disp #1	Low Disp #2	Low Cox	CellPx (kPa)	Chamber Temp (deg C)
1	-16.437508	0.818865	0.852661	-28.00549	-17.052633	0.817625	0.851111	-28.0336	104.25	43.96155
2	-16.3179	0.81902	0.852971	-28.01393	-17.052633	0.817625	0.851421	-28.0308	104.42	43.98244
3	-16.352074	0.838088	0.869249	-28.02236	-45.809729	0.8184	0.852041	-28.0617	104.7	44.00639
4	-41.725982	0.841499	0.87297	-28.04203	-48.987875	0.836538	0.868164	-28.0645	104.51	44.0279
5	-39.81226	0.858552	0.888008	-28.04766	-71.832935	0.840569	0.87142	-28.0842	104.79	44.04766
6	-39.248395	0.866459	0.895604	-28.05047	-80.273818	0.84708	0.877311	-28.0983	104.66	44.06932
7	-39.026267	0.878551	0.904596	-28.05609	-92.422537	0.851576	0.881031	-28.1067	104.93	44.09142
8	-39.00918	0.887853	0.913433	-28.05328	-103.528962	0.855762	0.883512	-28.1207	104.7	44.11188
9	-38.376968	0.897775	0.922579	-28.06452	-114.977122	0.859948	0.886458	-28.1236	104.46	44.13576
10	-38.325707	0.908782	0.931106	-28.06452	-125.827245	0.863513	0.889558	-28.1432	104.39	44.15767
11	-37.898537	0.919789	0.939633	-28.07014	-137.241231	0.867389	0.893124	-28.1545	104.47	44.17555
12	-37.590975	0.929866	0.948469	-28.07296	-148.074267	0.87142	0.895604	-28.1657	104.06	44.19593
13	-37.146718	0.941338	0.958701	-28.08139	-160.154639	0.875605	0.89948	-28.177	104.15	44.21479
14	-36.634114	0.95188	0.967848	-28.08139	-171.927449	0.879636	0.903201	-28.191	104.35	44.23424
15	-36.463246	0.963972	0.978235	-28.08139	-184.913422	0.883822	0.907231	-28.2023	103.74	44.254
16	-35.916468	0.97715	0.989242	-28.09544	-200.12068	0.887388	0.911417	-28.2191	103.93	44.27191
17	-35.865207	0.989552	0.999939	-28.09544	-211.961837	0.892814	0.915603	-28.2276	104.21	44.28822
18	-35.130475	1.002109	1.011411	-28.10106	-226.17806	0.89762	0.920099	-28.25	104.39	44.30521
19	-35.164648	1.014822	1.022108	-28.10388	-238.719776	0.902426	0.924595	-28.2585	104.1	44.3214
20	-34.429916	1.027534	1.034045	-28.1095	-252.713871	0.907386	0.928936	-28.2782	104.13	44.33571

Figure 3.9 An Example of a Test Data File Generated by the Tri-Axial Testing Equipment

Next, the resilient deformations and resilient strains were calculated. The resilient deformations (Δ_{r1}, Δ_{r2}) were the differences between the high and low displacement readings for each step over channel 1 and 2. An average of the two resilient deformations ($\Delta_{r\ avg}$) divided by the average over the initial and final specimen height was used to determine the average resilient strain ($\varepsilon_{r\ avg}$).

The resilient modulus was calculated for each of the 1500 load cycles using the relation of stress over strain.

$$M_r = \frac{\sigma_{d\ dynamic}}{\varepsilon_{r\ avg}} \tag{48}$$

AASHTO T294-94 specifies 15 separate load steps with varying σ_3's and σ_d's. An average is calculated on the last 5 cycles from each of those load steps. These averages are the final resilient modulus numbers generated for analysis. Table 3.10 shows the σ_3's and σ_d's specified in AASHTO T294-94.

Table 3.10 Testing Sequence for Type 1 Soils

Sequence No	σ_3 (kPa)	σ_d (kPa)	Load Applications
0*	103	103	1000
1	21	21	100
2	21	41	100
3	21	62	100
4	34	34	100
5	34	69	100
6	34	103	100
7	69	69	100
8	69	138	100
9	69	207	100
10	103	69	100
11	103	103	100
12	103	207	100
13	138	103	100
14	138	138	100
15	138	276	100

* preconditioning

3.3.4.2 Permanent Deformation (Rutting) Calculations

The data generated from the rutting tests is in the same format as those from the resilient modulus tests. However, the σ_3's and σ_d's are constant over a test length of 1000 to 6000 cycles. The calculations used to generate the final results also differ from those of the resilient modulus tests.

An Excel rutting template is used to generate the final results. The data is pasted into the template then it is sorted and any negative deformation values are removed. Only strain values need to be generated for these tests. The low readings from the LVDTs (Δ_d) are added to the starting deformation (Δ_0) and divided by the initial specimen height or gage length. These permanent strains (ε_p) are plotted against the load repetition number (N). These plots are, then, used for the analysis of the data.

CHAPTER FOUR

FIELD TESTING RESULTS AND ANALYSIS

This chapter presents the entire field data collected during this study. The first section covers the back-calculation method used by the research group headed by Young (1997). The second section looks at the resilient modulus by presenting the corresponding layer coefficients produced by the methods outlined in the 1993 AASHTO Guide for Design of Pavement Structures. Figures 4.1 and 4.2 provide examples of the data generated by the FWD. The drop height represents the height used in the FWD testing. Different heights provide an indication of the linearity of the materials and the effect of higher impact load on the deflection basin.

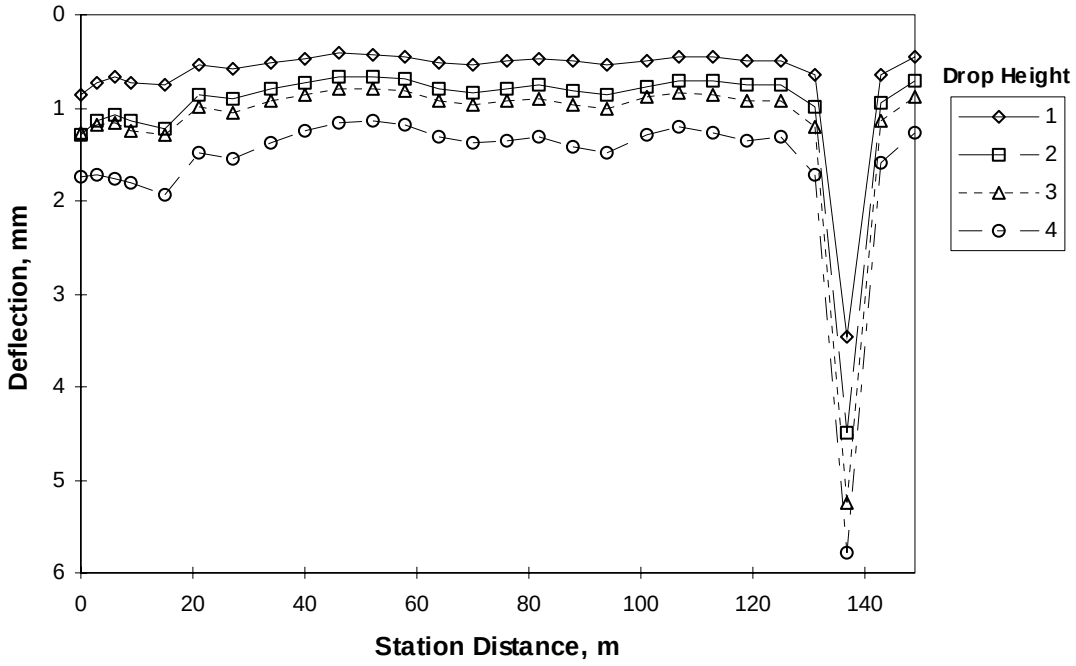

Figure 4.1 Deflection from MV Section Sub-base

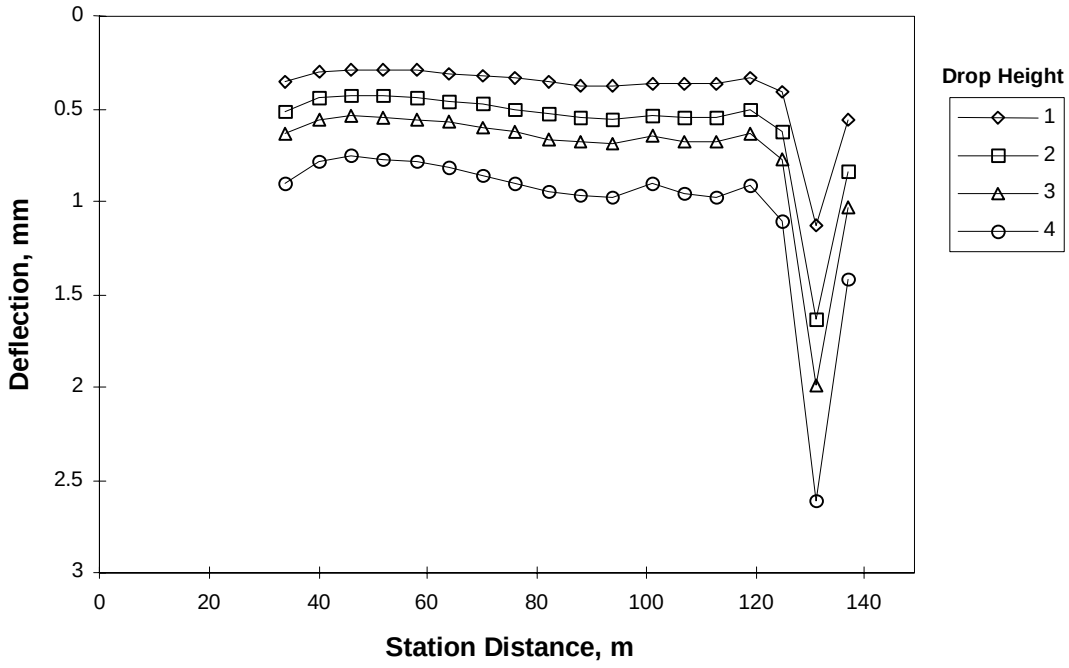

Figure 4.2 Deflection from MV Section AC Surface

4.1 Resilient Modulus Calculations

All of the moduli backcalculations were performed by MODULUS, which is a software program for backcalculating layer moduli. This program can be applied to a two-, three-, or four-layer system with or without a stiff layer. The latter is a theoretical line past which no deformations will occur. MODULUS is a linear elastic program that generates a database of deflection bowls by assuming different modulus ratios. Measured and calculated bowls are run through a pattern search routine that minimizes the error function between the measured and calculated bowls.

To complete the backcalculations, a seed modulus and moduli ratios are required. Once these values are determined, another pattern search routine is used to find the optimum set of modulus ratios so that a minimum error is obtained.

Stiff layer type analyses were used on all of the test sections. The number of layer analysis was determined by the pavement geometry of each test section. The pavement geometries can be seen in Table 4.2. A discussion of the results is found in the next section.

4.2 Field Testing Results

Table 4.1 shows the average M_r obtained from each of the sections material types tested. A detailed discussion of the backcalculation technique can be found in the literature review. Table 4.2 shows the corresponding layer thickness of each section.

The final M_r results for the MV section are shown in Figure 4.3. As or Figure 4.4, it shows the M_r values obtained from the SHRP field data. To achieve the final M_r values for this section, the test on the ABC layer itself was used instead of the test on the entire completed asphalt pavement. The results from ABC pavement are shown in Figure 4.5. All of these sections were analyzed using the stiff layer technique with the stiff layers recommended by MODULUS being utilized.

The M_r values calculated by Jong et al. (1997) were analyzed using the equations suggested by Mustaque and his co-reserarchers in 1997 presented in section 2.2.1.1 of this report. Table 4.1 is a summary of M_r and a_i estimated from FWD results.

Table 4.1 Summary of M_r and a_i Estimated from FWD Results

Material		Resilient Modulus M_r (MPa)	Layer Coefficient a_i	Test Temp (°C)	Wisconsin Layer Coefficients	
					1972	1997
SHRP	Max	2225	0.388	15.6	0.44	0.44
	Avg	1645	0.336			
	Min	1550	0.325			
MV	Max	455	0.112*	32.2	0.44	0.44
	Avg	385	0.083*			
	Min	312	0.047*			
ABC	Max	1060	0.2	6.1	0.3	0.34
	Avg	714	0.13			
	Min	275	0.05			
Pul	Max	1814	0.39*	15.6	0.1	0.1-0.25
	Avg	814	0.31*			
	Min	250	0.195			

* values lie outside the suggested range of the equation

Table 4.2 Section Layer Thickness

Thickness	SHRP (in)	ABC (in)	MV-29 (in)	Pulverized Asphalt (in)
Asphalt Layer	9	7	7	4.5
Base Layer	13	12	6	6
Subbase	-	4	-	8.6
Subgrade	Infinite	infinite	infinite	infinite

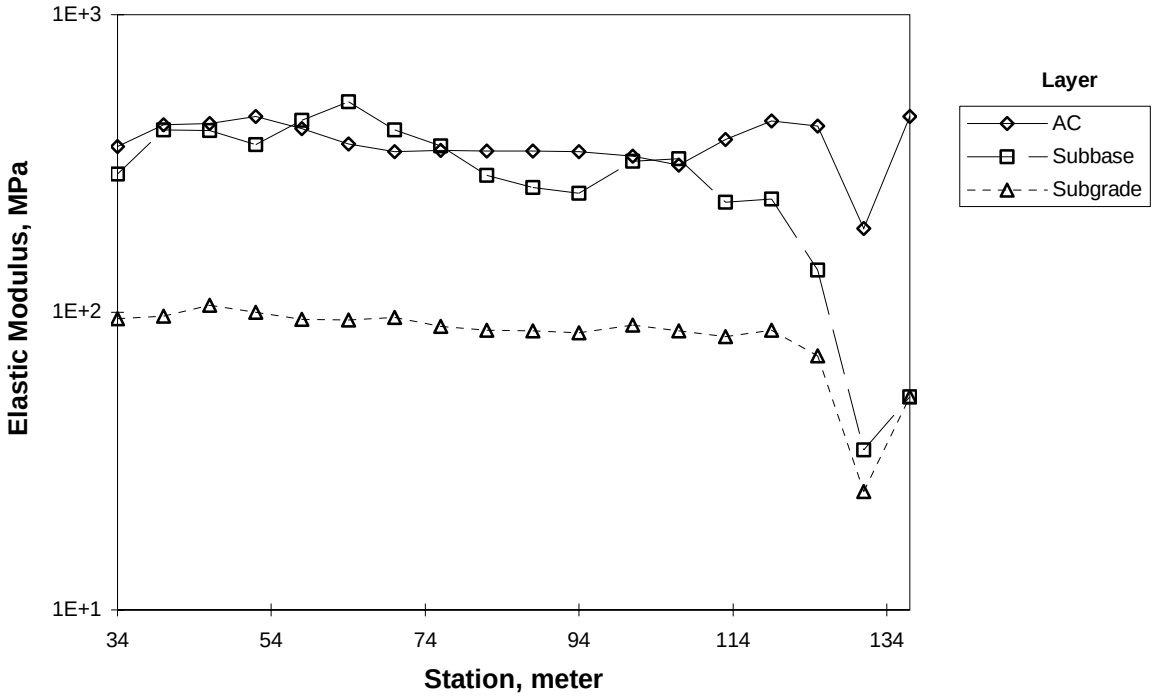

Figure 4.3 The Backcalculated M_r Results from the MV Section

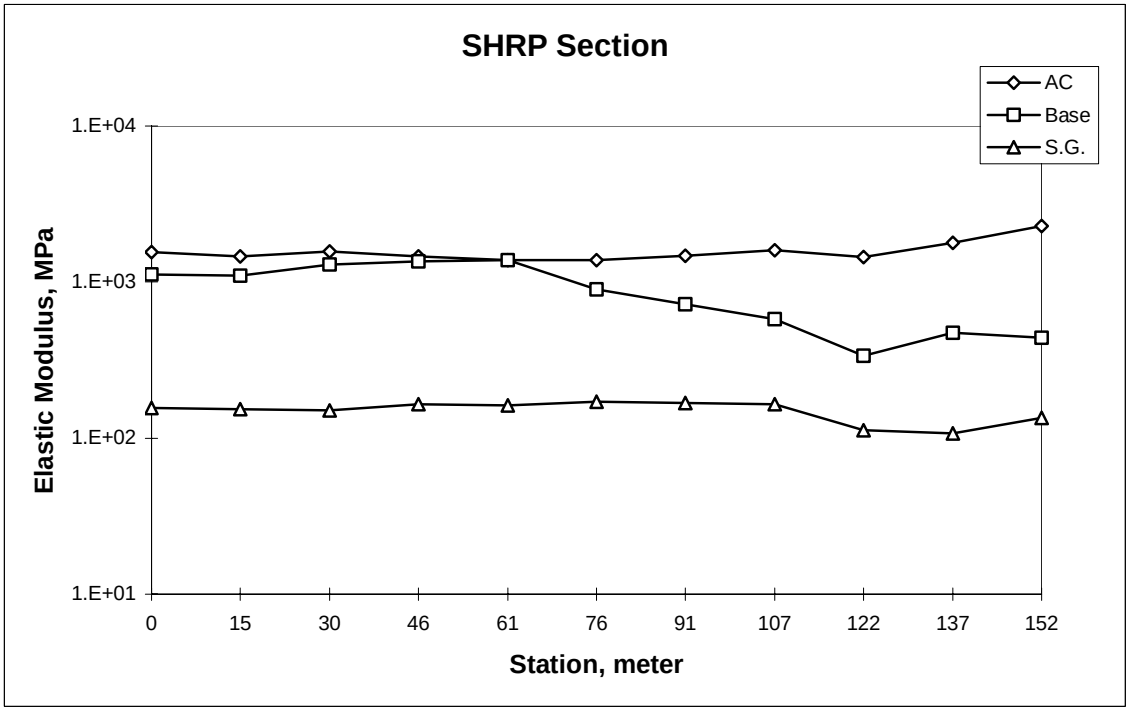

Figure 4.4 The Backcalculated M_r Results from the SHRP Section

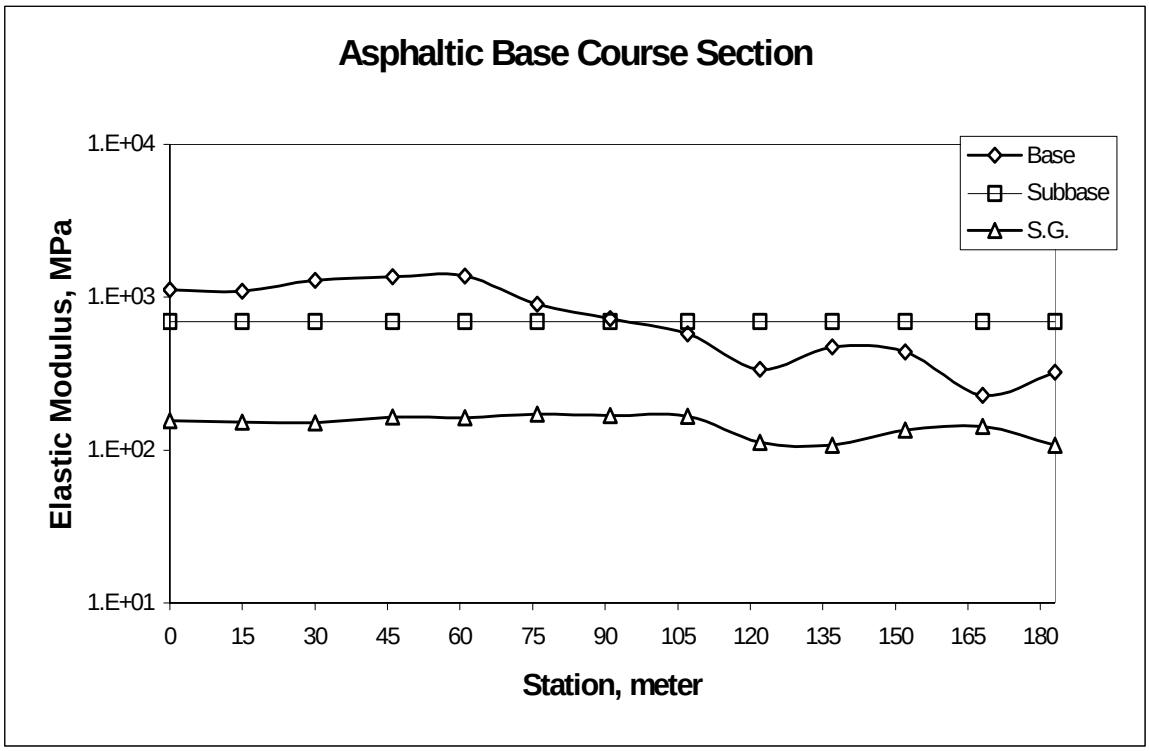

Figure 4.5 The Backcalculated M_r Results from the ABC Section

CHAPTER FIVE

LABORATORY RESULTS AND ANALYSIS

This chapter is divided into three sections: the first part covers the testing conducted to establish the repeatability of test results. The second part covers the laboratory results collected for the granular materials included in the study. The third part presents the results of testing the different asphalt mixtures included in the study. It is worth noting that the chapter includes only samples of the data collected. Tables of the entire collection of laboratory M_r and rutting tests are shown in Appendix B.

5.1 Repeatability Testing and Confining Pressure Control

Duplicate measurements were conducted for resilient modulus testing of all materials. Because of the limited amount of materials available from the field, it was realized that in some cases samples will have to be made out of compacted materials. Duplicate measurements were, therefore, conducted to compare virgin-to-virgin materials and virgin-to-recompacted material. The tests were performed on both the asphalt and granular materials. The tests showed good repeatability in all areas tested. Figure 5.1 shows the results for two tests conducted on the 50-50 material in the dry condition; both specimens were produced from re-compacted material. There is, on average, a 5% difference between the two test results. In addition to the material variability, two different testing frames were used in this study. Therefore, multiple trials were performed to test and verify that the results collected by the two testing frames are comparable. The comparison indicated that the test results remained in a range of 10% difference or less.

The procedure to produce an asphalt specimen from material already compacted and tested included heating two or more used specimens in a pan covered with aluminum foil, mixed thoroughly, and then recompacted. This process was developed to insure that the materials used in preparing specimens were homogenous and representative. The aluminum foil was used to lessen the aging process by protecting the material from the hot air flow within the oven. To reproduce the granular specimens, the material was dried, mixed with the necessary amount of water, and then recompacted.

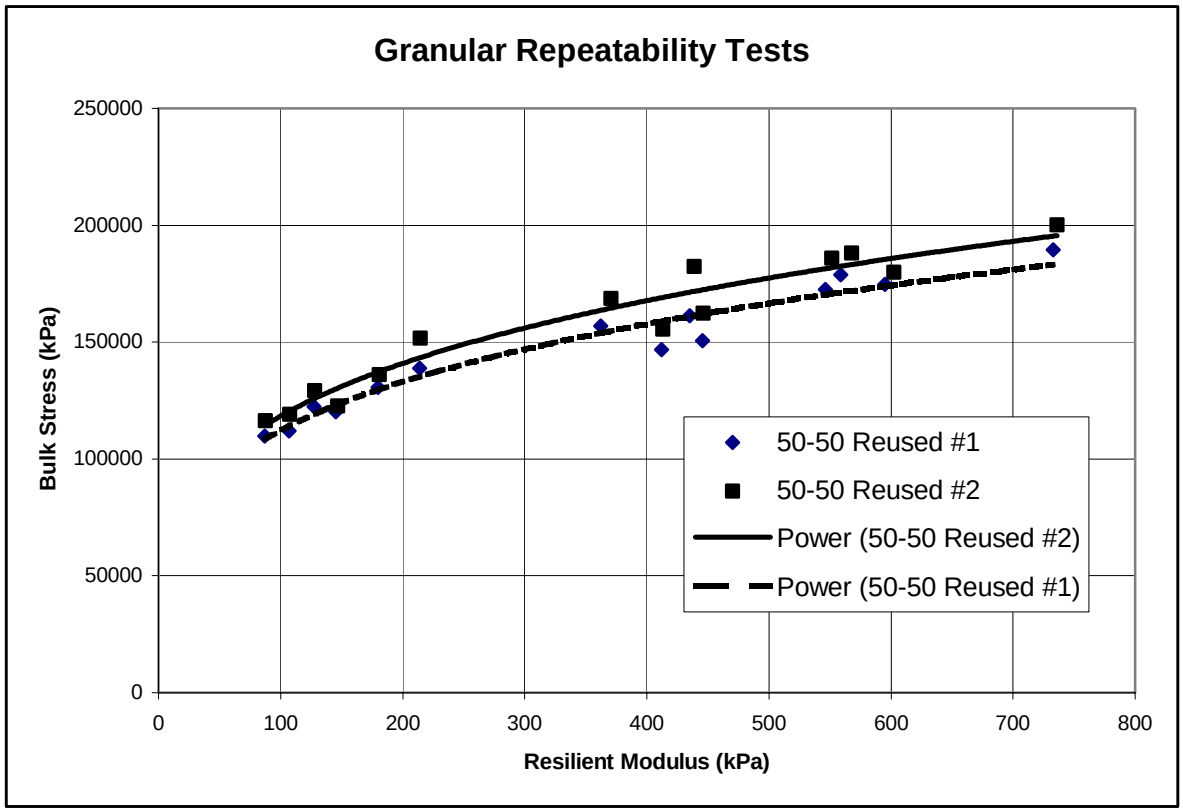

Figure 5.1 50-50 M_r Trials Showing Test Repeatability

To keep the variability due to equipment to a minimum, all of the granular rutting tests and asphalt tests were conducted in the new test equipment. Repeatability tests were conducted to test the repeatability of materials and equipment involved.

Controlling the confining pressure was another challenge faced in conducting the triaxial testing. During the early testing of the asphalt mixtures. It was also observed that the resistance to rutting was relatively low compared to what is reported in the literature. Also it was observed that the confining pressure did not affect the results significantly, which was something unexpected. Careful examination of the equipment indicated that there were two holes in the steel top plate. These holes allowed the pressurized air to access the inside of the specimen by effectively eliminating any confining pressure effects. Because of this problem, the specimens failed prematurely. Under these harsh conditions, specimens failing in 500 cycles or less, good repeatability was still achievable. Once the confining pressure problem had been discovered and corrected, many tests had to be performed again; these were referred to as second-generation tests. Repeatability tests were again conducted to verify results and

trends. Figure 5.2 shows the repeatability of two SHRP 103-450-64 tests. One of the specimens came from material that was reused only once; on the other hand, the second specimen was made from material that had been reused several times. The two tests remained nearly consistent over the entire test length of 6000 cycles. A difference of 0.063% strain had been identified.

The repeatability was seen in asphalt rutting tests, asphalt M_r tests, and in granular rutting tests. With the repeatability of these tests confirmed the remaining tests were only run once. However, some other repeats were performed when those tests did not conform to developing trends.

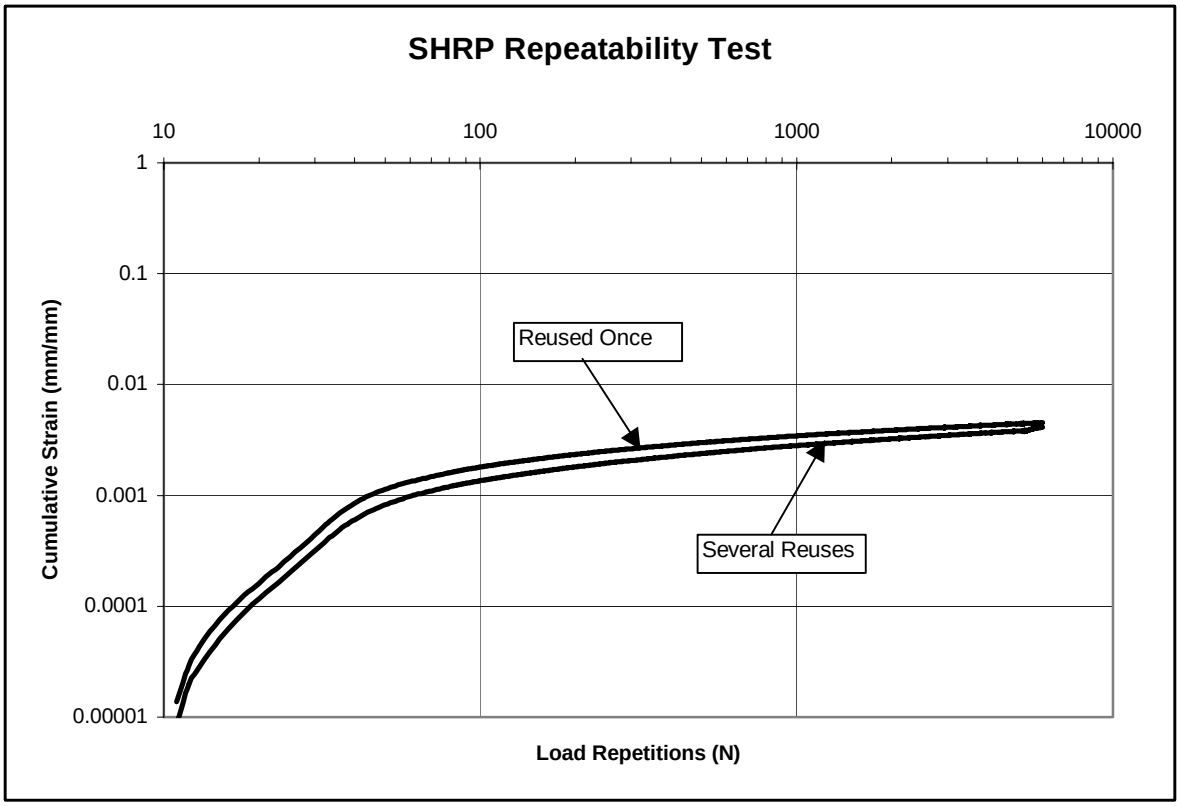

Figure 5.2 SHRP Rutting Repeatability – Confining Pressure Applied

5.2 Unbound Material Laboratory Results and Analysis

This section presents the results of the testing of the granular unbound materials. It is divided into two subsections: the first covers the resilient modulus testing and the second the rutting testing.

5.2.1 Resilient Modulus Results

Five recycled asphalt materials were tested for this research. One was a milled asphalt with 50% virgin aggregate added in (50-50); another was a pulverized asphalt that included 13% shoulder aggregate (Pul). The remaining materials were combinations of recycled portland cement concrete and recycled asphalt materials (90P-10A, 70P-30A, and 50P-50A). Whereas the 50-50 and Pul materials were tested for resilient modulus (M_r) and permanent deformation (rutting) at two water contents, the others were tested in dry conditions only. While this section covers the M_r results, the next highlights the rutting results.

Multiple M_r tests were run for each combination of testing parameters according to the AASHTO standard procedure. Using the resilient strain, the resilient modulus values (Mr) were calculated and plotted as a function of the bulk stress. A power-law curve was fitted to the plots for each material to represent the variation of Mr with bulk stress

An example of results for the pulverize dry M_r tests is shown in Figure 5.3. The power model fit generates two parameters, K1 and K2. As shown in Figure 5.3, a K1 of 21624 and a K2 of 0.3925 were estimated for the material tested, with the K2 being the exponent. The K1 and K2 values obtained from the power-law equation were averaged over all the tests, and an average M_r curve was generated for each material in both the wet and dry condition. The final M_r results for the granular (unbound) materials tested in this study are shown in Figure 5.4.

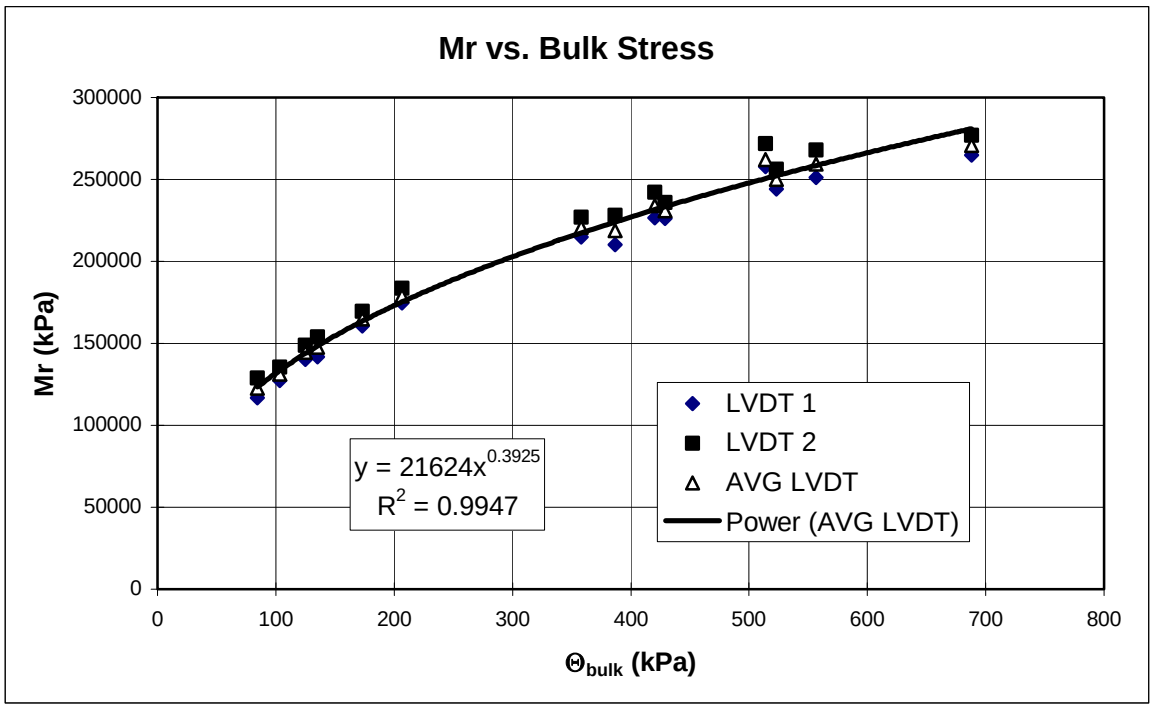

Figure 5.3 Pulverize with 13% Shoulder Aggregate – Dry M_r Test Results

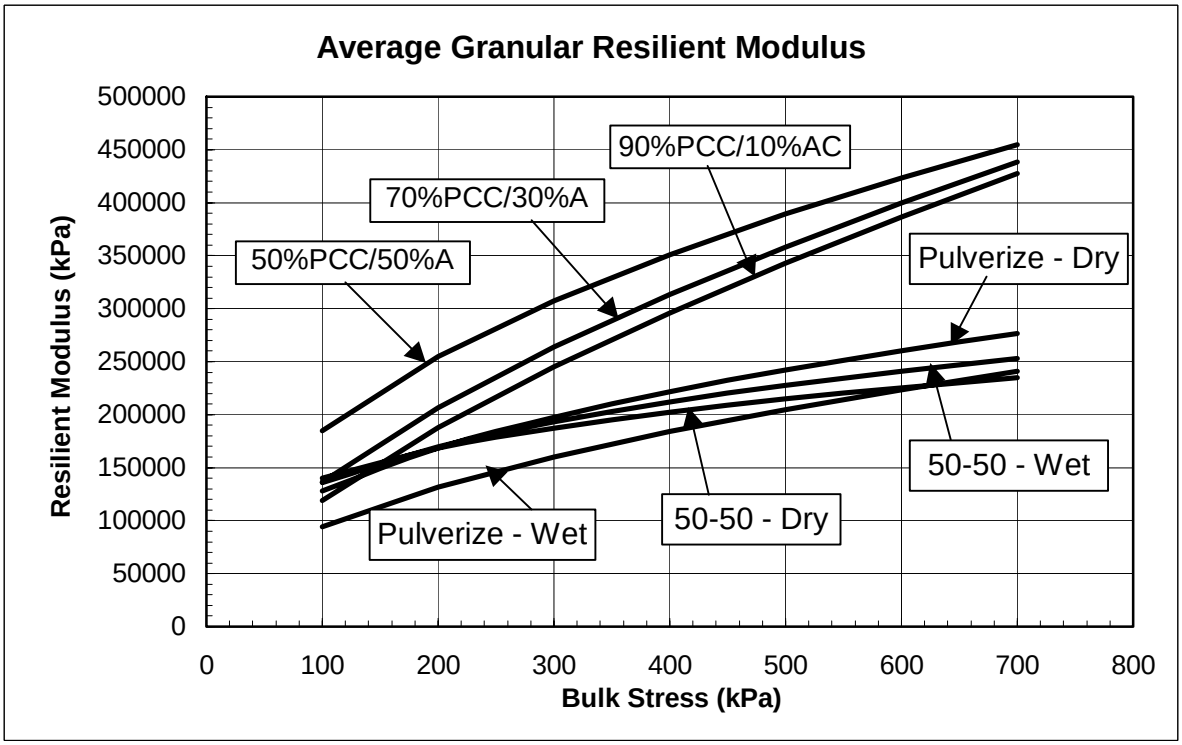

Figure 5.4 Final M_r Test Results for the Granular Base Course Materials

5.2.1.1 A Comparison of the Results of Different Materials

The results for the unbound recycled materials at the bulk stresses of 200 Kpa and 400 Kpa are shown in Table 5.1. The first part of the table shows the results are for the dry and wet conditions of the pulverized and the 50-50 mixes. The second part shows the results for the dry condition of the PCC-AC recycled materials. The PCC-AC recycled materials were not tested wet because they contain no granular materials that could be sensitive to moisture. The low (200 Kpa) and high (400 Kpa) bulk stress levels are shown to simulate various depths within a typical pavement structure.

The pulverized mixture shows the highest sensitivity to bulk stress and to moisture condition. Higher M_r values are calculated for a higher bulk stress and lower moisture content.

The 50-50 mixture shows negligible sensitivity to moisture. The dry and wet results are within the repeatability range. The effect of bulk stress is similar in trend to the pulverized mixture, although slightly lower. On average, the M_r values of the dry 50-50 mixture are similar to those of the dry pulverize material. The wet M_r values for the 50-50 mixtures are, however, higher than those of the pulverize wet mix, particularly at the low bulk stress.

All the PCC-AC materials show higher M_r values compared to the 50-50 and the pulverized material. It is also observed that Mr values of the PCC-AC material increase as the percentage of recycled asphalt material (AC) increases in the mix.

Table 5.1 Base Material M_r and a_2 Values

Bulk Stress (kPa)	Pulverize				50-50			
	Dry		Wet		Dry		Wet	
	M_r (MPa)	a_2	M_r (MPa)	a_2	M_r (MPa)	a_2	M_r (MPa)	a_2
200	168	0.155	132	0.131	168	0.155	170	0.156
400	221	0.182	184	0.167	202	0.173	212	0.178

Bulk Stress (kPa)	90P-10A		70P-30A		50P50A	
	Dry		Dry		Dry	
	M_r (MPa)	a_2	M_r (MPa)	a_2	M_r (MPa)	a_2
200	188	0.166	207	0.176	255	0.196
400	296	0.208	313	0.214	351	0.226

5.2.1.2 Calculation of Layer Coefficients for Unbound Materials

Once the M_r values have been calculated, layer coefficients can be estimated using equation (4) presented in Chapter 2. The bulk stress (Θ) value of 200kPa (σ_3 = 34kPa and σ_d = 103kPa) was selected because it represents the worse case scenario found at the top of a base layer: a low σ_3 (confining pressure) and a high σ_d (deviator stress or vertical pressure) value. The Θ value of 400kPa represents an area near the bottom of the base layer where the σ_3 values are higher (σ_3 = 103kPa and σ_d = 69kPa). The layer coefficients for the base materials are presented in Table 5.1 above. Figure 5.5 shows a bar chart comparing the layer coefficients of the materials tested in this study. These layer coefficients compare reasonably well with the existing recommendations and give an estimate of how to rank these unbound materials based on their resilient modulus values.

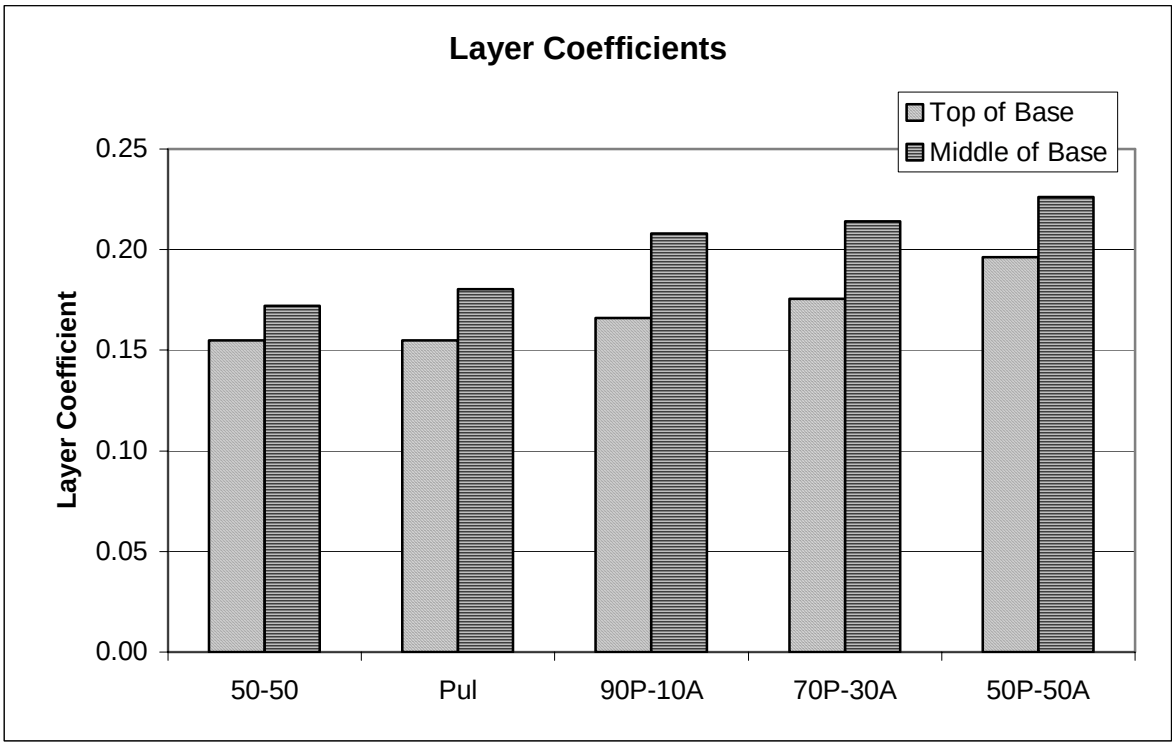

Figure 5.5 Layer Coefficients Estimated for Unbound Material

5.2.2 Permanent Deformation Results

This section covers the rutting tests of all the unbound materials. The results will be analyzed by grouping them in terms of material and stress level. Figures 5.6 and 5.7 give examples of the data generated from the permanent deformation tests. These data were used to estimate the potential for rutting resistance using commonly used modeling techniques. These models, called damage functions, represent the accumulation of permanent deformation.

5.2.2.1 Permanent Deformation Damage Functions

To compare the permanent deformation results to the layer coefficients generated by the resilient modulus tests, the concept of damage functions was used to estimate the rate of permanent strain. The mathematical form of the damage function is shown in equation 49. It is used to determine the linear strain rates (m) observed on a log-log plot of the permanent deformation results.

$$\log(y) = m * \log(x) + b \qquad (49)$$

where

y = permanent strain (mm/mm)

x = number of load repetitions (N)

m = slope of the line

b = y or strain intercept

The strain intercept represents the initial amount of conditioning deformation that occurs during the first load cycle. The slope of the line represents the rate of the increased accumulation of permanent strain. Both values, which are critical to determining the rutting performance of he materials, are shown in Figures 5.8 and 5.9. This model was used to fit the data and estimate the parameters m and b for each of the materials tested.

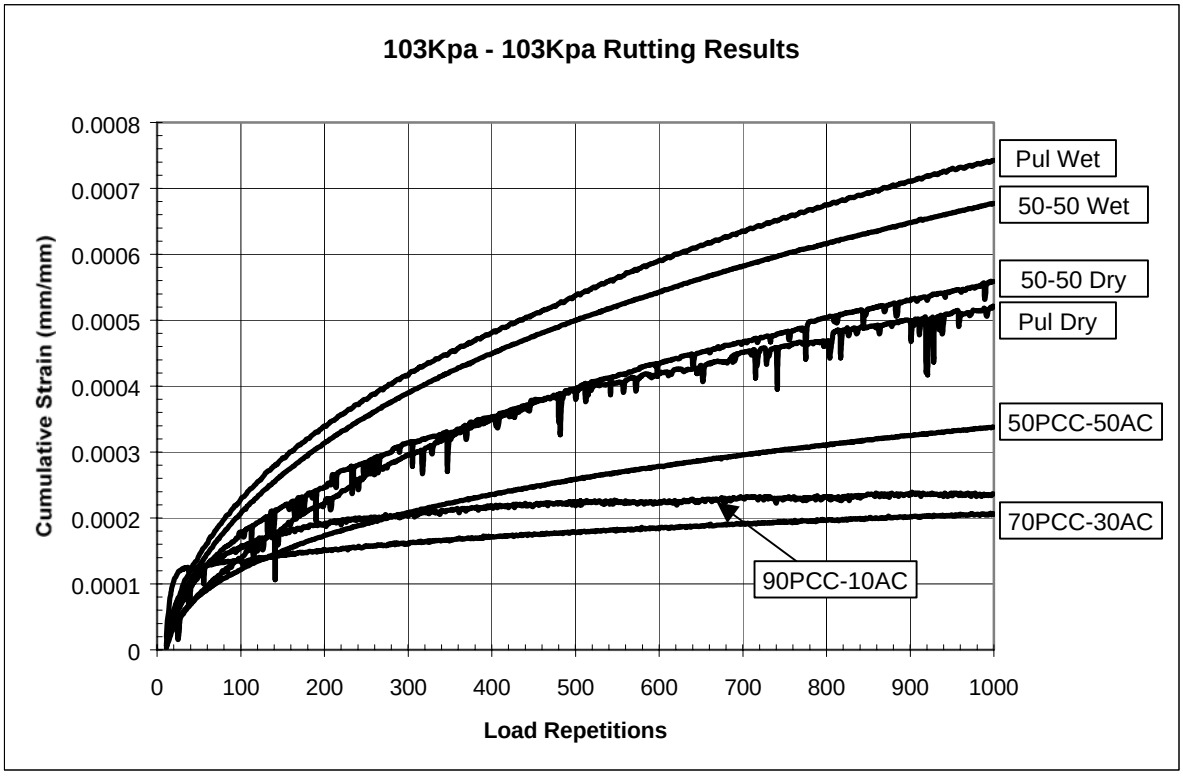

Figure 5.6 Rutting Results of unbound materials at the stress condition of 103kPa σ_3 – 103kPa σ_d

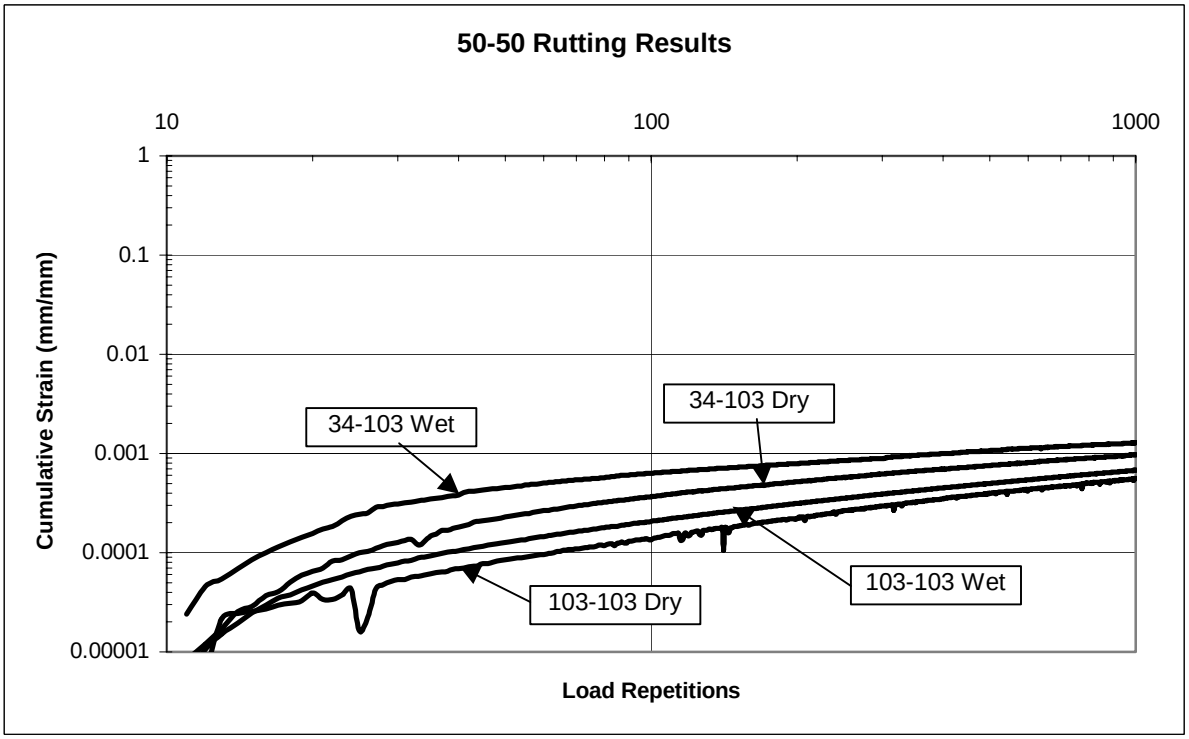

Figure 5.7 Rutting Results for the 50-50 Material at Different Moisture and Stress Conditions

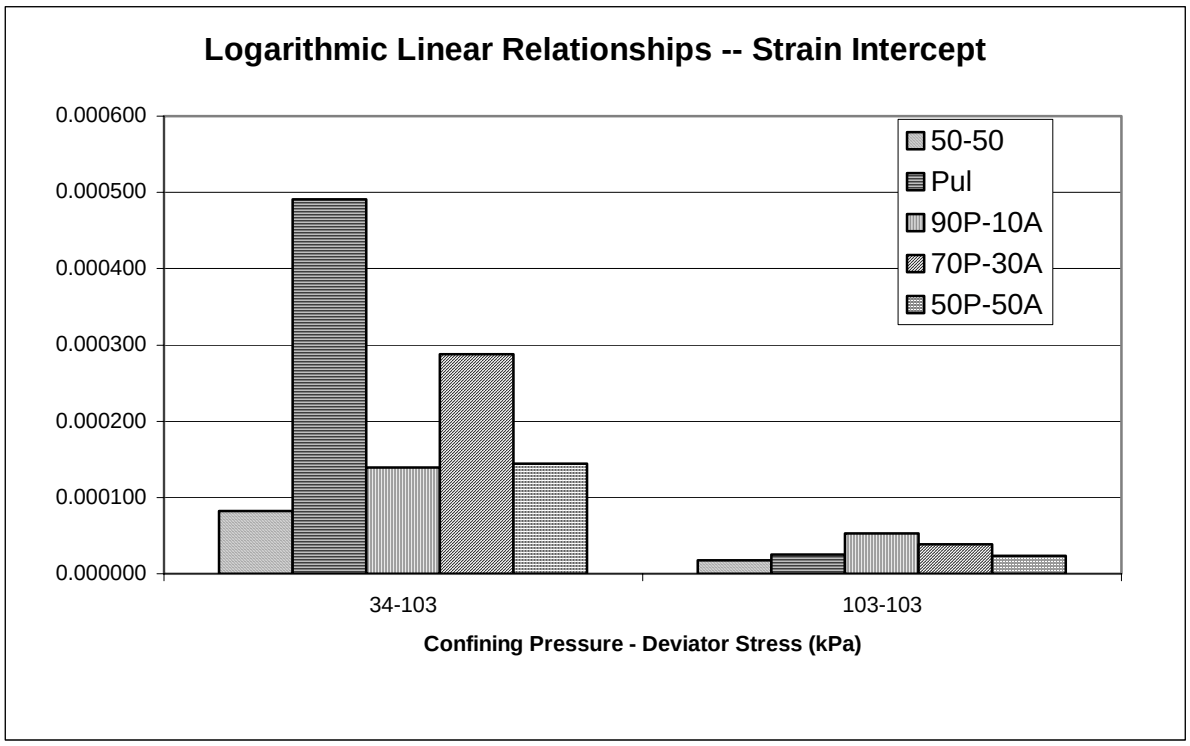

Figure 5.8 Strain Intercepts for Unbound Materials

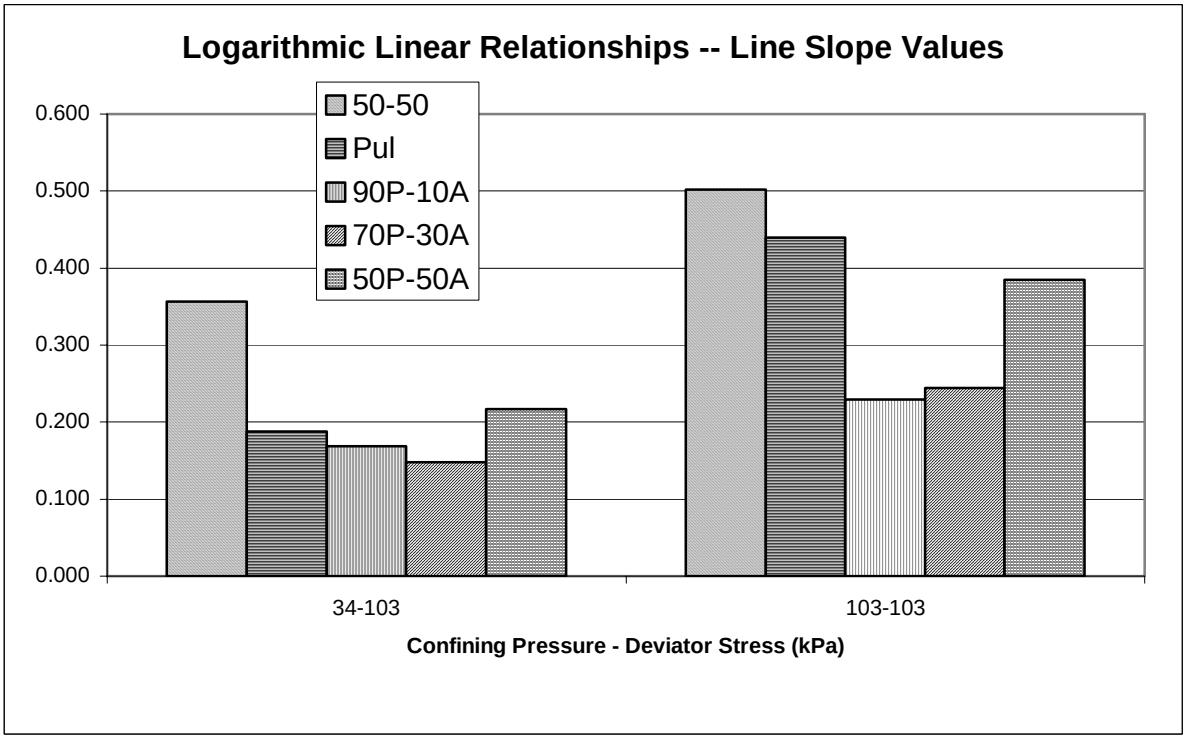

Figure 5.9 Line Slope Values for Unbound Materials

The model parameters can be used to derive the number or repetitions required to reach a certain permanent strain. The number of repetitions can be used to estimate the potential for rutting under a given amount of traffic. Although it is not known how each cycle in the testing is related to number of traffic applications ; these cycles to failure, given permanent strain, can be used for comparative purposes to rank the materials tested. An example is shown in Figure 5.10 at two different combinations of stress conditions.

The testing parameters chosen for analysis were the same as the ones used for the M_r analysis, 34-103 and 103-103 (σ_3-σ_d). The σ_3, which represents the depth from of the pavement surface, will be smallest at the top of the layer and largest at the bottom. The σ_d represents the additional vertical stress applied. The value of σ_d will decrease from the top of the layer to the bottom as the area of stress distribution gets wider. The σ_d was held constant for the analysis in order to maintain a comparison between σ_1-σ_3 ratios. Figure 5.10 shows the number of load repetitions needed to reach a strain of 0.003 for each of the testing parameters analyzed.

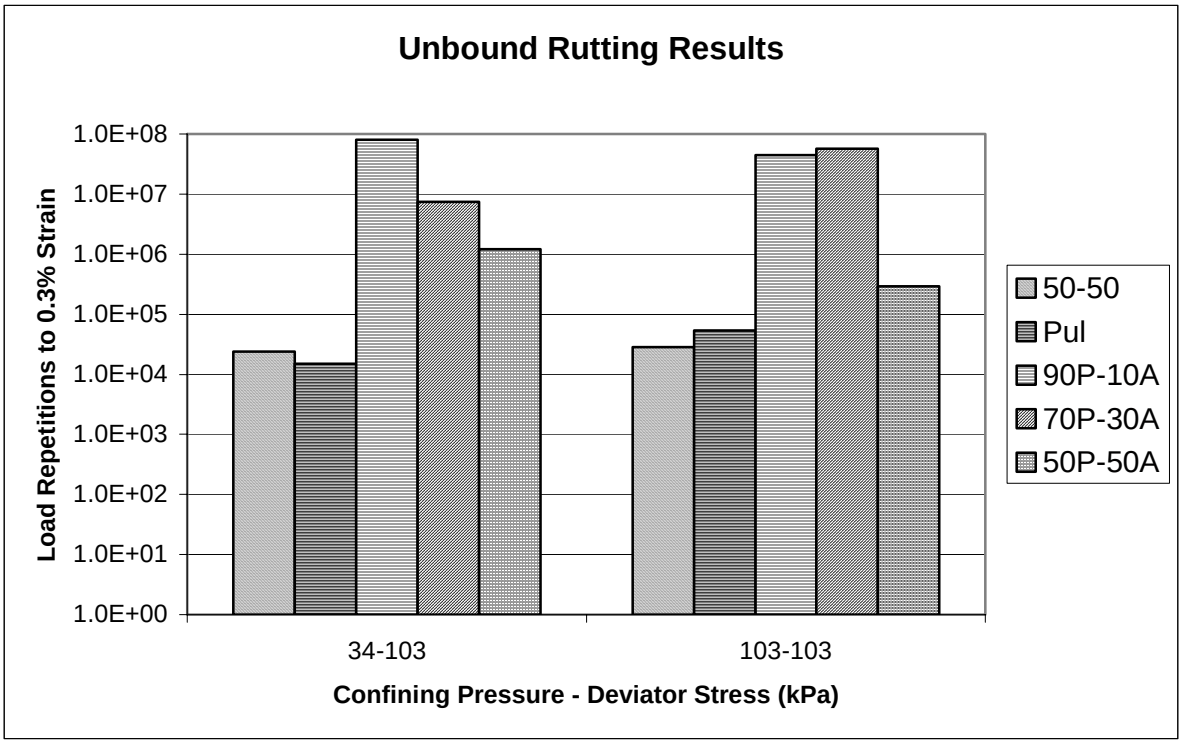

Figure 5.10 Load Repetitions Required to Reach 0.3% Strain for Granular Materials

5.2.2.2 Comparisons of Rutting Behavior

The pulverized material and the 50-50 mixture show very similar average rutting performance. They both show relatively low sensitivity to stress conditions and they both show slightly higher load repetitions under increased confining pressure, which is something expected. The PCC-AC materials outperform both the pulverized and 50-50 materials in rutting resistance. The difference in number of repetitions to failure ranges from 2 to 4 orders of magnitude, depending on the PCC-AC mixture percentages.

Table 5.2 shows the summary of the rutting results and the estimated a_2 factors. Although the 50-50 material does not show high sensitivity to stress ratio, it displays a moderate level of sensitivity to moisture conditions. The a2 values do not match the relative change in N0.003 values for this material. In fact, at the ratio σ_1-σ_3 of 4, the trend of the $N_{0.003}$ values is opposite to the trend of the a_2 values.

The pulverized material shows dependency on moisture content and on the σ_1-σ_3 ratio, with the σ_1-σ_3 ratio having a larger effect. The trends are reasonable since a higher σ_1-σ_3 ratio or more moisture should result in more permanent deformation. The a2 values for the pulverized material correlate well with the N0.003 values, which is an encouraging finding.

Table 5.2 Base Material a_2 values and $N_{0.003}$ Results

Recycled Asphalt	50-50				Pul			
	Dry		Wet		Dry		Wet	
Θ (kPa)	200	400	200	400	200	400	200	400
σ_1/σ_3	4	2	4	2	4	2	4	2
$N_{0.003}$	23799	28212	32168	30483	15510	53061	2041	47531
a_2 (20°C)	0.155	0.173	0.153	0.178	0.155	0.182	0.131	0.167
PCC-AC Mix	90P-10A		70P-30A		50P-50A			
	Dry		Dry		Dry			
Θ (kPa)	200	400	200	400	200	400		
σ_1/σ_3	4	2	4	2	4	2		
$N_{0.003}$	8E+07	5E+07	8E+06	6E+07	1E+06	3E+05		
a_2 (20°C)	0.166	0.211	0.176	0.217	0.197	0.228		

The PCC-AC materials generally show higher resistance to permanent strain compared to the 50–50 or pulverized. The results also show that as the PCC percentage increases the rutting

performance becomes more favorable. This trend is in opposition to the M_r trend, which exhibits higher M_r values when the AC percentage increases. The only exception which deviates from this trend is the 70P-30A material tested at 103-103. The PCC-AC mixtures show some dependence on σ_1-σ_3 but this dependence is opposition to the trend seen in the recycled asphalt material results. With the exception of the 70P-30A, the amount of load repetitions to 0.3% strain decreases as the σ_1-σ_3 ratio decreases.

The trend in the N0.003 data does not match the trend in the values of the a2 values. The lowest a2 value corresponds to the highest N0.003 value for all the combinations of the PCC-AC materials.

5.2.2.3 Deriving the a_2 Values

Table 5.2 shows the comparisons between the M_r a_2 values established from M_r and the $N_{0.003}$ results. It is clear that the a_2 values and the N0.003 values are sensitive to moisture, σ_1-σ_3 ratio, and material type. It is also observed that the a2 and N0.003 values do not correlate very well.

These results are not surprising since the moisture and σ_1-σ_3 ratio are known to have an effect on performance. In addition, the a2 values are derived directly from the resilient modulus, which is a measure of resilient non-permanent strain; while the N0.003 is an indication of permanent (non-resilient strain).

There are serious difficulties in deriving the layer coefficient from the data collected because of two reasons.

(1) Some of the materials are sensitive to stress. It is however difficult to determine which stress level should be used in selecting the a2.

(2) Rutting performance do not necessarily match the resilient modulus trend. The layer coefficients in the current AASHTO recommendations are based solely on the resilient modulus and there is no method for taking into account the rutting performance.

To address these difficulties, some assumptions have to be made. Regarding the effect of stress conditions, an average value of the layer coefficients could be justified because within any layer in the pavement structure, stress conditions will vary with depth. With regard to the rutting performance, there are many interacting factors that influence the progression of rutting. It is difficult with this initial set of data to determine how the layer coefficients should be adjusted to account for the difference in rutting behavior. It is believed that this study should be expanded to verify first that the measured rutting

characteristics are related to rutting resistance in the field. If this can be accomplished, there are several concepts that could be utilized to account for this property in pavement design. One of these concepts is explained in the latter parts of this chapter. The concept can be applied for unbound and bound materials. At this time, however, it is premature to recommend any procedure for taking the rutting behavior into account before it is validated in the field.

5.3 Bound Material Results

5.3.1 Resilient Modulus Results

All of the asphalt materials were tested for resilient modulus according to AASHTO T294. The data collected were also analyzed employing the same method used for the granular (unbound) materials. K1 and K2 values were generated using a power curve from the relationship of the resilient modulus (Mr) with the bulk stress (Θ). Similar to the granular materials the power curve relationship had reliabilities in at least the 90^{th} percentile. Figure 5.11 presents an example of the results for the M_r testing of one of the asphalt mixtures. The fitted power curve can be seen as well as the K1 and K2 values estimated for the specimen. Figure 5.12 shows the fitted curves only for all the bound (asphalt) materials tested in this study.

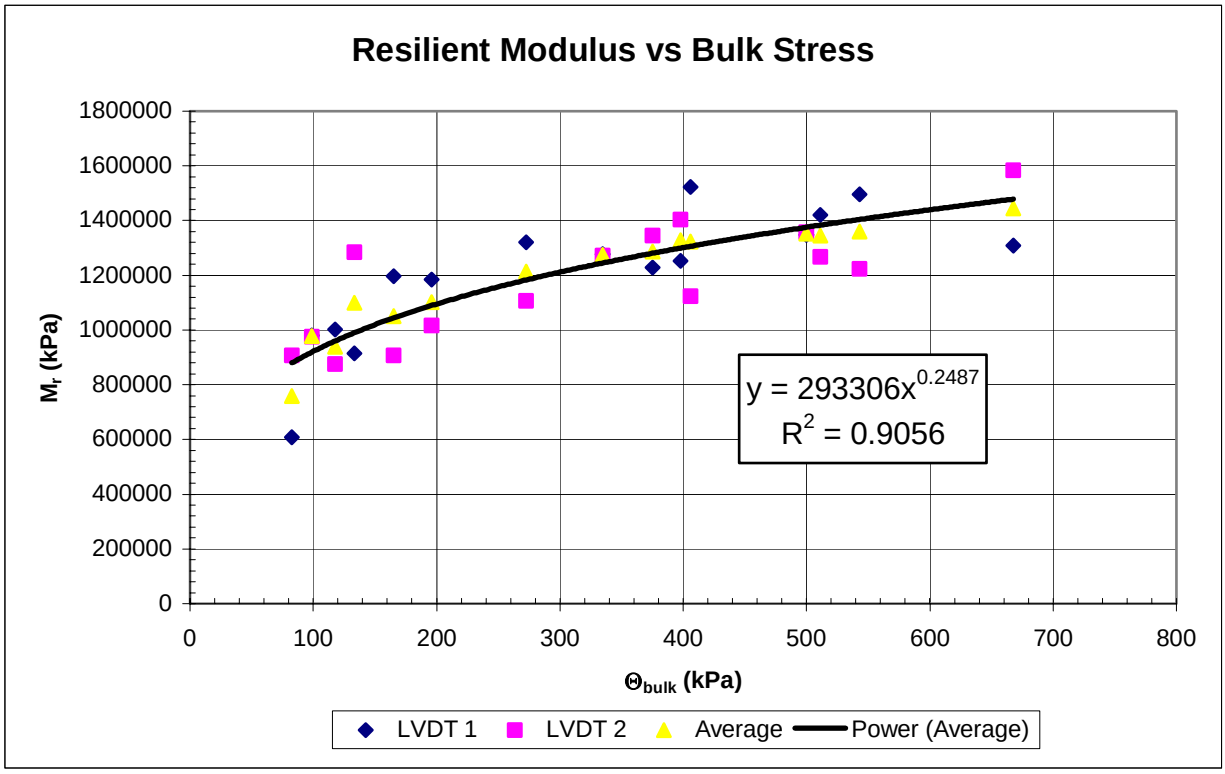

Figure 5.11 Results of Testing the HV mixture for Mr at 20°C

Figure 5.12 Asphalt Material M_r Results @ 20°C

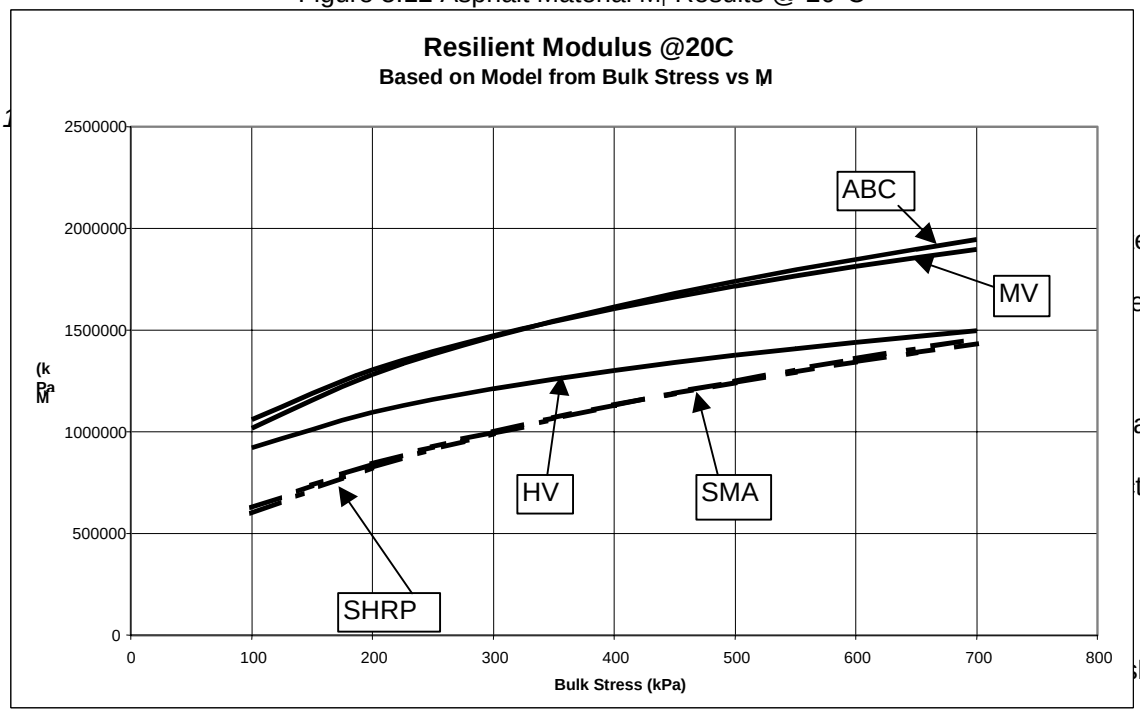

5.3.1

erials.

elastic

aterial

ted, it

given

slightly

higher M_r than the more coarse grained mixes. However, based on the repeatability of the testing, there is no obvious M_r difference among all the materials tested. The range is within

10-20 % of the average values. The consequence is that the layer coefficients derived from the resilient modulus values only should be very similar among all the materials.

5.3.1.2 Resilient Modulus Layer Coefficients

To derive the layer coefficient, the equation presented below was used to calculate the a_1 values from the M_r results. This equation was derived from field AASHTO experiments and numerical analysis, as discussed in Chapter 2.

$$a_1 = 0.4(\log M_r) - 0.951$$

To use this equation, a value for M_r has to be selected for a given Θ value. For the purposes of this study, two Θ values were chosen to represent a surface layer and a binder layer. A Θ value of 550kPa was chosen because it represents the surface layer where low σ_3 and high σ_d values exist (i.e., 34kPa and 450kPa, respectively). Asphalt surface layers usually experiences the lowest σ_3 values in a pavement structure. The surface layer will also experience the highest σ_d values.

The binder layer is represented by a Θ value of 620kPa, where σ_3 values are higher and σ_d values are lower (i.e., 103kPa and 310kPa, respectively).

As for the ABC mixture, a Θ value of 200kPa was chosen to represent its use as a base layer material. The a_2 values for the ABC were derived from charts for bituminous treated base in the AASHTO 1993 Guide.

Table 5.3 shows the calculated layer coefficients and their corresponding M_r values. The differences in these a_1 values are very small. The range is between a low value of 0.267 to a high value of 0.290. These values are, however, higher than the a2 values calculated for the ABC base material. Figure 5.14 shows a comparison of the layer coefficient values of all the materials calculated to represent different layers.

It seems that, for asphalt materials, the effect of the layer depth is rather minimal. It is, therefore, reasonable to recommend that the effect of layer depth be ignored in calculating the layer coefficients.

What is important to notice, however, is that the asphalt mixtures tested in this study are known to have different performances and produced with aggregates of different quality. This raises some

concerns about relying on the Mr values to estimate material contribution to performance. This concern can be considered well founded because the resilient modulus is designed to measure only the elastic-recoverable component. Asphalt mixtures are known to be visco-elasto-plastic in behavior and to exhibit significant non-elastic behavior. This known fact leads to the belief that a consideration of other properties that are non-elastic is necessary to reflect the known differences in the materials used. The next section covers the analysis of the rutting data, which considers the combined effect of viscosity and plasticity of asphalt mixtures.

Table 5.3 Asphalt Mixture a_i and M_r Values

	SHRP		SMA		MV		HV		ABC	
Bulk	20°C		20°C		20°C		20°C		20°C	
Stress (kPa)	M_r (MPa)	a_1	M_r (MPa)	a_1	M_r (MPa)	a_1	M_r (MPa)	a_1	M_r (MPa)	a_2
550	1153	0.274	1168	0.276	1240	0.286	1111	0.267	903*	0.17*
620	1195	0.28	1195	0.28	1270	0.29	1141	0.272	1077**	0.20*

*A bulk stress of 200kPa was used to reqresent the top of the base layer

** A bulk stress of 380 was used to represent the mid to lower portion of the base layer

Figure 5.13 Layer Coefficients of Asphalt Mixtures Estimated for 2 Depths to Represent a Surface and a Binder Layer

5.3.2 Permanent Deformation Results for Asphalt Mixtures

The data for the permanent deformation of asphalt mixtures are presented in this section They are sorted according to material type and test conditions (σ_3, σ_d, temperature). Figure 5.14 shows an example of the results for the SHRP mixture under different test conditions. The plots show the ε_p accumulated in the specimen as a function of the load repetition (N). The designations used include three numbers, with the first referring to confining pressure, the second to the deviator stress, and the third to

the testing temperature in degrees Celsius. As shown in the Figure 5.14, the permanent strain (ε_p) is higher at higher temperatures (64°C) than at lower temperatures (52°C). It can also be observed that a higher deviator stress (450kPa) results in more ε_p at both temperatures. The full set of permanent deformation plots for the materials tested are included in Appendix C.

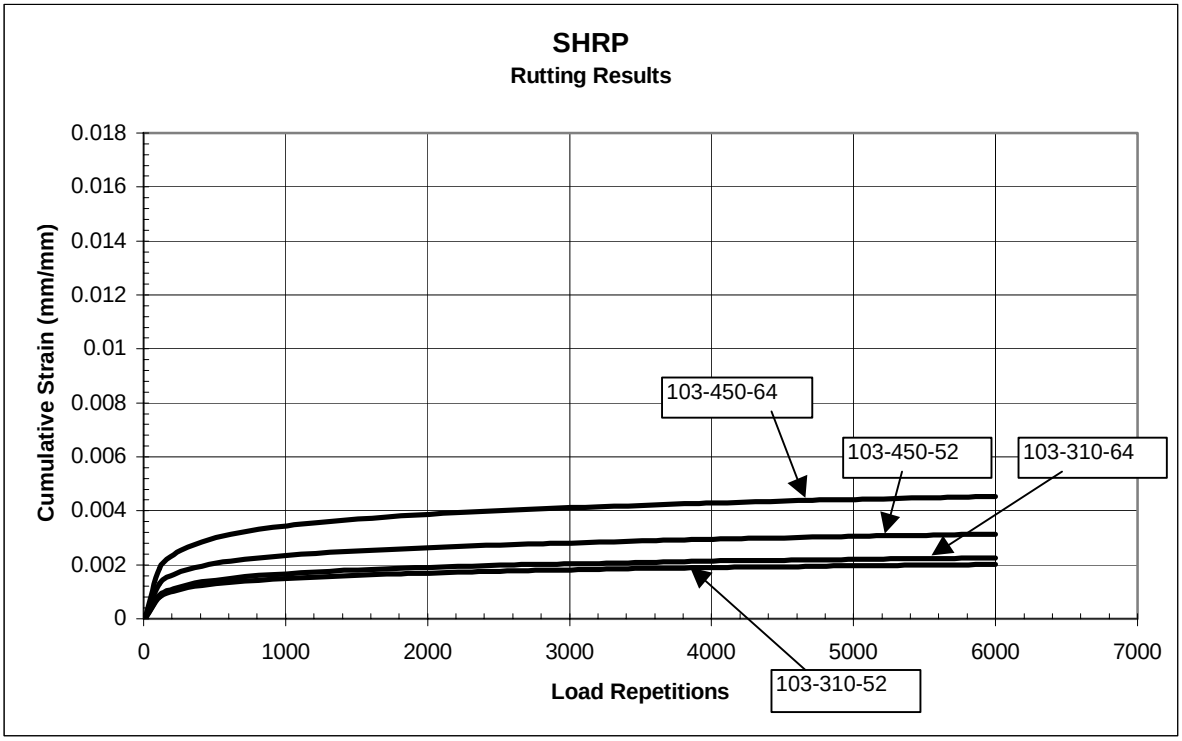

Figure 5.14 Rutting Results for the SHRP Mixture at Different Combinations of Stresses and Temperatures

Figure 5.15 is intended to display comparisons between materials at selected conditions of 103 Kpa confining pressure, 450 Kpa deviator stress, and a temperature of 64°C, (103- 450-64). The data in the figure indicates that there are significant differences between the asphalt mixtures. Whereas the SHRP mixture shows the best performance (i.e., low permanent strain), the SMA shows the least favorable performance (i.e., high permanent strain). The following sections include an in-depth analysis of the data.

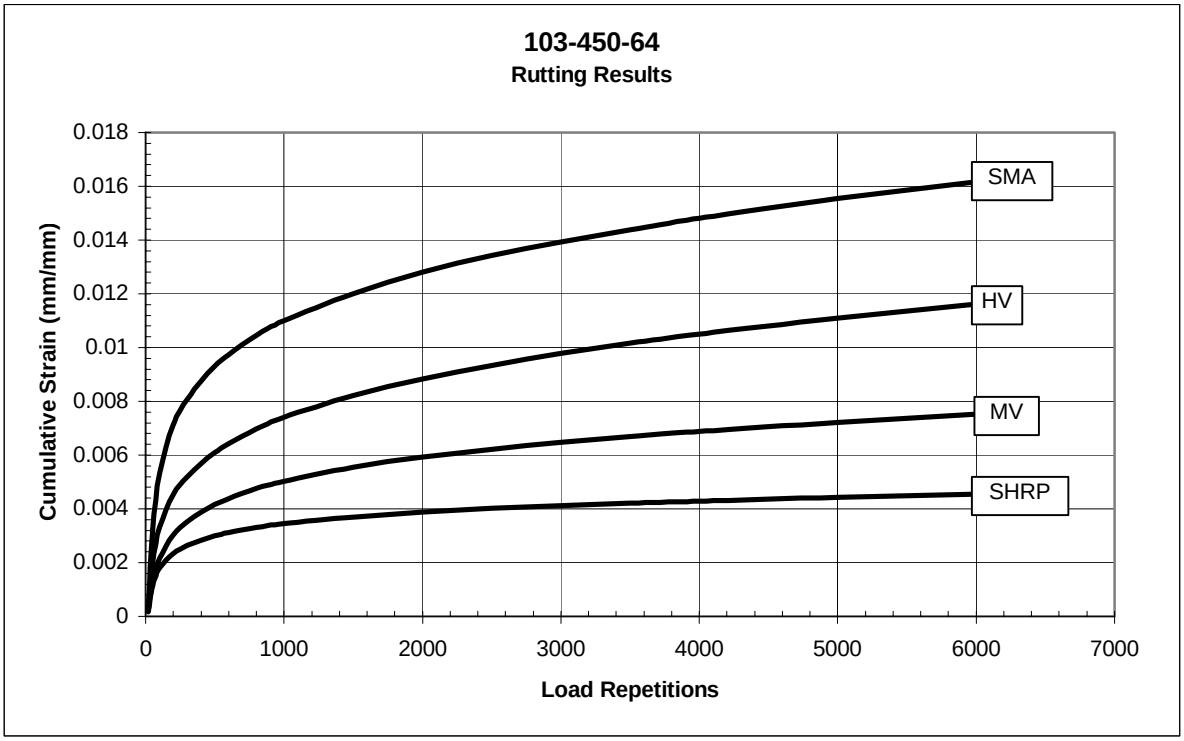

Figure 5.15 Rutting Tests Results at a σ_3 of 103kPa, σ_d of 450kPa, and a temperature of 64°C

5.3.2.1 Permanent Deformation Damage Functions

To estimate the rutting damage function parameters, the logarithmic transformations of the data, shown in Figure 5.15, were used to estimate the strain intercept and the logarithmic rate of strain accumulation as explained in section 5.2.2.1. Figures 5.17 and 5.18 show the strain intercept values and the line slope values, respectively, for the mixtures tested.

The strain intercept, the b-value, represents the initial response of the mixtures. Higher values are not favorable because they represent a potential for early rutting. The results shown indicate that the SHRP and the MV mixtures show the best performance while the SMA shows the lowest.

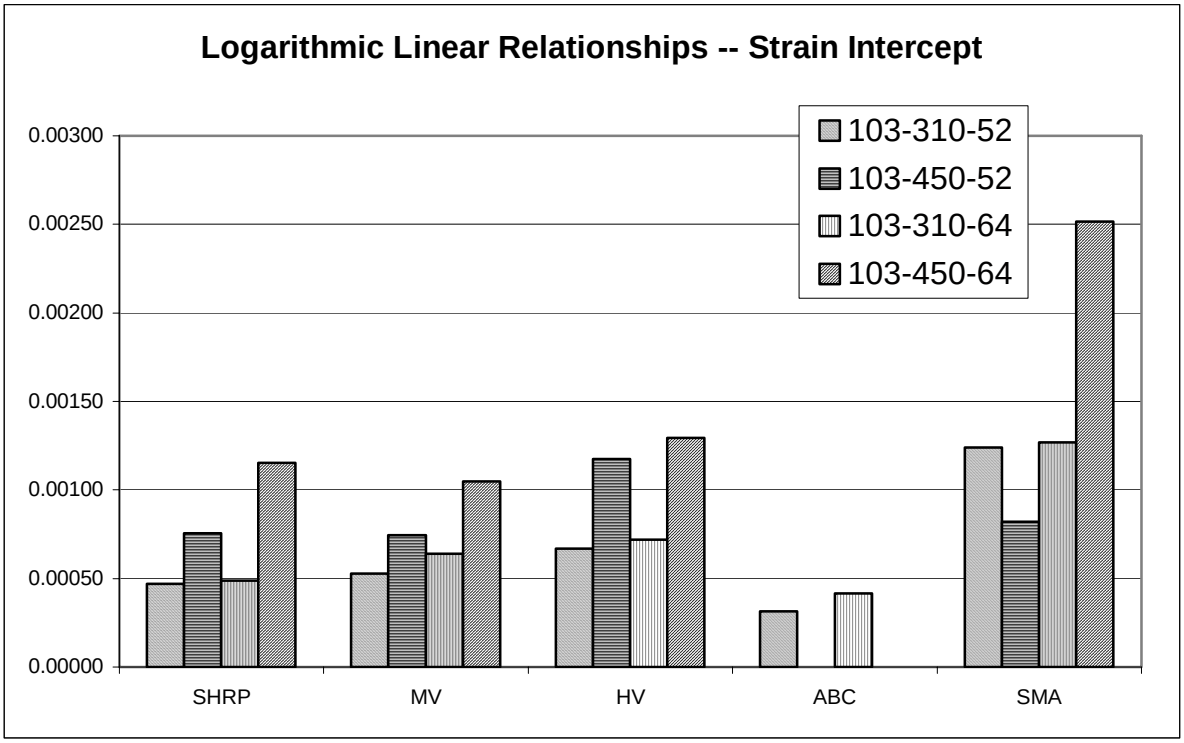

Figure 5.16 Strain Intercepts from Logarithmic Linear Relationships

The results also show that there is a significant effect of tire pressure (i.e., deviator stress) and temperature. They also show that the sensitivity of some of these mixtures to an increase in the temperature is rather low, particularly at lower deviator stress levels. The strain intercept is higher for higher temperatures, as well as higher stress levels for all mixtures, which is an expected outcome.

The results of estimating the logarithmic slope, shown in Figure 5.18, indicate that the trend in the rate of strain accumulation is similar to the intercept value. The values of the rate are lower for the SHRP and the MV mixtures compared to the other mixtures. The rate, however, appears to be less sensitive to temperature and stress conditions. The SMA mixture shows an anomalous behavior at 52°C, at which the intercept value is very low and the rate of accumulation is very high. The SMA aggregate structure is known to be sensitive to stress conditions, which might explain these results.

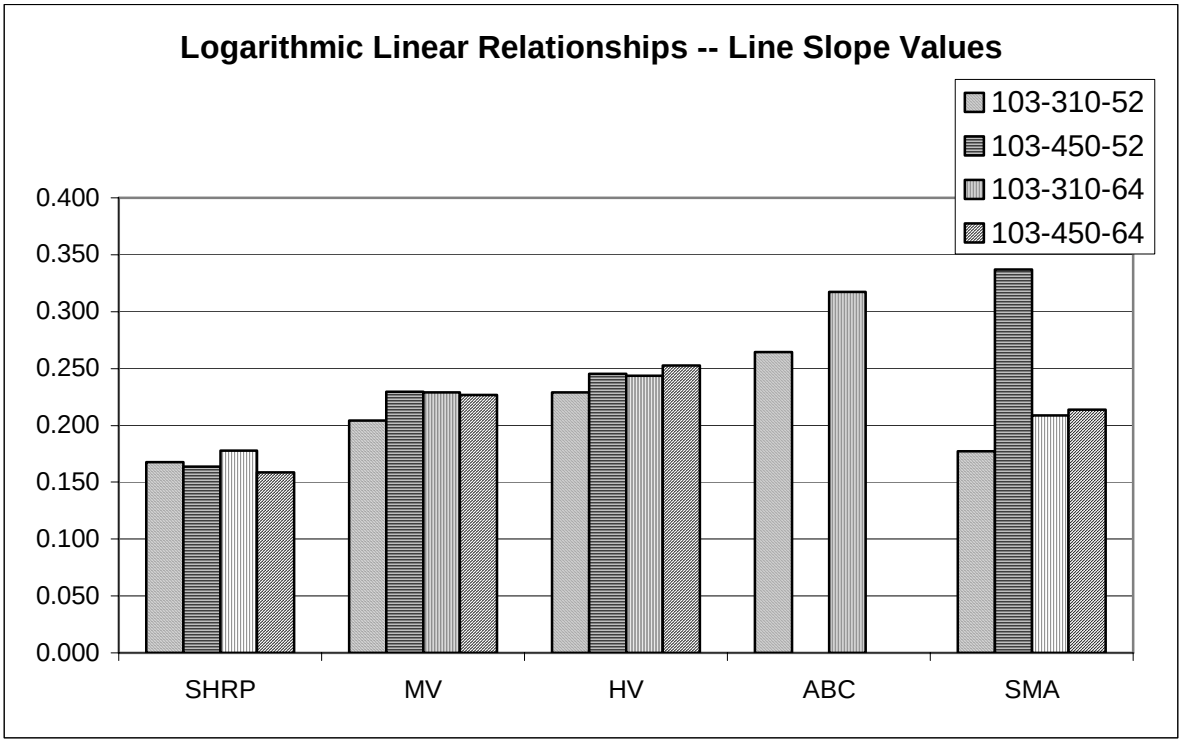

Figure 5.17 Line Slope Values from Logarithmic Linear Relationships

Although it is important to study the intercept and the rate of the accumulation of strain, it is more practical and more related to the actual pavement conditions to compare the mixtures by estimating the number of cycles required to reach a certain level of permanent strain. Such analysis was conducted for the granular materials in the previous sections.

The calculation of the damage functions was identical to the process used for the granular materials. Logarithmic linear equations were derived from the data and then used to determine the number of repetitions (N) needed to reach a specified strain level. The strain level chosen for asphalt was 1% ($N_{0.01}$). This represents a vertical rut depth of 2mm in a pavement layer which is 20mm (8in) thick. This strain level was selected for analysis purposes to create a reference point to compare mixtures and relate the behavior to the M_r results and the layer coefficients.

Figure 5.19 shows the $N_{0.01}$ values for all surface mixtures. The data shown confirm that the mixture type has the most significant effect on permanent strain behavior, compared to the other factors. The SHRP mixture shows the best performance because it requires the highest number of cycles

necessary to reach 1% rut depth. On the other hand, the SMA mixture shows the worst performance because of the low number of cycles required to achieve the same rut depth.

The results also indicate that σ_d, which represents tire pressure, can also be as important as changing the temperature by 12°C (52 to 64°C).

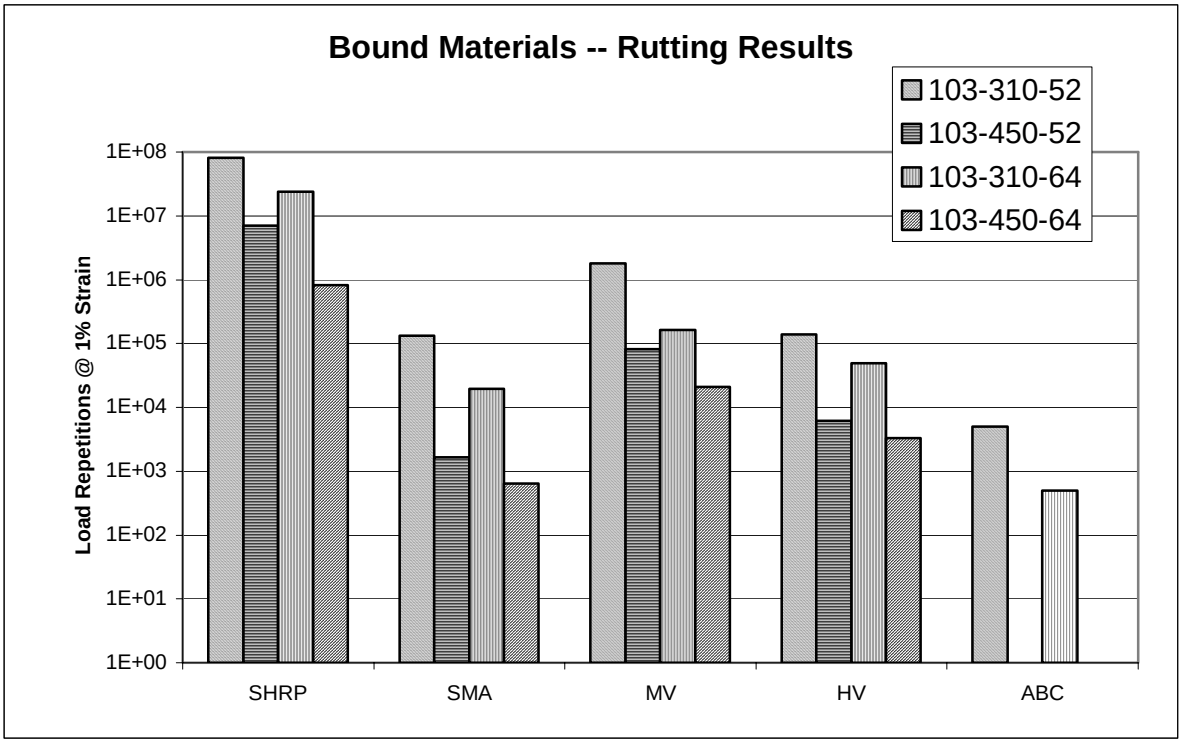

Figure 5.18 Asphalt Surface Mixtures Rutting Performance

The results from the rutting tests give a different view of the relative behavior of the asphalt mixtures. While the resilient modulus and the layer coefficients appear to be relatively similar across all asphalt mixtures, the number of cycles required to achieve 1 % rut depth is significantly higher for the SHRP mixture compared to the other mixtures. The results also show that the MV mixture is superior to the SMA and the HV mixtures. The ABC material, under the conditions tested, shows a rutting behavior that is comparable to the SMA.

Some of the results collected for rutting show the kind of superior performance expected in the case of high quality mixtures, such as the SHRP mixture. Other results, such as the comparison between the SMA and the ABC, however, deserve further analysis to confirm the un-expected trend observed.

The SMA is expected to perform significantly better than the other mixtures tested in this program. Without the knowledge of the performance of this specific SMA mixture in the field, it is very difficult to determine whether or not these results reflect the actual relative performance of these mixtures.

5.3.2.2 Temperature and Principle Stress Effects

The first noticeable trend that is observed from this data is that a higher temperature caused more permanent deformation for the same σ_1/σ_3 ratio. The second is that the σ_1/σ_3 seems to have a greater impact on permanent deformation than the temperature.

The higher temperature trend is expected. Asphalt stiffness reduces significantly when temperature is raised, which translates into lower stiffness in asphalt mixtures. This goes hand in hand with field results, which show that rutting presents a great problem in warmer climates.

When the testing parameters were developed, it was thought that raising the temperature would be more of a factor than increasing the applied stress. The results, however, proved otherwise; the asphalt mixes appear to be more dependent on the σ_1/σ_3 ratio than on the temperature in the ranges tested. The two permanent deformation curves corresponding to the same σ_1/σ_3 ratio are relatively close to one another. However, there is a significant difference between the lower and higher σ_1/σ_3 ratios. This implies that rutting may be more dependent on loading than on temperature.

The differences between the materials becomes greater as the σ_1/σ_3 ratio and temperature increase. Distinct and significant differences can be seen between the different mixes, especially at the σ_1/σ_3 ratio of 4.

5.3.2.3 Layer Coefficients and Permanent Deformation Comparisons

Table 5.4 shows the layer coefficients derived by the resilient modulus at 20ºC. The SHRP mixture was not associated with the highest a_1 value. The MV mixture showed the best results; there are only minor differences among the layer coefficients of these materials.

The rutting results differentiate among the asphalt mixtures very well, which is not the case when the results from the M_r tests are considered. According to the M_r testing, the MV should be the best mixture while the rutting testing is showing that the SHRP mixture has the best performance.

The lack of agreement between the Mr and the rutting results is also seen at different stress conditions. When changes are made in the Θ values the corresponding a_1 values do not change significantly. However, the $N_{0.01}$ values change drastically (as much as an order of magnitude) when the σ_1/σ_3 ratio is raised from 4 to 5.4.

Table 5.4 Asphalt Surface Material Layer Coefficients

	SHRP		SMA		MV		HV		ABC	
Θ (kPa)	600	760	600	760	600	760	600	760	400	600
a_1(20ºC)	0.28	0.29	0.28	0.29	0.29	0.30	0.27	0.28	0.20	0.22

In summary, the rutting tests exhibit significant differences in the materials, which suggests that the materials do not behave similarly. The permanent deformation results can vary by as much as 3 orders of magnitude from one material to another over the same σ_1/σ_3 ratio. The changes in a_1 values are small and show no significant differences in materials.

5.3.2.4 Other Trends and Comparisons

One trend that can be seen from strain intercept and line slope value plots is that an increase in either the temperature or the σ_1/σ_3 ratio causes the initial strain accumulated during conditioning to increase. The σ_1/σ_3 ratio has a more significant effect. This trend was observed to occur in all of the surface mixtures tested.

The slope of the damage line plot shows an increase in temperature and/or σ_1/σ_3 ratio causes an increase in the rate of accumulation of damage. As these parameters rise the rate at which a material accumulates permanent deformation, except for SHRP, increases. The change in the slopes of the damage lines is consistent among the parameters and is relatively small. However, a small change in slope can cause a large change in the accumulated strain at a high number of load repetitions. A smaller

slope value means that a material will accumulate permanent strains at a slower rate. The SHRP shows the smallest slope followed by SMA, MV, HV and ABC, respectively.

To summarize the rutting data, Figure 5.21 is prepared to show the rutting results for all the materials tested. The asphalt material data is selected for the low temperature and the granular data for the dry condition. This data gives an overall idea of the relative rutting resistance of these materials. This type of data could help determine which part of a pavement structure is the most susceptible to rutting. An interesting observation is that the recycled granular materials perform better in permanent deformation than three types of asphalt mixtures when compared at the selected stress conditions. The selected stress conditions are typical of sub-surface layers, binder or base course.

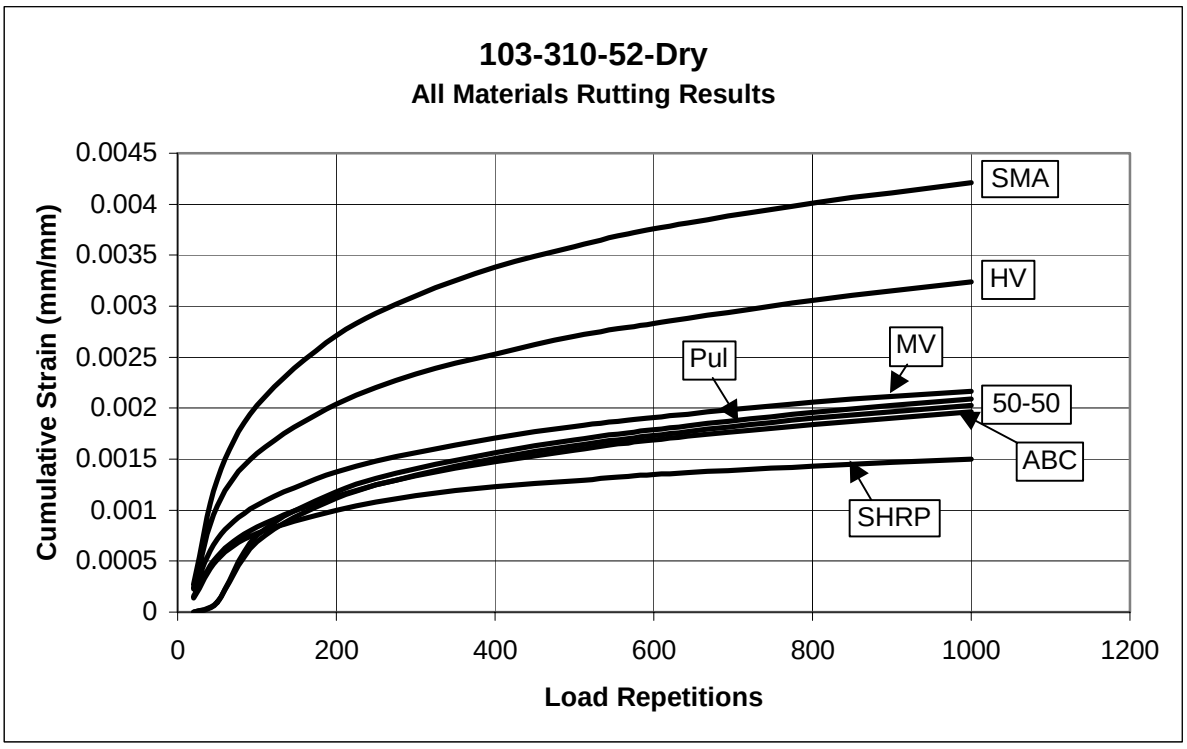

Figure 5.19 103-310-52-Dry Rutting Results for All Materials

5.4 Derivation of New Layer Coefficients

It is important to indicate that the formula used to estimate layer coefficients from the Mr value of asphalt mixtures, s recommended in the AASHTO 1993 manual, does not consider the effect of stress conditions as it is derived for measurements conducted at 20^{o}C only. This formula was based on a

comparative analysis of a single surface asphalt mixture that was used in the AASHTO experiment that started in 1958. It is, therefore, necessary to proceed with extreme caution when using the Mr values to derive the layer coefficients for newer materials.

Many State highway agencies have recognized this problem and used a layer coefficient of 0.44 for the best asphalt mixtures as a reference for their materials. Based on the research conducted in this study, there appears to be minor differences in Mr values among asphalt mixtures. There also appears to be major concerns regarding the reliance on the Mr values to derive new layer coefficients because of the lack of a relationship with other performance measures, such as the rutting test results.

The only approach that could be offered to mitigate this problem is to derive layer coefficients based on a collection of factors that affect pavement performance. These factors include resilient modulus, damage functions, stress and temperature variations, and type of pavement structure.

For an asphalt layer, this would entail testing the resilient modulus at 20°C and 64°C, determining rutting behavior at 64°C (# of cycles to 1% strain), and determining fatigue behavior at a temperature of 20°C (# of cycles to a 50% loss in stiffness). The layer coefficient will be based on a combination of adjustment factors that give an equal contribution to each of the factors.

The layer coefficients would be determined by using the following general equation:

$$a_1 \propto A\int M_R\Big|_{20^\circ C} + B\int N_{Rutting}\Big|_{64^\circ C} + C\int N_{Fatigue}\Big|_{20^\circ C} \qquad (50)$$

where

A = resilient modulus adjustment factor

B = rutting resistance adjustment factor

C = fatigue resistance adjustment factor

$N_{Rutting}$ = # of load repetitions to 1% strain

$N_{Fatigue}$ = # of load repetitions to 50% loss in stiffness.

The adjustment factors could be derived by correlating the resilient modulus and damage testing results of an asphalt surface mix to the layer coefficient of a reference material. These factors will adjust the layer coefficient based on how a particular mixture performs in comparison to the reference material.

The resilient modulus adjustment factor would be a ratio of the resilient modulus of the reference material and the resilient modulus of the mixture that is being investigated.

The rutting resistance adjustment factor is derived by using the following equation:

$$B = \frac{SN_R - SN_1 + a_R d_R}{d_R} \quad (51)$$

where

SN_R = The rutting structural number of the reference material

SN_1 = The rutting structural number of the tested material

a_R = The layer coefficient of the reference material

d_R = The layer thickness of the reference material

SN_R is determined by using the number of cycles needed to reach 1 % permanent strain, measured from testing the reference material, as the number of ESAL's. Using the AASHTO design nomograph for flexible pavements, the required structural number for these ESAL's is determined using an assumed pavement structure and roadbed characteristics. After taking the rutting results for the new material and the same pavement structure, the same procedure is used to determine SN_1.

The fatigue resistance adjustment factors could be found in a manner similar to the one just described. However, the number of cycles to failure should be measured or estimated using the models proposed in the literature. Since the fatigue testing is extremely time consuming and requires special samples, it is recommended that the number of cycles-to-failure be determined using an existing model. One of the widely used model is published by the Asphalt Institute (AI, 1982) expressed by the following equation:

$$N_f = 0.0796\varepsilon_t^{-3.291}\left(M_R\right)^{-0.854} \quad (52)$$

where

N_f = number of repetitions to fatigue failure

ε_t = strain of asphalt mixture at the bottom of the surface layer.

The stain at the bottom of the layer can be determined by one of the existing multi-layer elastic analysis systems, such as the KENLAYER pavement analysis software package. It can also be assumed based on the pavement structure being designed.

The N_f of the reference material is found by taking the ε_t and M_r and using the equation above. The calculated number is assumed to represent the EASLs in a pavement design. The EASLs are used in the AASHTO flexible nomograph to determine a structural number for the reference material. To find the N_f of a particular asphalt mixture, its measured resilient modulus is used to determine its Nf and its structural number value. The following equation could be used to generate the fatigue resistance adjustment factor.

$$C = \frac{SN_F - SN_2 + a_R d_R}{d_R} \tag{53}$$

where

SN_F = The fatigue structural number of the reference material

SN_2 = The fatigue structural number of the tested material

a_R = The layer coefficient of the reference material

d_R = The layer thickness of the reference material

For the granular unbound materials, the layer coefficients could be found by using a slightly different equation:

$$a2 \propto A\int M_R\Big|_{Dry} + B\int M_R\Big|_{Wet} + C\int N_{Rutting}\Big|_{20^\circ C} \tag{54}$$

The equation includes the effect of moisture conditions by using the wet and dry resilient modulus, as well as the number of cycles to failure in rutting measured, at 20°C. This approach to determining the layer coefficient of the unbound base material utilizes current resilient modulus methods; however, it also takes into account the material's property of weakening when moisture contents are

increased. In addition, it includes a factor for rutting failure criterion. The unbound adjustment factors can be found by following the processes described above.

The procedure described in the last few paragraphs includes using the inherent advantages of the current resilient modulus tests. It also includes the failure criterion of rutting and fatigue. Another advantage of this method is that it allows us to use the current methodologies of design, as well as include some mechanistic analysis approach. The additional testing required to complete this method of assigning layer coefficients includes the rutting testing which can be conducted using the same specimen and testing set-up. It is relatively simple and has been successfully completed in this, as well as other research.

CHAPTER SIX

FINDINGS AND FUTURE RECOMMENDATIONS

6.1 Summary of Findings

Based on the analysis of the results collected in this project, we summarize our findings below according to area of research or group of materials tested.

Laboratory VS Field Measurements

The resilient modulus values measured in the laboratory for samples recovered from the field could be successfully related to the values estimated from the non-destructive testing of pavements in the field. The values estimated from field measurements are sensitive to the back calculation procedure and the assumptions made in the analysis. It is, therefore, more realistic to measure resilient modulus in the laboratory under different stress and temperature conditions.

Results of Unbound Reprocessed Materials

The resilient modulus values of the 50-50 mixture (i.e., 50% recycled asphalt mixture mixed with 50% virgin aggregates) and the pulverized material vary within a narrow range depending on stress and moisture conditions. Both these materials are found to have a lower resilient modulus than the PCC-AC recycled mixtures. Based on the results collected in comparison with the AASHTO layer coefficient equations, the following layer coefficients are recommended for the interim use:

- 50Pcc-50Ac – 0.23
- 70Pcc-30Ac – 0.21
- 90Pcc-10Ac – 0.21
- 50-50 Milled – 0.17
- Pulverized – 0.18

These layer coefficients should be used with caution because in this study it has been found that the

rutting performance measured in the laboratory does not rank these materials in the same order as indicated by the layer coefficients. It is believed that the current method of estimating layer coefficients is biased toward resilience behavior. A conceptual method is presented for future consideration.

Results of Asphalt Mixtures

The resilient modulus values of the asphalt mixtures at 20^{o}C vary within a narrow range. The values are not highly sensitive to stress conditions but are sensitive to temperature. The rutting results of the asphalt mixtures show very important differences between the materials; the SHRP mixture showed the highest resistance to rutting, whereas the SMA mixture showed the least resistance to rutting. Based on the procedure for estimating the layer coefficient values recommended by AASHTO, the asphalt mixtures range in their layer coefficients between 0.26 and 0.30 depending on material type and stress conditions. It is unrealistic to recommend using these values because of the significant differences in rutting performance observed in the laboratory and the possible effect of temperature or age that is not considered in the AASHTO procedure. It is important that the Wisconsin DOT establishes a reference material with a reference layer coefficient. Deriving a realistic list of layer coefficients could be done only on the basis of a comparison with this reference material. If the HV mixture tested in this project was considered as the reference material with a layer coefficient of 0.44, the layer coefficients of the other materials should not be any different because of the similarities in the resilient modulus values that have been measured.

The layer coefficient of the asphalt base course is estimated at approximately 70 % of the values for the surface layer materials. In other words, if the HV mixture is considered at 0.44, the asphaltic base course should be at 0.31. If the actual values of Mr are used, the base material should be considered at 0.18.

A conceptual procedure is offered in this study to account for rutting and fatigue damage in deriving a layer coefficient. The procedure requires testing mixtures for rutting, as well as the measuring resilient modulus. The procedure could not be verified in this project and more work is required before its implementation.

6.2 Conclusions and Recommendations

The present AASHTO method of determining layer coefficients is based on using resilient modulus measured values to estimate the layer coefficients using specific empirical relationships. This method can be used to consider material properties under different traffic loads, confining pressure and deviator stress. Based on the methodology recommended by the AASHTO, the following layer coefficients are recommended for the interim use.

- 50Pcc-50Ac – 0.23
- 70Pcc-30Ac – 0.21
- 90Pcc-10Ac – 0.21
- 50-50 Milled – 0.17
- Pulverized – 0.18

It should be mentioned however, that the research team believes that the AASHTO methodology largely ignores other relevant factors, such as temperature sensitivity, air void, layer thickness, rutting behavior, fatigue behavior, and age effects.

Because of this problem, it is concluded that the layer coefficients derived from resilient modulus values should be used with certain caveats. A method is proposed that can combine resilient modulus values with other damage factors to derive the layer coefficients. It is recommended that this method be further explored and verified. This will require further testing and selection of reference materials that would allow for an accurate estimation of layer coefficients.

REFERENCES

The Asphalt Institute, 1982. "Research and Development of The Asphalt Institute's Thickness Design Manual (MS-1), (9th ed.). *Research Report 82-2*. Asphalt Institute.

ASTM, 1989. *Nondestructive Testing of Pavements and Backcalculation of Moduli* . *First* Volume", ASTM STP 1026. Harold, L. et al. (Eds.) : Philadelphia.

ASTM, 1994. *Nondestructive Testing of Pavements and Backcalculation of Moduli*. *Second Volume*", ASTM STP 1198, Harold, L. et al, (Eds.) : Philadelphia.

Brown, E. R., Haddock, J. E., Mallick, R. B., & Lynn, Y. A., 1997. "Development of a Mixture Design Procedure for Stone Matrix Asphalt (SMA)", *Journal of the Association of Asphalt Paving Technologists*. Vol. 66, pp. 1-24.

Bosscher, P. J., Benson, C.H., & Jong, D., 1997. "Method Development for Determining the Effect of Thermal Cycles and Moisture Conditions on Pavement Structure". *Interim Report to Wisconsin Department of Transportation*

Carpenter, 1990. "Layer Coefficients for Flexible Pavements". *Report No. WI/HPR-08-90, Wisconsin Department of Transportatio*n.

Chen, D. H. , Zaman, M. M. , and Laguros J.G. 1995, "Characterization of Base/Sub-base Materials Under Repetitive Loading," *Journal of Testing and Evaluation,* Vol. 23, N. 3, pp. 180-188.

Coree, W., 1988. "Layer Coefficients in Terms of Performance and Mixture Characteristics," *Report Number FHWA/IN/JHRP-88/13*. Indiana Department of Highways: Indiana

Cowher, K., 1975. "Cumulative Damage of Asphalt Materials Under Repeated-Load Indirect Tension". *Research Report Number 183-3*. Center For Highway Research – University of Texas: Austin.

Dawson, A. R., Thom N. H., & Paute J.L., 1993: Mechanical Characteristics of Unbound Granular Materials as a Function of Condition, Flexible Pavements, A. Gomes Correia, pp 35-44

Ewing, W.M., Jordetsky, W. S., & Press, F., 1957. *"Elastic Waves in Layered* FHWA (1994), "*Pavement Deflection Analysis*". *National Highway Institute.* Report No. 13127*.*

FHWA, 1994. "Pavement Deflection Analysis," *National Highway Institute.* Report No. 13127*.*

Fwa, T. F., Low B. H., & Tan, S. A., "Compaction of Asphalt Mixtures for Laboratory Testing: Evaluation Based on Density Profile". *Journal of Testing and Evaluation (JTEVA*). Vol. 21, No. 5, September 1993, PP. 414-421.

Galjaard, P.J., Paute, J.L., & Dawson A. R., 1993. Comparison and Performance of Repeated Load Triaxial Test Equipment for Unbound Granular Materials, Flexible Pavements, A. Gomes Correia, pp 7-21

George, K.P., & Asce, M., 1984. "Structural Layer Coefficient for Flexible Pavement". *Journal of Transportation Engineering.* Vol. 110 (3), pp. 251-267.

George, K.P., and Uddin, Waheed., 1994, "In situ and laboratory characterization of nonlinear pavement layer moduli," ASTM Special Technical Publication Proceedings of the Symposium on

Nondestructive Testing of Pavements and Backcalculation of Moduli, Jun 1993, n 1198, (12), Atlanta. pp. 203-217.

Gomez, T., & Thompson, M., R. 1983. "Structural Coefficients and Thickness Equivalency Ratios," *Report Number FHWA/IL/UI-202: Illinois Department of Transportation.*

Hall, J.R., & Woods, R.D., 1970. *Vibrations of Soils and Foundations*. Englewood Cliffs, Prentice-Hall: New Jersey.

Hicks, R.G., & Monismith, C. L., 1971. Factors influencing the resilient response of granular materials. *Highway Research Record No 345*, pp 15-31

Horak, E., 1987. "The Use of Surface Deflection Basin Measurements in the Mechanistic Analysis of Flexible Pavements," *Proc., Vol. 1, Sixth International Conference Structural Design of Asphalt Pavements*. University of Michigan: Ann Arbor.

Hossain, M., & Habib, A. 1997. "Development of Structural Layer Coefficients of Crumb Rubber Modified Asphalt Mixes from In-Situ Deflection Tests," *Report Number K-TRAN: KSU-96-2, Kansas Department of Transportation.*

Houston, W.N., Mamlouck, M.S., & Perera R.W. (1990), "Laboratory versus Nondestructive Testing for Pavement Design," *Journal of Transportation Engineering*, ASCE. Vol. 118, No.2, pp207-222.

Huang, Y.H. 1993. *Pavement Analysis and Design.* Prentice Hall: New Jersey.

Jong, D., 1997. *Freeze-Thaw Effects on Stiffness of Pavement Systems*. Masters thesis, University of Wisconsin: Madison.

Jong, D., & Christensen, J. D., 1997, "Layer Coefficients for New and Reprocessed Asphaltic Mixes – Field Testing Report*", Research Report*. University of Wisconsin: Madison.

Khanal, P. P., & Mamlouk, M. S., 1992 "Tensile Versus Compressive Moduli of Asphalt Concrete," Transportation Research Record 1492, pp. 144-150.

McCollough, B.F., Van Til, C .J ., and Hicks, R.G. "Evaluation of AASHO Interim Guides for Design of Pavement Structures". *NCHRP Report 128*, 1972.

Michalak, C.H., Scullion, T., 1995, "Modulus 5.0: Users Manual". Texas Transportation Institute, The Texas A&M University System.

Nazarian, S., 1984. *In Situ Determination of Elastic Moduli of soil Deposits and Pavement Systems by Spectral-Analysis-of-Surface-Waves Method.* Ph.D. Dissertation. University of Texas: Austin.

Nazarian, S., & Stokoe, K., H. 1984. "Nondestructive Testing of Pavements Using Surface Waves," *Transportation Research Record 993*, TRB, National Research Council, pp. 67-79.

Nazarian, S., and Stokoe, K., H. 1986. "Use of Surface Waves in Pavement Evaluation," *Transportation Research Record 1070*, TRB, National Research Council. pp 132-144.

Paute J.L., Dawson A.R. & Galjaard P., J. 1993. "Recommendations for Repeated Load Triaxial Test Equipment and Procedure for Unbound Granular Materials, Flexible Pavements", A. Gomes Correia, pp 23-34

Paute J. L., Hornych P., & Benaben J., P. 1993. Repeated Load Triaxial testing of Unbound Granular Materials in the French Network of “Laboratories des Ponts et Chaussees”. *Euroflex 1993*, session 1, Lisbon: Portugal

Ping, W., V. , G. l., & Zhiliang, Y. 1996. “Evaluation of Pavement Bearing Characteristics Using Florida Limerock Bearing Ration Test”. *Transportation Research Record 1547*, pp. 53-60.

Rada, G., & and Witczak, M., W. 1981. “Comprehensive Evaluation of Laboratory Resilient Moduli Results for Granular Material*”. Transportation Research Record 810*, pp. 23-33.

Rada, G., & Witczak, M., W. 1982. “Material Layer Coefficients of Unbound Granular Materials from Resilient Modulus”. *Transportation Research Record 852*, pp. 15-21.

Rauhut, B., Lytton, B., & Darter, M. 1984. “Pavement Damage Functions for Cost Allocation, Executive Summary,” Report Number FHWA/RD-84/017, Federal Highway Administration.

Rauhut B., & Jordahl, B. 1984. “Pavement Damage Function for Cost Allocation, Vol. 3, Flexible Pavement Damage Functions Developed from AASHO Road Test Data,” Report Number FHWA/RD-84/020, Federal Highway Administration.

Richardson N., D. 1996. “AASHTO Layer Coefficients for Cement-Stabilized Soil Bases”. *Journal of Materials in Civil Engineering* v 8 n 2, pp. 83-87

Roberts, F. L., Kandhal, P. S., Brown, E. R., Lee, D. Y., & Kennedy, T. W., 1996. “Hot Mix Asphalt Material, Mixture Design, and Construction”, Lanham, Maryland, NAPA Education Foundation

Rohde, G. T., 1994. “Determining Pavement Structural Number from FWD Testing,” *Transportation Research Record 1448*, (10) pp. 61-68.

Sanchez-Salinero, I., Roesset, J. M., Shao, K., Stokoe, K.H., & Rix, G.J., 1987, “Analytical Evaluation Of Variables Affecting Surface Wave Testing of Pavements,” *Transportation Research Record 1136*, TRB, National Research Council. pp. 132-144.

Sebaaly, P., Tabatabaee, N., Bonaquist, R., & Anderson, D. 1989. “Evaluating Structural Damage of Flexible Pavements Using Cracking and Falling Weight Deflectometer,” *Transportation Research Record 1227*, TRB, National Research Council. pp. 44-52.

SHRP 1993a. “Layer Moduli Backcalculation Precedure: Software Selection”. SHRP-P-651, Strategic Highway Research Program, National Research Council, Washington, D.C.

Sheu, J., Stokoe, K.H., Roesset, J. M., and Hudson, W.R., “Applications and Limitations of the Spectral-Analysis-of-Surface-Waves Method,” *Center for Transportation Research 437-3F*, The University of Texas at Austin.

Stokoe, K.H., Lee, N.U., & Rits, M.P., 1994, “Repeated Measurements of In Situ Soil Stiffness with Permanently Embedded Geophones,” Dynamic Geotechnical Testing II, ASTM STP 1213, Ronald et al. (Eds.), ASTM, Philadelphia.

Tan, S. A., Low, B. H., & Fwa, T., F. 1994. “Behavior of Asphalt concrete Mixtures in Triaxial Compression,” *Journal of Testing and Evaluation, JTEVA.* Vol. 22, No. 3, pp. 195-203.

Thomas, S., 1997. *Investigation of Modified Asphalt Performance Using SHRP Binder Specification.* Masters Thesis, University of Wisconsin: Madison

Uzan, J. 1992. “Resilient Characteristics of Pavement Materials “. *Short Communication, International Journal for Numerical and Analytical Methods in Geomechanics*, Vol. 16, No. 6, pp. 453-459.

Witczak, M. W., & Uzan, J. 1988. ”The Universal Airport Pavement Design System; Report I of IV: Granular Material Characterization”. University of Maryland, Dept. Of C. E.

Wisconsin Department of Transportation, 1994. “Facilities Development Manual,” Department of Transportation, State of Wisconsin.

APPENDIX A

Survey Results of Midwestern States

Wisconsin	
Material	**Layer Coefficient**
New AC	0.44
CABC	
Crushed stone	0.14
Crushed gravel	0.1
OGBC #1	
Crushed stone	0.14
Crushed gravel	0.1
OGBC #2	
Crushed stone	0.14
Crushed gravel	0.1
Breaker Run	
Crushed stone	0.14
Crushed gravel	0.1
Granular Subbase	From graph
Asphaltic Base Course	0.34
Cement Stabilized Open Graded Base Course	
Crushed stone	0.14
Crushed gravel	0.1
Asphalt Stabilized Open Graded Base Course	
Crushed stone	0.14
Crushed gravel	0.1
Rubblized PCC	0.20-0.24
Milled and Relayed Asphaltic Concrete	0.10-0.25
Pulverized Asphaltic Concrete	0.10-0.25

Design Methods Used by Surveyed States					
			AASHTO DM		
State	**Design Agency**	**Contact Name**	**86**	**93**	**other**
Illinois	DOT	David Lippert			X
Indiana	DOT	Dave Andrewski		X	
Iowa	DOT	Chris Brakke		X	
Kansas	DOT	Rick Barezinsky		X	
Kentucky	DOT	Gary W Sharpe			X
Michigan	DOT	Curtis Bleech		X	
Minnesota	DOT	Duane Young		X	X
Missouri	DOT	Denis Glascock	X	X	
Nebraska	DOT	Dan Nichols	X		
North Dakota	DOT	Darcy Rosendahl		X	
Ohio	DOT	Aric A Morse		X	
South Dakota	DOT	Gill Hedman		X	

Kansas			
	Coefficient		
Material	**New**	**Aged 10 yr.**	**Aged 20 yr.**
All Surface Course Material	0.42	0.34	0.28
Base Course Materials Except BM-4 and Cold Recycle	0.34	0.28	0.2
BM-4	0.28	0.2	0.15
Cold Recycle	0.25	0.18	0.11
Aggregate Bases	0.14	0.1	0.08
Lime Treated Subgrade	0.11	0.08	---
Rubblized Concrete Including Crack and Seat	0.18	0.12	0.08
Plant Mix Bituminous Mixture-Commercial Grade	0.34		
The aged coefficients are given for rehabilitation alternatives.			

Ohio	
Material	**LC**
Asphalt Concrete	0.35
Aggregate Base	0.14
Subbase	0.11
Broken and Seated Concrete	0.27
Existing Asphalt	0.23
Rubblized Concrete	0.14

Illinois	Layer Coefficients		
Bituminous Surface	**a_1**	**a_2**	**a_3**
Road Mix (Class B)	0.20		
Plant Mix (Class B)			
Liquid Asphalt	0.22		
Asphalt Cement	0.30		
Class I Bituminous Concrete	0.40		
Base Course			
Aggregate, Type B			
Uncrushed		0.10	
Crushed		0.13	
Aggregate, Type A		0.13	
Waterbound Macadam		0.14	
Bituminous Stabilized Granular Material			
MS 300		0.16	
MS 400		0.18	
MS 800		0.23	
MS 1000		0.25	
MS 1200		0.27	
MS 1500		0.30	
MS 1700		0.33	
Class I Binder		0.33	
Pozzolanic, Type A		0.28	
Lime Stabilized Soil		0.11	
Select Soil Stabilized w/ Cement			
300 psi		0.15	
500 psi		0.20	
Cement Stabilized Granular Material			
650 psi		0.23	
750 psi		0.25	
1000 psi		0.28	
Subbase			
Granular Material, Type B			0.11
Granular Material, Type A			
Uncrushed			0.12
Crushed			0.14
Lime Stabilized Soil			0.12

Indiana		Iowa	
Material	**LC**	**Material**	**LC**
Surface	0.34	Top 4" AC	0.44
Intermediate	0.36	AC Layers Below 4"	0.38
Base	0.34	Granular Material	0.14
Compacted Agg	0.14		

Michigan		Minnesota	
Material	**LC**	**Material**	**LC**
Top and Leveling	0.42	Asphalt	0.44
Base Courses	0.36	Cold Inplace Recycle	0.21
		Base	0.14
		Subbase	0.11

Nebraska		North Dakota	
Material	**LC**	**Material**	**LC**
Asphalt	0.44	Class 33 and Large	
Bituminous Milling	0.20	Stone Mix	0.40
Crushed Conc. Base	0.20	Class 31	0.38
Fly-ash Stabilized	0.25	Class 29	0.36
Asphaltic Conc. Stab.	0.25	Class 27	0.34
		Class 25	0.32
		Existing HBP	0.25
		Emulsified Base	0.1-0.2
		Aggregate Base	0.10

Kentucky	
Material	**LC**
AC	0.36-0.4
Agg Base	0.14
Broken/Seated PCC	0.18

Missouri	
Material	**LC**
High Type Surface	0.44
High Type Base	0.43
Other Asphalt	0.42
Permeable Base	0

South Dakota	
Material	**LC**
Asphalt	0.40
Ledge Rock Bases	0.14
All Other Bases	0.10

APPENDIX B

Tables of Testing Results

50% Milled Asphalt & 50% Virgin Aggregate

Resilient Modulus			
w = 1.8% K1= 40971, K2= 0.2665		w = 5% K1= 31013, K2= 0.3206	
Bulk Stress (kPa)	M_r (kPa)	Bulk Stress (kPa)	M_r (kPa)
100	139835	100	135729
300	187408	300	193029
500	214743	500	227374
700	234892	700	253270

Rutting Tests							
Dry w = 1.8%							
σ_3 (kPa)	34.5	σ_3 (kPa)	34.5	σ_3 (kPa)	103	σ_3 (kPa)	103
σ_d (kPa)	34.5	σ_d (kPa)	103	σ_d (kPa)	103	σ_d (kPa)	310
N	Cumulative Strain (mm/mm)	N	Cumulative Strain (mm/mm)	N	Cumulative Strain (mm/mm)	N	Cumulative Strain (mm/mm)
500	0.00018987	500	0.00075477	500	0.00039556	500	0.0016628
1000	0.00025248	1000	0.00097194	1000	0.0005589	1000	0.0020489

Rutting Tests							
Wet w = 5%							
σ_3 (kPa)	34.5	σ_3 (kPa)	34.5	σ_3 (kPa)	103	σ_3 (kPa)	103
σ_d (kPa)	34.5	σ_d (kPa)	103	σ_d (kPa)	103	σ_d (kPa)	310
N	Cumulative Strain (mm/mm)	N	Cumulative Strain (mm/mm)	N	Cumulative Strain (mm/mm)	N	Cumulative Strain (mm/mm)
500	0.00052807	500	0.00106715	500	0.00049938	500	0.0037037
1000	0.00063793	1000	0.00128155	1000	0.00067725	1000	0.0047493

Pulverized Asphalt with 13% Shoulder Aggregate

Resilient Modulus			
w = 1.5% K1= 20591, K2= 0.3965		w = 5% K1= 10316, K2= 0.4809	
Bulk Stress (kPa)	M_r (kPa)	Bulk Stress (kPa)	M_r (kPa)
100	127816	100	94473
300	197581	300	160236
500	241935	500	204856
700	276461	700	240837

Rutting Tests Dry w = 1.8%							
σ_3 (kPa)	34.5	σ_3 (kPa)	34.5	σ_3 (kPa)	103	σ_3 (kPa)	103
σ_d (kPa)	34.5	σ_d (kPa)	103	σ_d (kPa)	103	σ_d (kPa)	310
N	Cumulative Strain (mm/mm)	N	Cumulative Strain (mm/mm)	N	Cumulative Strain (mm/mm)	N	Cumulative Strain (mm/mm)
500	0.00029471	500	0.0014109	500	0.0003799	500	0.001722
1000	0.00037299	1000	0.00178709	1000	0.0005211	1000	0.002106

Rutting Tests Wet w = 5%							
σ_3 (kPa)	34.5	σ_3 (kPa)	34.5	σ_3 (kPa)	103	σ_3 (kPa)	103
σ_d (kPa)	34.5	σ_d (kPa)	103	σ_d (kPa)	103	σ_d (kPa)	310
N	Cumulative Strain (mm/mm)	N	Cumulative Strain (mm/mm)	N	Cumulative Strain (mm/mm)	N	Cumulative Strain (mm/mm)
500	0.00086076	500	0.00207455	500	0.0005378	500	0.004672
1000	0.00102773	1000	0.00248477	1000	0.0007426	1000	0.005794

Asphalt Base Course

Resilient Modulus from Power Model			
52 C K1= 33220, K2= 0.4738		64 C K1= 20414, K2= 0.4877	
Bulk Stress (kPa)	M_r (kPa)	Bulk Stress (kPa)	M_r (kPa)
100	294441.9	100	192890
300	495518.3	300	329625
500	631206.7	500	422878.4
700	740298.9	700	498290.3

Rutting Tests							
52 C				64 C			
σ_3 (kPa)	103	σ_3 (kPa)	103	σ_3 (kPa)	103	σ_3 (kPa)	103
σ_d (kPa)	103	σ_d (kPa)	310	σ_d (kPa)	103	σ_d (kPa)	310
N	Cumulative Strain (mm/mm)	N	Cumulative Strain (mm/mm)	N	Cumulative Strain (mm/mm)	N	Cumulative Strain (mm/mm)
1000	0.0001142	1000	0.0019632	1000	0.0002758	1000	0.003734
2500	0.0001419	2500	0.0025199	2500	0.0003616	2500	0.0050181
4000	0.0001512	4000	0.0028326	4000	0.0004035	4000	0.0057991
6000	0.0001543	6000	0.0031207	6000	0.0004491	6000	0.0065681

Stone Matrix Asphalt

Resilient Modulus from Power Model			
52 C K1= 46874, K2= .3042		64 C K1= 13462, K2= 0.5153	
Bulk Stress (kPa)	M_r (kPa)	Bulk Stress (kPa)	M_r (kPa)
100	206189.4	100	144447.35
300	319868.7	300	254431.08
500	392323.8	500	331046.37
700	448799.2	700	393721.02

Rutting Tests							
52 C				64 C			
σ_3 (kPa)	103	σ_3 (kPa)	103	σ_3 (kPa)	103	σ_3 (kPa)	103
σ_d (kPa)	310	σ_d (kPa)	450	σ_d (kPa)	310	σ_d (kPa)	450
N	Cumulative Strain (mm/mm)	N	Cumulative Strain (mm/mm)	N	Cumulative Strain (mm/mm)	N	Cumulative Strain (mm/mm)
1000	0.0042115	1000	0.008426	1000	0.0053722	1000	0.0110072
2500	0.0050044	2500	0.0011442	2500	0.0065471	2500	0.0134177
4000	0.0053799	4000	0.012445	4000	0.0071748	4000	0.014803
6000	0.0057053	6000	0.015376	6000	0.007766	6000	0.0161769

SHRP (Superpave)

Resilient Modulus from Power Model			
52 C K1= 24529, K2= 0.4852		64 C K1 = 22012, K2 = 0.455	
Bulk Stress (kPa)	M_r (kPa)	Bulk Stress (kPa)	M_r (kPa)
100	229129	100	178920.3
300	390462	300	294950.9
500	500288	500	372126.7
700	589008	700	433689.7

Rutting Tests							
52 C				64 C			
σ_3 (kPa)	103	σ_3 (kPa)	103	σ_3 (kPa)	103	σ_3 (kPa)	103
σ_d (kPa)	310	σ_d (kPa)	450	σ_d (kPa)	310	σ_d (kPa)	450
N	Cumulative Strain (mm/mm)	N	Cumulative Strain (mm/mm)	N	Cumulative Strain (mm/mm)	N	Cumulative Strain (mm/mm)
1000	0.0015003	1000	0.0023453	1000	0.0016641	1000	0.0034437
2500	0.0017615	2500	0.0027366	2500	0.0019791	2500	0.0040134
4000	0.0018933	4000	0.0029247	4000	0.0021287	4000	0.0042905
6000	0.0020144	6000	0.0031409	6000	0.0022638	6000	0.0045387

Medium Volume

Resilient Modulus from Power Model			
52 C K1= 47523, K2= 0.3883		64 C K1= 34845, K2= 0.4133	
Bulk Stress (kPa)	M_r (kPa)	Bulk Stress (kPa)	M_r (kPa)
100	284121.3	100	233744
300	435281.3	300	368073.61
500	530779.2	500	454595.12
700	604860.8	700	522419.63

Rutting Tests							
52 C				64 C			
σ_3 (kPa)	103	σ_3 (kPa)	103	σ_3 (kPa)	103	σ_3 (kPa)	103
σ_d (kPa)	310	σ_d (kPa)	450	σ_d (kPa)	310	σ_d (kPa)	450
N	Cumulative Strain (mm/mm)	N	Cumulative Strain (mm/mm)	N	Cumulative Strain (mm/mm)	N	Cumulative Strain (mm/mm)
1000	0.0021632	1000	0.0036412	1000	0.0031103	1000	0.005022
2500	0.0026257	2500	0.0045279	2500	0.0038552	2500	0.006221
4000	0.002871	4000	0.0050054	4000	0.0042711	4000	0.006878

High Volume

Resilient Modulus from Power Model			
52 C K1= 24968, K2= 0.4426		64 C K1= 10922, K2= 0.5513	
Bulk Stress (kPa)	M_r (kPa)	Bulk Stress (kPa)	M_r (kPa)
100	191683.1	100	138325.5
300	311714.9	300	253477.3
500	390794	500	335926.6
700	453548.9	700	404394

Rutting Tests							
52 C				64 C			
σ_3 (kPa)	103	σ_3 (kPa)	103	σ_3 (kPa)	103	σ_3 (kPa)	103
σ_d (kPa)	310	σ_d (kPa)	450	σ_d (kPa)	310	σ_d (kPa)	450
N	Cumulative Strain (mm/mm)	N	Cumulative Strain (mm/mm)	N	Cumulative Strain (mm/mm)	N	Cumulative Strain (mm/mm)
1000	0.0032381	1000	0.0063924	1000	0.0038641	1000	0.0074015
2500	0.0040152	2500	0.0082629	2500	0.0048685	2500	0.009339
4000	0.0044462	4000	0.0089796	4000	0.0054161	4000	0.0105027
6000	0.0048607	6000	0.0095967	6000	0.0059165	6000	0.0116293

APPENDIX C

Asphalt Testing Results

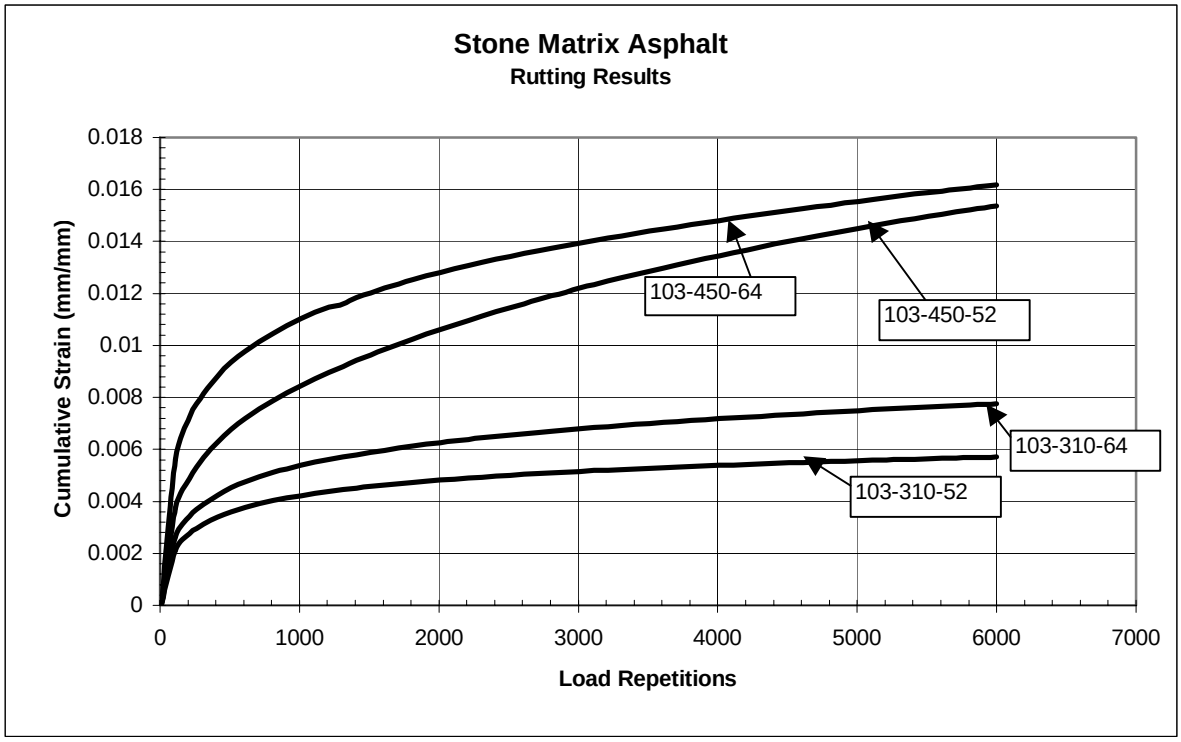

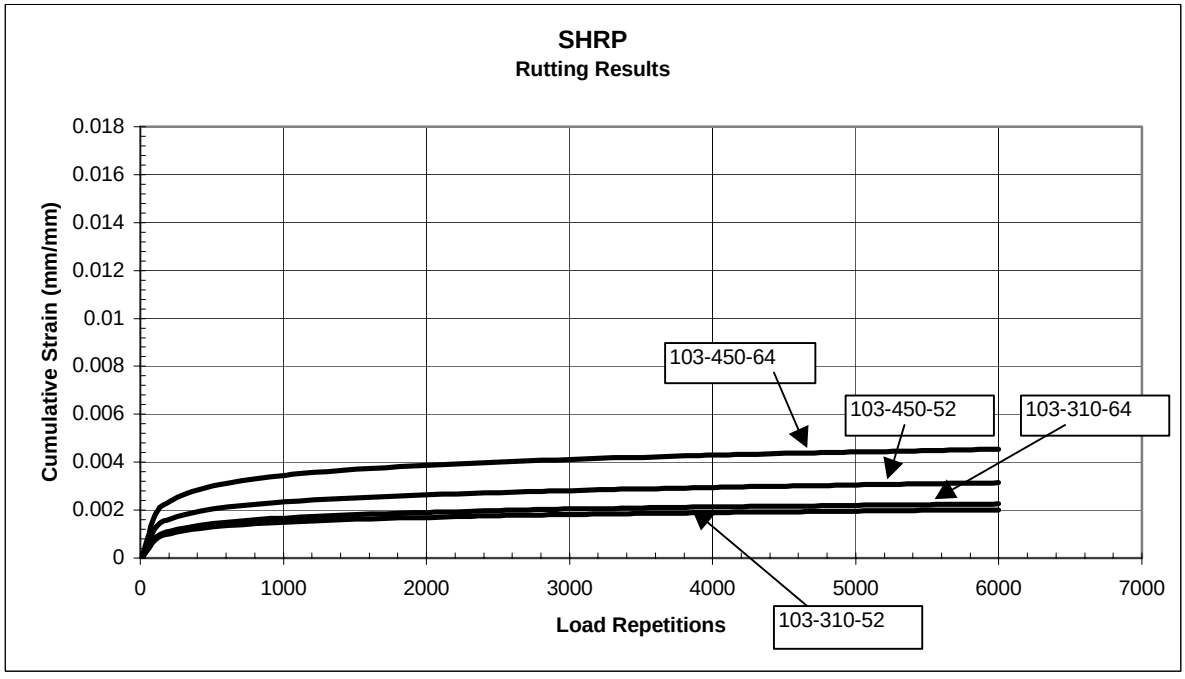

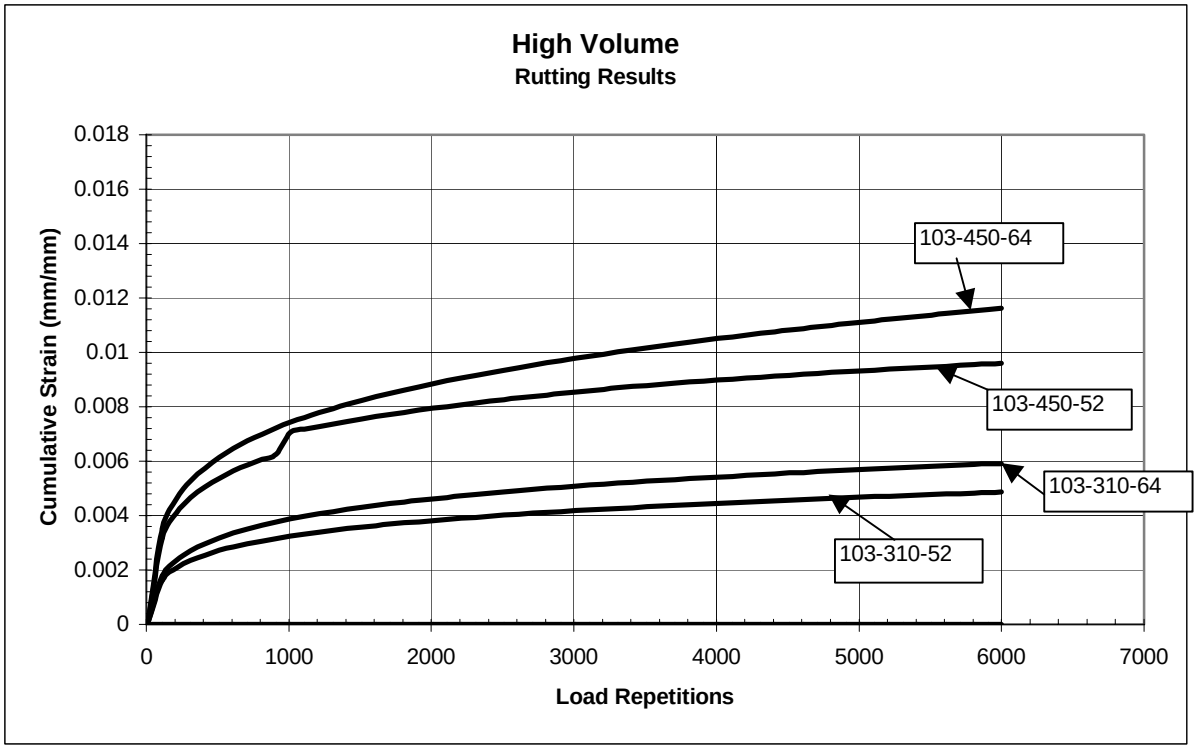
High Volume
Rutting Results
Cumulative Strain (mm/mm)
0.018
0.016
0.014
0.012
0.01
0.008
0.006
0.004
0.002
0
0
1000
2000
3000
4000
5000
6000
7000
Load Repetitions
103-450-64
103-450-52
103-310-64
103-310-52

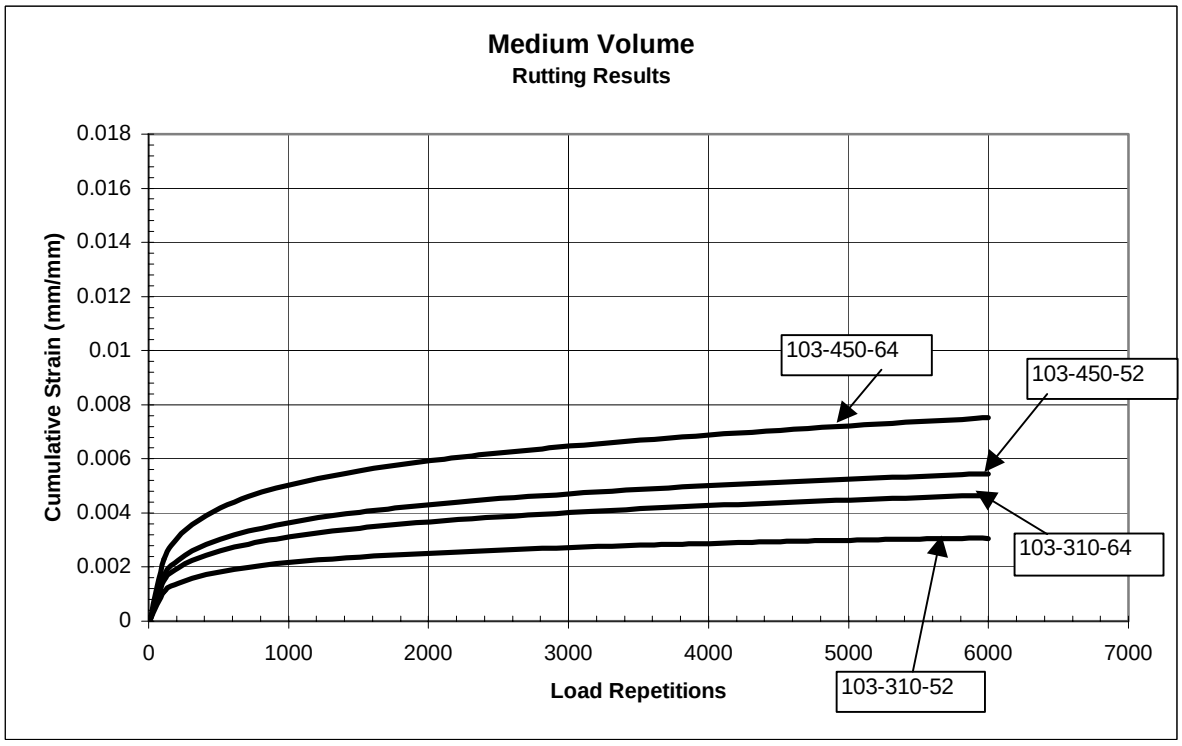
Medium Volume
Rutting Results
Cumulative Strain (mm/mm)
0.018
0.016
0.014
0.012
0.01
0.008
0.006
0.004
0.002
0
0
1000
2000
3000
4000
5000
6000
7000
Load Repetitions
103-450-64
103-450-52
103-310-64
103-310-52

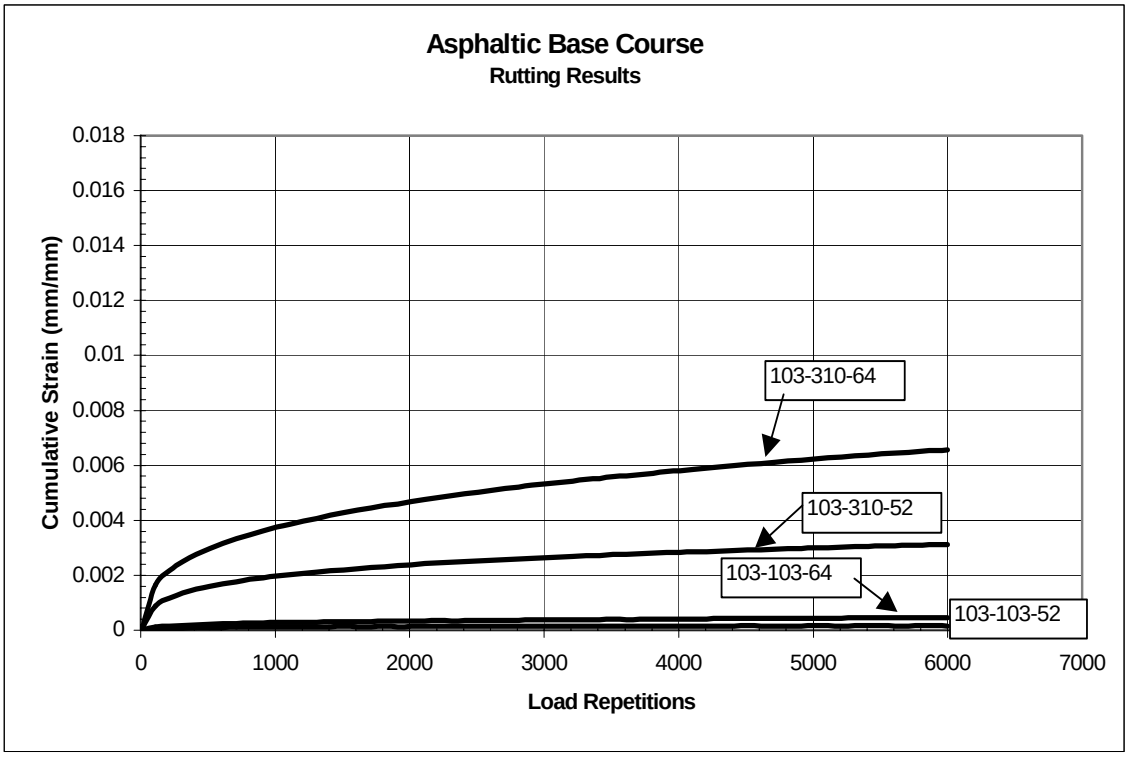
Asphaltic Base Course
Rutting Results
Cumulative Strain (mm/mm)
0.018
0.016
0.014
0.012
0.01
0.008
0.006
0.004
0.002
0
0
1000
2000
3000
4000
5000
6000
7000
Load Repetitions
103-310-64
103-310-52
103-103-64
103-103-52

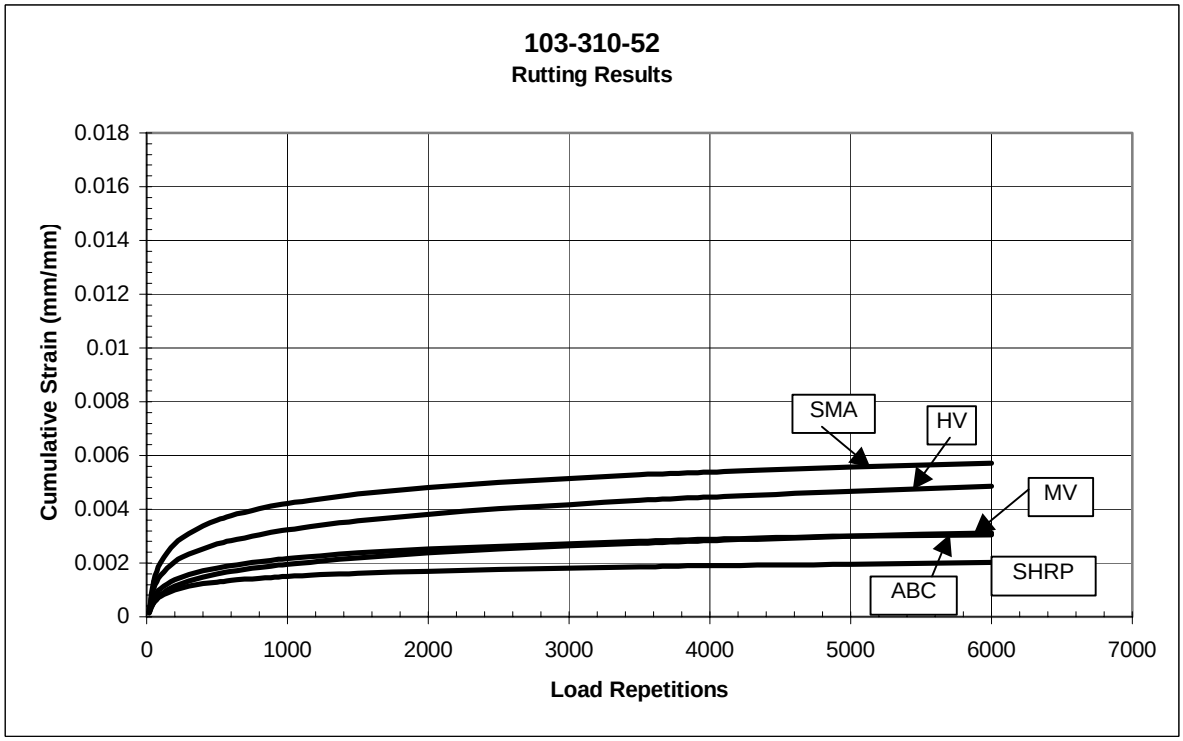
103-310-52
Rutting Results
Cumulative Strain (mm/mm)
0.018
0.016
0.014
0.012
0.01
0.008
0.006
0.004
0.002
0
0
1000
2000
3000
4000
5000
6000
7000
Load Repetitions
SMA
HV
MV
SHRP
ABC

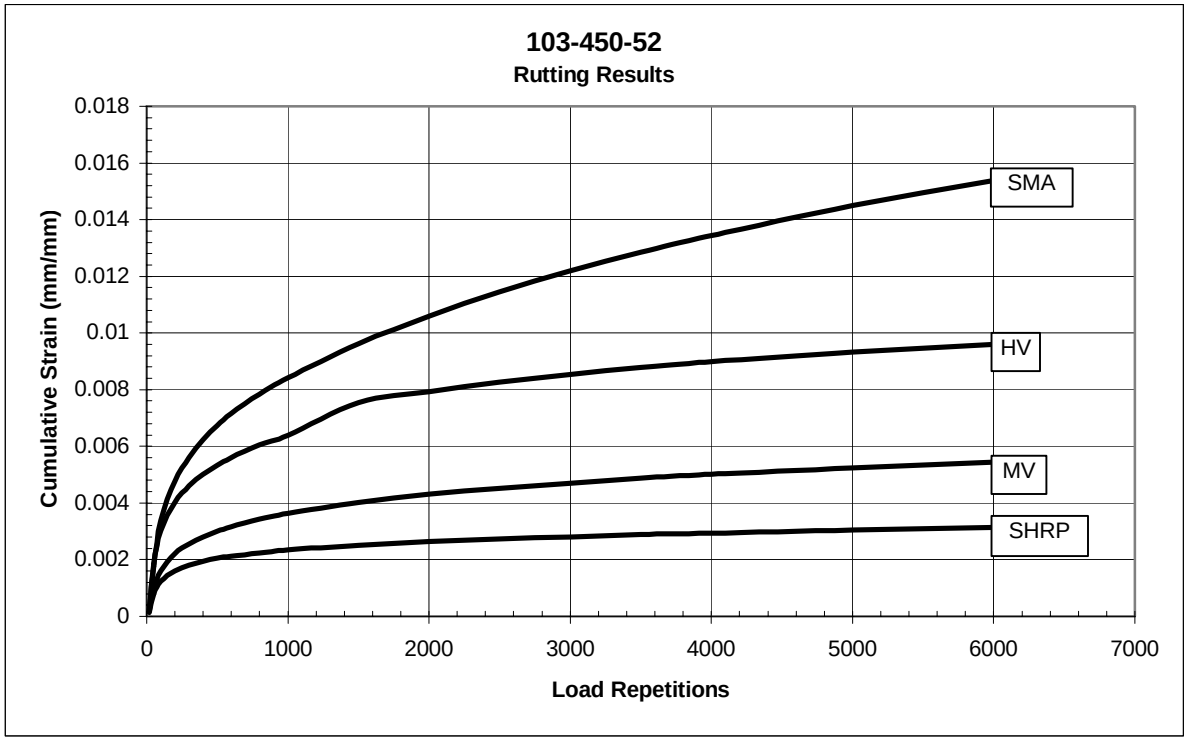
103-450-52
Rutting Results
Cumulative Strain (mm/mm)
0.018
0.016
0.014
0.012
0.01
0.008
0.006
0.004
0.002
0
0
1000
2000
3000
4000
5000
6000
7000
Load Repetitions
SMA
HV
MV
SHRP

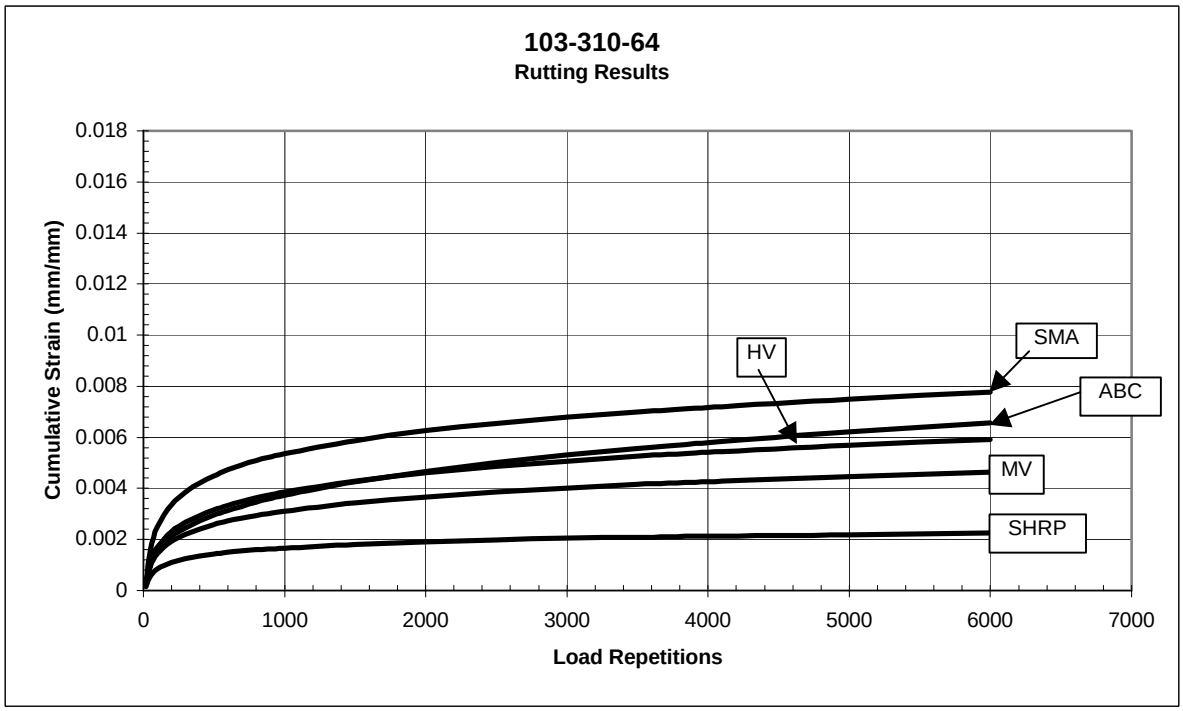
103-310-64
Rutting Results
Cumulative Strain (mm/mm)
0.018
0.016
0.014
0.012
0.01
0.008
0.006
0.004
0.002
0
0
1000
2000
3000
4000
5000
6000
7000
Load Repetitions
HV
SMA
ABC
MV
SHRP

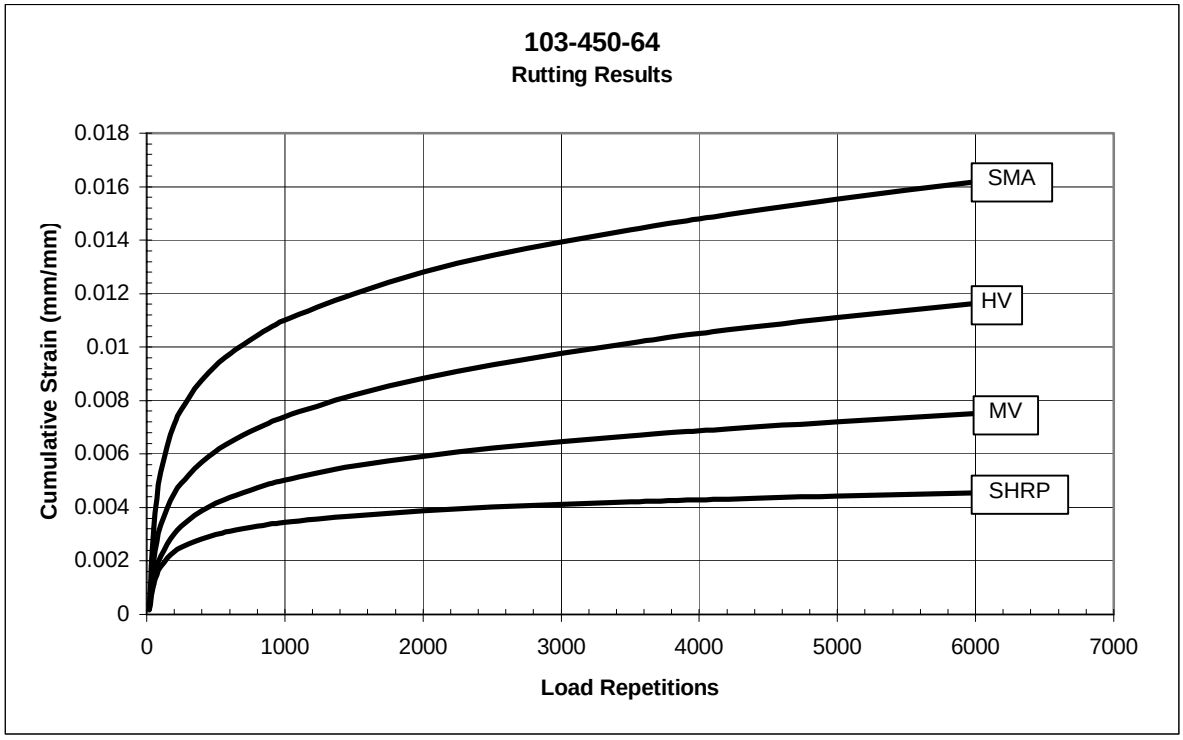
103-450-64
Rutting Results
Cumulative Strain (mm/mm)
0.018
0.016
0.014
0.012
0.01
0.008
0.006
0.004
0.002
0
0
1000
2000
3000
4000
5000
6000
7000
Load Repetitions
SMA
HV
MV
SHRP

APPENDIX D

Teflon Compliance

With the use of 8.8in asphalt specimens, edge friction between the specimens and the top and bottom plates became a concern. To alleviate the problem, the use of two Teflon discs was adopted. The discs are 3.023mm in thickness; it was assumed that the deformation would be negligible. However, this assumption proved to be incorrect.

The very first M_r tests performed (1^{st} generation tests) gave results that were too low and highly questionable. The values for asphalt M_r were lower than those of the granular materials. This directly led to the discovery of the confining pressure problem mentioned previously. However, even after this problem was corrected, the values for asphalt M_r seemed to be lower than those generated by the field tests and other previous research.

Newcomb (1987) compared laboratory M_r to field M_r and found that they varied by 0.3 to 0.4 for asphalt mixtures. Houston et al. (1992) found that the laboratory M_r on average were 1.5 times higher than the field M_r values. Khanal et al. tested asphalt using the diametrical resilient modulus method (ASTM D 4123) in harmonic compression and alternate tension and compression. They found laboratory moduli to average 1741MPa for harmonic M_r and 1378MPa for alternate M_r. Both of these came from tests at 40°C. Even though these previous studies did not use tri-axial equipment and the tests were conducted at lower temperatures, the values collected in this study still seemed to be on the low side.

Therefore, in the effort to determine where unwanted deformations might be coming from, an asphalt M_r test was conducted without the Teflon discs. This test showed a significant difference from the tests performed with the Teflon discs in place. Compliance tests were run on the Teflon discs. It was found that the Teflon discs were indeed deforming. The tests were conducted by placing the discs in between rigid steel plates and running the tri-axial at various deviator stresses. Then the discs were removed and the steel was tested solely under the same parameters. Figure D1 shows the deformation values of the Teflon discs in tri-axial compression; the steel deformation was subtracted out to arrive at the Teflon discs values.

Figure D1 shows that the deformation vs. σ_d follows a somewhat logarithmic trend. However, this trend was not reliable enough to be used as an adjustment for the data. Also, some of the deformations shown for the Teflon discs were greater than those from the asphalt M_r tests themselves. The deformation data could not be used directly; however, it showed that there was a problem and it needed to be explored.

In order to quantify the effect of the Teflon discs, additional M_r tests were preformed to see if a trend between the tests with and without the Teflon discs could be noticed. The result of the SMA testing is shown in Figure D2. The two additional testing results for the SHRP and MV mixtures are shown in Figures D3 & D4. The SMA and MV tests were conducted at 52°C and the SHRP mixture test was conducted at 64°C.

These three tests show that there is a similar trend in the effect of the Teflon discs. In all three cases the tests without the Teflon discs are approximately 100,000kPa higher at low bulk stress (Θ) and 150,000kPa higher at high Θ values. All of the specimens were compacted from reused material and were conducted under similar conditions. The analysis of these sets of tests is discussed further in the next chapter.

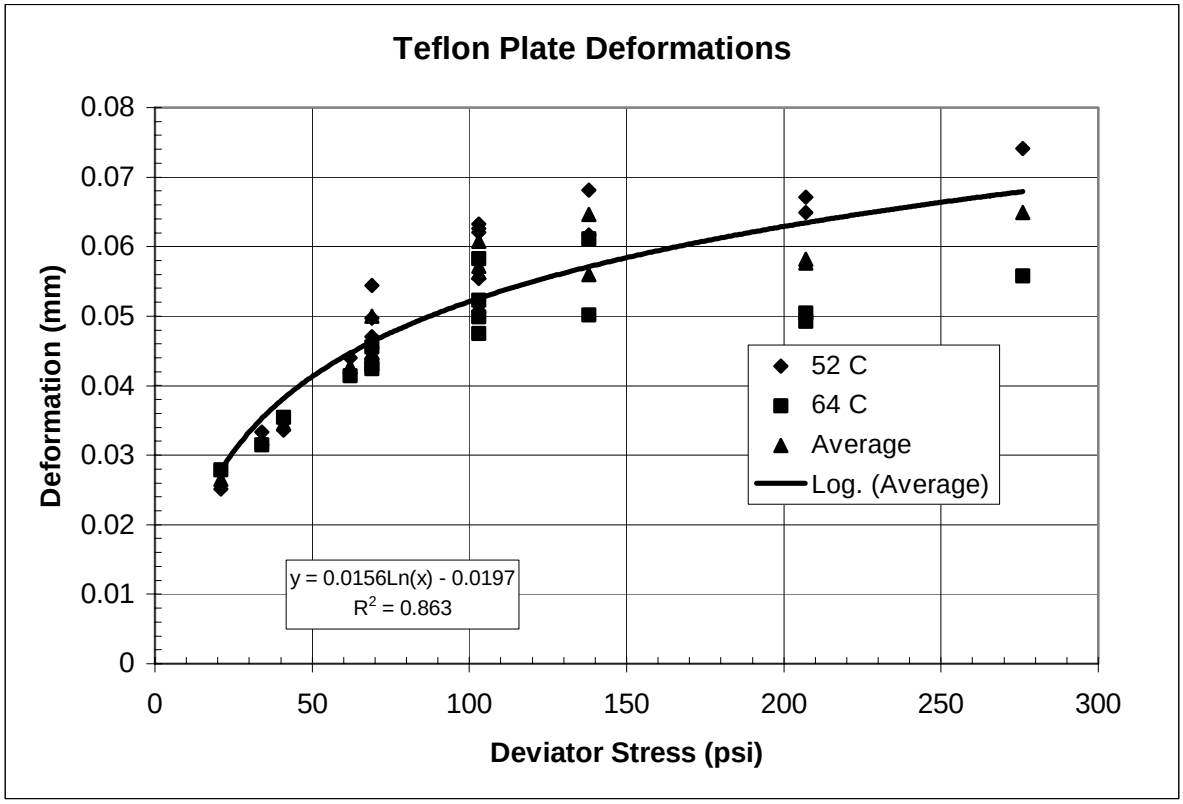

Figure D1 Teflon Plate Deformation at Various Deviator Stresses

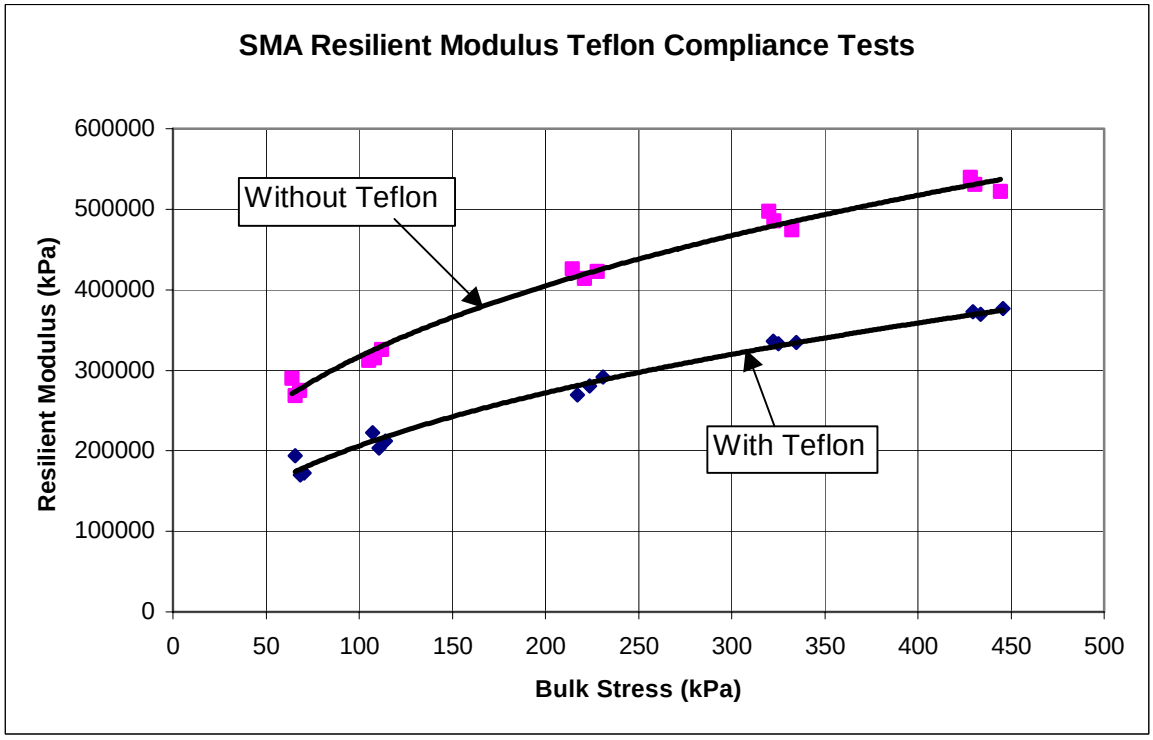

Figure D2 SMA M_r Tests @ 52°C With and Without Teflon

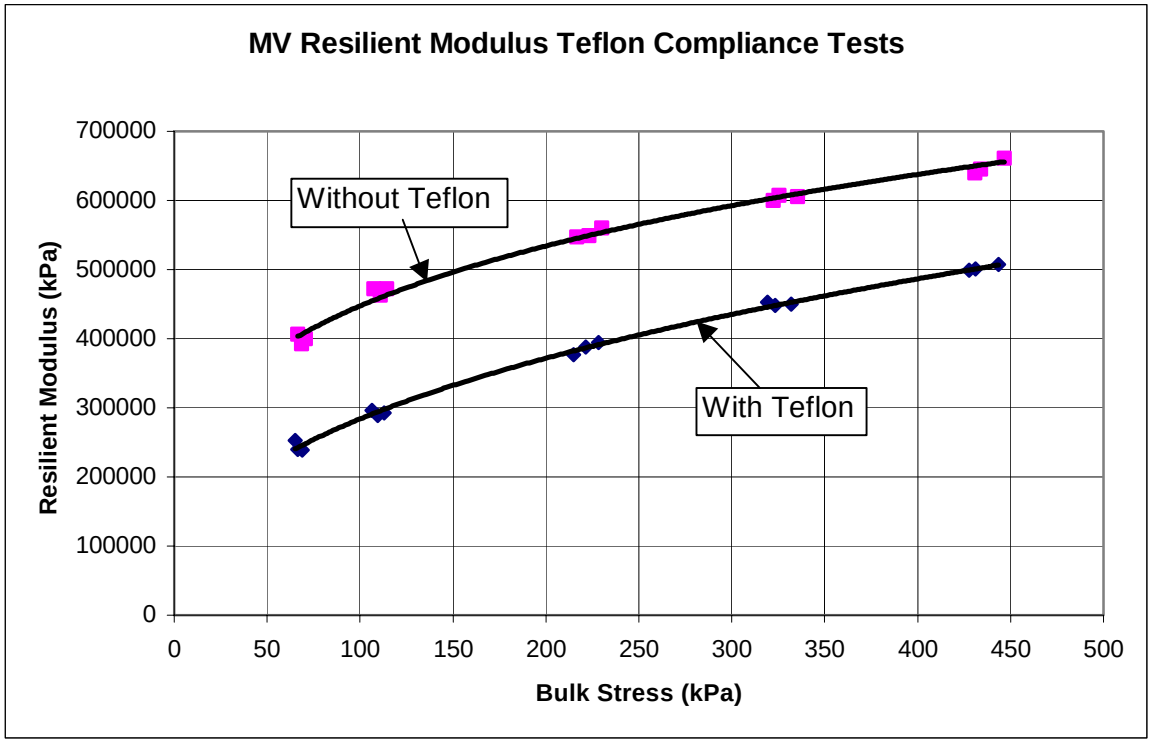

Figure D3 MV M_r Tests @ 52°C With and Without Teflon

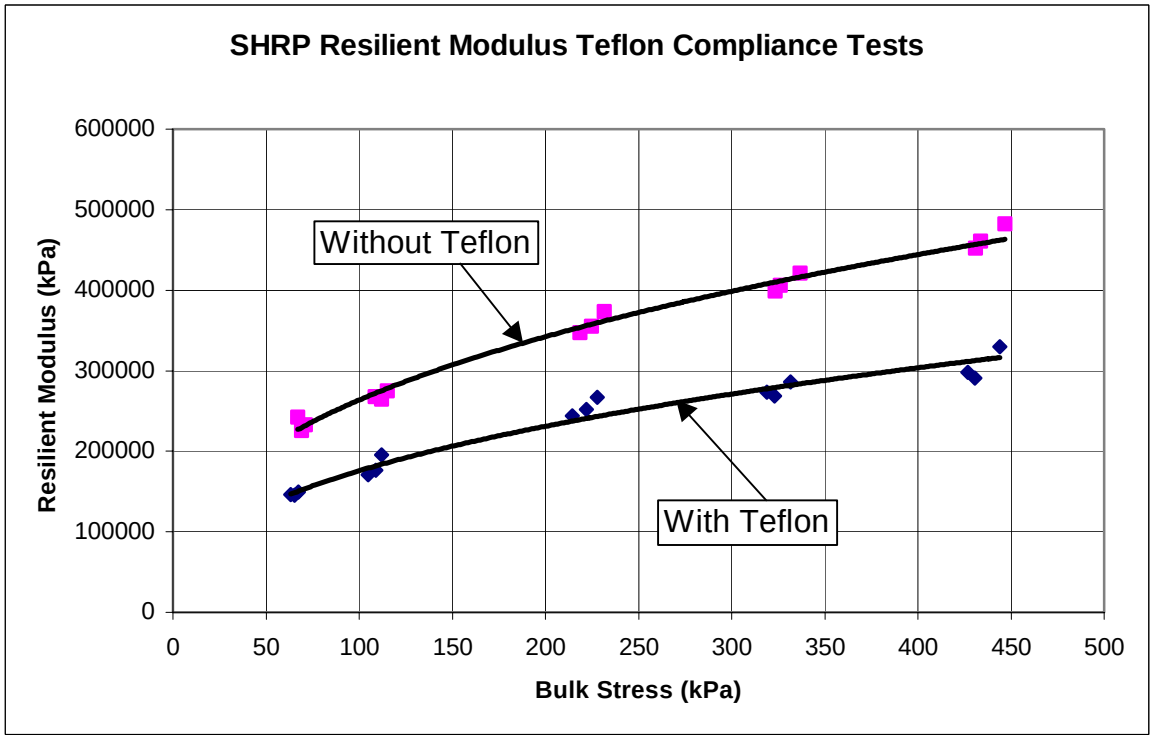

Figure D4 SHRP M_r Tests @ 64°C With and Without Teflon

APPENDIX E

High Temperature Resilient Modulus Results

All of the asphalt materials were tested for resilient modulus according to AASHTO T294. They were also analyzed with the same method used for the granular materials. K1 and K2 values were generated using a power curve from the relationship of Θ vs. M_r. Similar to the granular materials, the power curve relationship had reliabilities in at least the 95th percentile. All of the results presented are from tests performed with the Teflon discs in place. Figure E1 presents the results from a M_r test, the power curve can be seen as well as the K1 and K2 values for the specimen. Figures E2 & E3 show the final results obtained from all the tests.

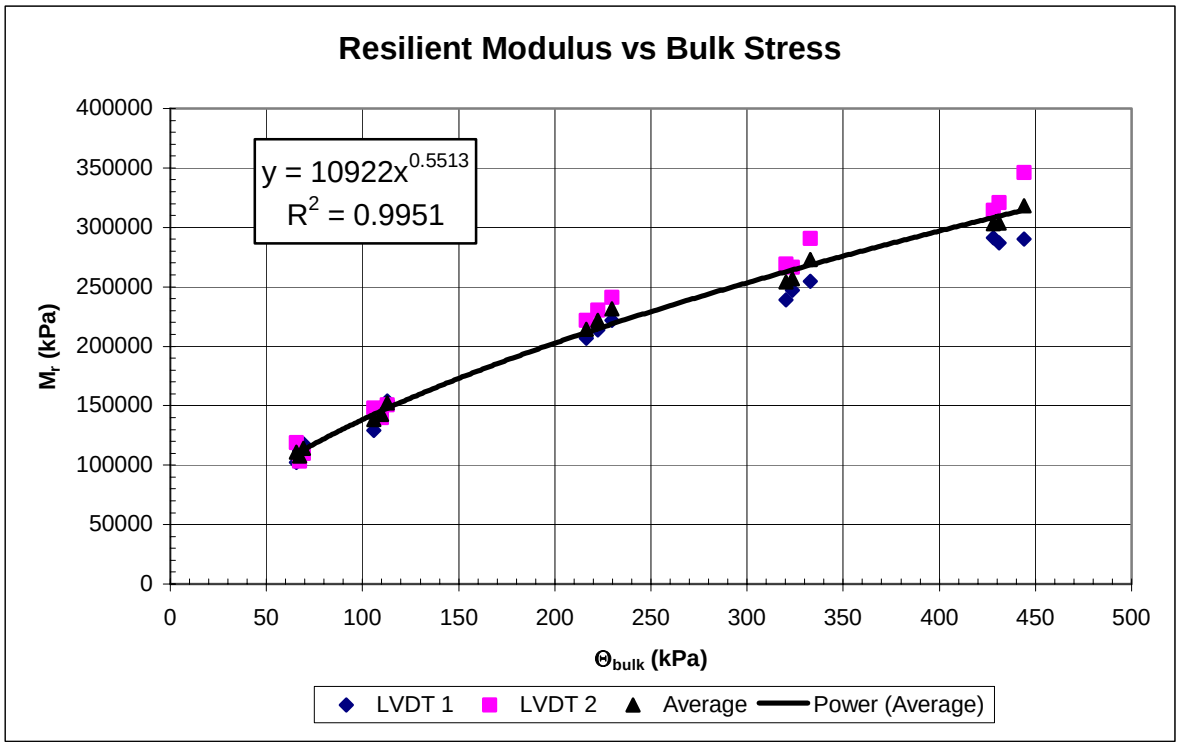

Figure E1 HV 64°C M_r Test Results

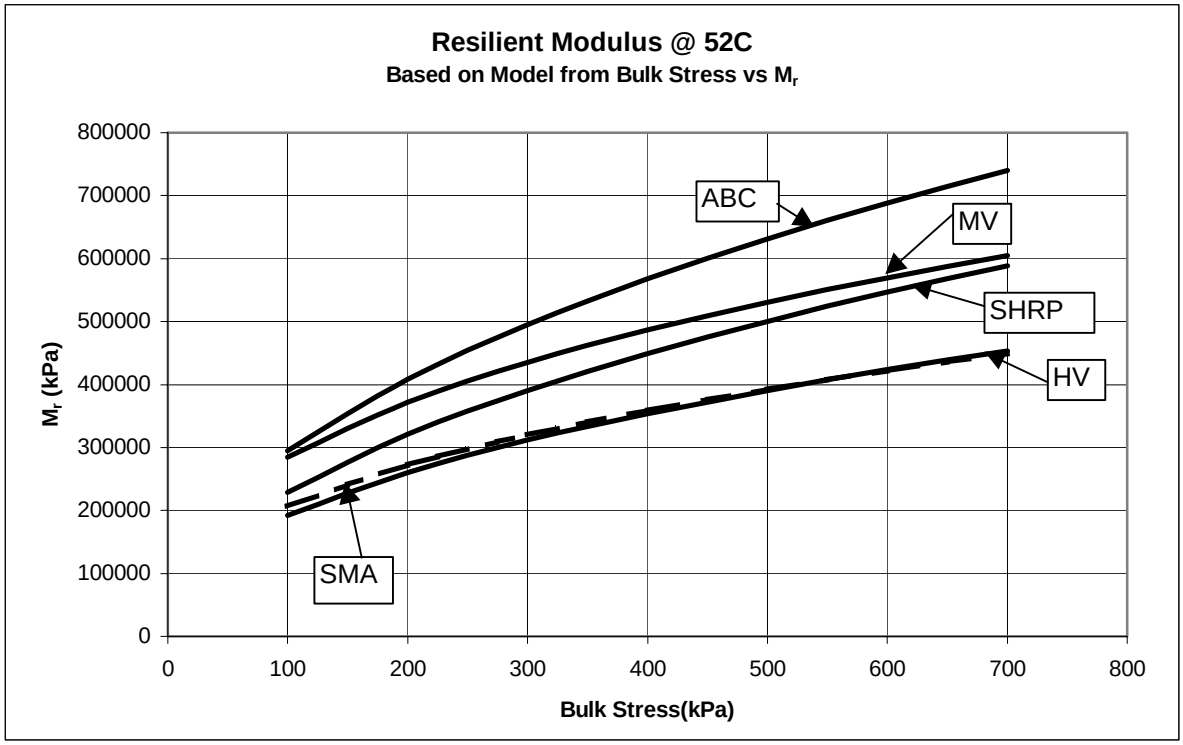

Figure E2 Asphalt Material M_r Results @ 52°C

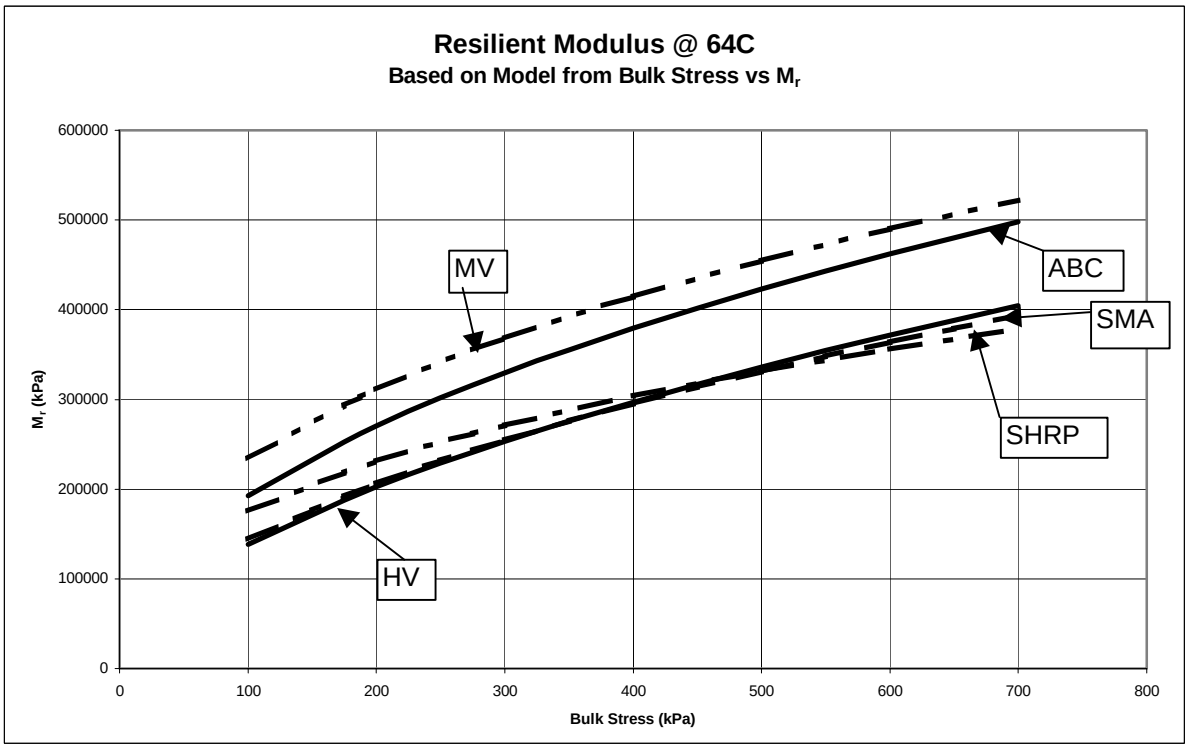

Figure E3 Asphalt Material M_r Results @ 64°C

E.1 Material Comparisons

The M_r data show two trends: the first is that asphalt performs better than granular materials. The second is that the finer mixes have a higher M_r. The MV and ABC materials, which are the finest of all the mixes tested, consistently performed better than the more coarse grained mixes. The difference over both temperature levels was approximately 20%. The HV mixture and SMA, which were tested almost identically at both temperatures, were the worst resilient performers while SHRP fell into the middle. This could suggest that the gradation of the mix influences the M_r of an asphalt mixture.

All of the surface materials maintained constant differences between them over the range of Θ values, except the SHRP mixture. The SHRP mixture at 52°C shows a relatively better performance at the high Θ values. However, when the same material is tested at 64°C, the opposite is true ; the performance is relatively poor at high Θ values.

E.2 Temperature Effects

As expected, the temperature caused differences in the M_r of the materials. The temperature shift was not always consistent. The HV and SMA showed less of a temperature dependency than the MV and ABC. The SHRP mixture had the highest temperature shift of all, especially at high Θ values. This may suggest that materials with a lower M_r are less temperature- dependent and vice versa.

Generally, all of the materials show a parallel relation to one another except for SHRP. The SHRP material also behaves differently at the two temperatures in relation to the other materials. When tested at 64°C the SHRP, the specimen's M_r decreases in relation to the other tests, but at 52°C the SHRP specimen shows an increasing M_r.

Finally, in all cases, the M_r values for the asphalt materials are higher than those of the recycled granular materials. The factors range from 1.7 at 64°C and 2.2 at 52°C. This trend is not unusual, nor surprising.

The temperature shifts were used to compare the M_r results to one another at 20°C and to current layer coefficient values. Shifting the M_r values to 20°C allows for the calculation of

asphalt concrete layer coefficients (a_1). Those a_1 values are in turn used for comparison with permanent deformation results, granular results, and field results.

E.3 Resilient Modulus Layer Coefficients

The temperature shifts mentioned above were used in a process that is identical to the one used shifting the ABC M_r values in the previous section. Again it was assumed that the asphalt mixtures shift linearly on a logarithmic scale versus temperature. The equations presented were used to calculate the a_1 values from the shifted M_r results. A Θ value of 400kPa was chosen because it represents a high σ_d and low σ_3 values, 207kPa and 69kPa respectively. Asphalt surface layers usually experience the lowest σ_3 values of any other layer in a pavement structure. The surface layer will also experience the highest σ_d values. These σ_3 and σ_d values meet both of those criterions.

Table E1 shows the calculated layer coefficients and their corresponding M_r values. There are significant differences in these a_1 values and it clearly suggests that these materials are not the same and most likely should not have identical layer coefficients.

Table E1 Asphalt Mixture a_1 and M_r Values

	SHRP		SMA		MV		HV	
Bulk	20°C		20°C		20°C		20°C	
Stress (kPa)	M_r (MPa)	a_1	M_r (MPa)	a_1	M_r (MPa)	a_1	M_r (MPa)	a_1
400	1352	0.302	605	0.162	743	0.198	565	0.15